

Ninevah University

College of Electronics Engineering

Electronic Engineering Department



**Comparative Analysis of Rectifier Circuits at 2.4 GHz for
Energy Harvesting Applications**

Othman Anwar Mohammed

A Thesis in

Electronic Engineering

Supervised by

Asst. Prof.

Dr. Ahmed Mohammad Sabaawi

1445 AH

2024 AD

**Comparative Analysis of Rectifier Circuits at 2.4 GHz for
Energy Harvesting Applications**

A Thesis Submitted by

Othman Anwar Mohammed

To

The Council of the College of Electronics Engineering

Ninevah University

As a Partial Fulfillment of the Requirements

For the Degree of Master of Science

In

Electronic Engineering

Supervised by

Asst. Prof.

Dr. Ahmed Mohammad Sabaawi

1445 AH

2024 AD

بِسْمِ اللّٰهِ الرَّحْمٰنِ الرَّحِیْمِ

وَقُلْ اَعْمَلُوا فِی سَبِیْلِ اللّٰهِ عَمَلِكُمْ وَرَسُوْلُهُ وَالْمُؤْمِنُوْنَ وَاسْتُرِدُوْنَ
اِلَى عِلْمِ الْغَیْبِ وَالشَّهَادَةِ فِی نَبِئِكُمْ بِمَا كُنْتُمْ تَعْمَلُوْنَ (105)

صَدَقَ اللّٰهُ الْعَظِیْمُ

سورة التوبة

ACKNOWLEDGEMENTS

In the name of Allah, and prayers and peace be upon the Messenger of Allah and his family and companions all until the Day of Judgment. Oh Allah, praise be to You as it should be for the majesty of Your countenance and the greatness of Your authority. Praise be to Allah who has enabled me to complete this work, helped me, and guided me to be on the straight path.

The duty of loyalty invites me to extend my thanks and gratitude to everyone who extended a helping hand, and gave me guidance.

I am pleased to extend my sincere thanks and appreciation to my teacher and supervisor, Assist. Prof. Dr Ahmed Mohammed Sabaawi, for the sound advice, correct guidance and abundant knowledge he gave me.

My thanks and gratitude to the President of the University of Ninevah and the Dean of the College of Electronics Engineering for their contribution to maintaining the continuity of the science and learning process.

My thanks and gratitude to the Head of the Department of Electronic Engineering and to all my professors in the College of Electronics Engineering who were a source of knowledge.

My thanks and gratitude go to the one who honored me with bearing his name and who spent the precious and precious things in order for me to reach a high academic degree, and today my father sees the fruit of what my he planted (may Allah have mercy on him) .

My thanks and gratitude to the light of my eyes, the light of my path, and the joy of my life, whose prayers and words were a shield and a fortress for me (my dear mother).

Abstract

Energy harvesting is the technique of taking energy from the external environment of a system and converting it into usable electric power. Electronics may operate without a conventional power source; thanks to energy harvesting, which eliminates the need for frequent cable hookups and battery changes. Circuitry for controlling electricity and safeguarding an energy storage cell are usually included in an energy harvesting system. Advanced Design System (ADS) software is used to simulate the proposed structures. In this work, a comparison between different types of rectifier circuits for RF energy harvesting is conducted. Six types of rectifier circuits consisting of half-wave, full-wave, voltage doubler, Villard charge pump, Graetz charge pump, and Dickson charge pump are designed and simulated. These various types of rectifier circuits are designed for different resistance loads, HSMS282X diodes and standard substrate materials that represent various dielectric constant values (ϵ_r). Firstly, the rectifiers are designed on an FR-4 substrate with a thickness of 1.6 mm using a single-stage LC-match method at 2.4 GHz. The studied range of the input power was from 0 dBm to 30 dBm. The dielectric constant is 4.3, the resistance load is 3k ohm, and the HSMS2820 diode is used. The highest recorded output voltage for the Graetz charge pump was around 27 V, while the highest recorded efficiency for the Graetz charge pump was also 27%. Again, a comparative study between rectifier circuits using the LC-match method and rectifier circuits using the TL-match method is presented. Furthermore, the Graetz charge pump is the best among other rectifier circuits, having recorded 73% efficiency and 26.8 V in terms of V_{out} when using the TL-match method. On the other hand, the Dickson charge pump showed the worst performance compared with other rectifier circuits.

Table of Contents

Subject	Page
CHAPTER ONE INTRODUCTION AND LITERATURE REVIEW	1
1.1 Radio Frequencies (RF)	1
1.2 Literature review	4
1.3 Aims of the thesis	11
1.4 Thesis Layout	12
CHAPTER TWO THEORETICAL BACKGROUND	14
2.1 Introduction	14
2.2 Wireless Power Transfer (WPT)	15
2.3 Rectifier Characteristics	16
2.4 Rectifier Circuits	17
2.4.1 Half Wave Rectifier	17
2.4.2 Full Wave Rectifier	18
2.4.2.1 Center Tapped Rectifier	18
2.4.2.2 Bridge Rectifier	18
2.4.3 Voltage Doubler	19
2.4.4 Villard Charge Pump	19
2.4.5 Graetz Charge Pump	20
2.4.6 Dickson Charge Pump	21
CHAPTER THREE ANALYSIS OF VARIOUS RECTIFIER CIRCUITS WITH THE LC-MATCH METHOD	24
3.1 Impedance Matching Circuit using LC-match method	25
3.2 Half-wave rectifier circuit using LC-match method	29
3.3 Full-wave rectifier circuit using LC-match method	37
3.4 Voltage doubler rectifier circuit using LC-match method	44
3.5 Villard rectifier circuit using LC-match method	49
3.6 Graetz charge pump rectifier circuit using LC-match method	55
3.7 Dickson charge pump rectifier circuit using LC-match method	60
CHAPTER FOUR COMPARISON BETWEEN DESIGN OF RECTIFIER CIRCUITS WITH LC-MATCH METHOD AND TL-	69

MATCH METHOD AT 2.4 GHZ	
4.1 Impedance Matching Circuit using TL-match method	69
4.2 Half-wave rectifier circuit using TL-match method	73
4.3 Full-wave rectifier circuit using TL-match method	77
4.4 Voltage doubler rectifier circuit using TL-match method	80
4.5 Villard rectifier circuit using TL-match method	83
4.6 Graetz charge pump rectifier circuit using TL-match method	86
4.7 Dickson charge pump rectifier circuit using TL-match method	89
CHAPTER FIVE	
CONCLUSIONS AND FUTURE WORKS	
98	
5.1 Conclusions	98
5.2 Future works	100
References	102

List of Figures

No.	Subject	Page
1.1	Schematic block diagram of RF energy harvesting.	2
2.1	Radio Frequency Energy Sources.	14
2.2	Half-Wave Rectifier circuit.	17
2.3	Full-Wave Rectifier circuit.	18
2.4	Voltage doubler rectifier circuit diagram.	19
2.5	Villard charge pump rectifier circuit diagram.	20
2.6	Graetz charge pump rectifier circuit diagram.	21
2.7	Dickson charge pump rectifier circuit diagram.	23
3.1	LC-Matching Method.	25
3.2	Equivalent Circuit for LC-Circuit.	26
3.3	Simulated circuit to find Z_{in} for half-wave at frequency band 2.4 GHz.	27
3.4	Simulated value of Z_{in} .	27
3.5	Half-wave rectifier circuit operating at 2.4 GHz with LC-circuit.	30
3.6	Simulated S_{11} of half-wave rectifier circuit at 2.4 GHz with LC-circuit.	30
3.7	V_{in} (V) of half-wave rectifier circuit at 2.4 GHz with LC-circuit.	31
3.8	V_{out} (V) of half-wave rectifier circuit at 2.4 GHz with LC-circuit.	32
3.9	Output current of half-wave rectifier circuit at 2.4 GHz with LC-circuit.	32
3.10	V_{out} versus P_{in} of half-wave rectifier circuit for different resistance values of load (R_L) at 2.4 GHz with LC-circuit.	33
3.11	V_{out} (V) versus P_{in} (dBm) of Half-wave rectifier circuit for different Diodes at 2.4 GHz with LC-circuit.	34
3.12	V_{out} (V) versus P_{in} (dBm) of half-wave rectifier circuit for different ϵ_r at 2.4 GHz with LC-circuit.	35
3.13	Efficiency (η) versus P_{in} (dBm) of half-wave rectifier circuit for different values of resistance load (R_L) at	35

	2.4 GHz with LC-circuit.	
3.14	Efficiency (η) versus Pin (dBm) of half-wave rectifier circuit for different Diodes at 2.4 GHz with LC-circuit.	36
3.15	Efficiency (η) versus Pin (dBm) of half-wave rectifier circuit for different ϵ_r at 2.4 GHz with LC-circuit.	37
3.16	Full-wave rectifier circuit operating at 2.4 GHz with LC-circuit.	38
3.17	Simulated S11 of full-wave rectifier circuit at 2.4 GHz with LC-circuit.	38
3.18	Vout (V) versus Pin (dBm) of full-wave rectifier circuit for different resistance load (R_L) at 2.4 GHz with LC-circuit.	39
3.19	Vout (V) versus Pin (dBm) of full-wave rectifier circuit for different resistance load (R_L) at 2.4 GHz with LC-circuit.	40
3.20	Vout (V) versus Pin (dBm) of full-wave rectifier circuit for different diodes at 2.4 GHz with LC-circuit.	41
3.21	Efficiency (η) versus Pin (dBm) of voltage doubler rectifier circuit for different values of resistance load (R_L) at 2.4 GHz with LC-circuit.	42
3.22	Efficiency (η) versus Pin (dBm) of full-wave rectifier circuit for different Diodes at 2.4 GHz with LC-circuit.	43
3.23	Efficiency (η) versus Pin (dBm) of full-wave rectifier circuit for different ϵ_r at 2.4 GHz with LC-circuit.	43
3.24	Voltage doubler rectifier circuit operating at 2.4 GHz with LC-circuit.	44
3.25	Simulated S11 of voltage doubler rectifier circuit at 2.4 GHz with LC-circuit.	45
3.26	Vout (V) versus Pin (dBm) of voltage doubler rectifier circuit for different values of resistance load (R_L) at 2.4 GHz with LC-circuit.	45
3.27	Vout (V) versus Pin (dBm) of voltage doubler rectifier circuit for different Diodes at 2.4 GHz with LC-circuit.	46

3.28	Vout (V) versus Pin (dBm) of voltage doubler rectifier circuit for different ϵ_r at 2.4 GHz with LC-circuit.	47
3.29	Efficiency (η) versus Pin (dBm) of voltage doubler rectifier circuit for different values of resistance load (R_L) at 2.4 GHz with LC-circuit.	47
3.30	Efficiency (η) versus Pin (dBm) of voltage doubler rectifier circuit for different Diodes at 2.4 GHz with LC-circuit.	48
3.31	Efficiency (η) versus Pin (dBm) of voltage doubler rectifier circuit for different ϵ_r at 2.4 GHz with LC-circuit.	49
3.32	Villard charge pump rectifier circuit operating at 2.4 GHz with LC-circuit.	50
3.33	: Simulated S11 of Villard charge pump rectifier circuit at 2.4 GHz with LC-circuit.	50
3.34	Vout (V) versus Pin (dBm) of Villard charge pump rectifier circuit for different values of resistance load (R_L) at 2.4 GHz with LC-circuit.	51
3.35	Vout (V) versus Pin (dBm) of Villard charge pump rectifier circuit for different Diodes at 2.4 GHz with LC-circuit.	52
3.36	Vout (V) versus Pin (dBm) of Villard charge pump rectifier circuit for different ϵ_r at 2.4 GHz with LC-circuit.	52
3.37	Efficiency (η) versus Pin (dBm) of Villard charge pump rectifier circuit for different values of resistance load (R_L) at 2.4 GHz with LC-circuit.	53
3.38	Efficiency (η) versus Pin (dBm) of villard charge pump rectifier circuit for different Diodes at 2.4 GHz with LC-circuit.	54
3.39	Efficiency (η) versus Pin (dBm) of Villard charge pump rectifier circuit for different ϵ_r at 2.4 GHz with LC-circuit.	54
3.40	Graetz charge pump rectifier circuit operating at 2.4 GHz with LC-circuit.	55
3.41	Simulated S11 of Graetz charge pump rectifier circuit	55

	at 2.4 GHz with LC-circuit.	
3.42	Vout (V) versus Pin (dBm) of Graetz charge pump rectifier circuit for different values of resistance load (R_L) at 2.4 GHz with LC-circuit.	56
3.43	Vout (V) versus Pin (dBm) of Graetz charge pump rectifier circuit for different Diodes at 2.4 GHz with LC-circuit.	57
3.44	Vout (V) versus Pin (dBm) of Graetz charge pump rectifier circuit for different ϵ_r at 2.4 GHz with LC-circuit.	57
3.45	Efficiency (η) versus Pin (dBm) of Graetz charge pump rectifier circuit for different values of resistance load (R_L) at 2.4 GHz with LC-circuit.	58
3.46	Efficiency (η) versus Pin (dBm) of Graetz charge pump rectifier circuit for different Diodes at 2.4 GHz with LC-circuit.	59
3.47	Efficiency (η) versus Pin (dBm) of Graetz charge pump rectifier circuit for different ϵ_r at 2.4 GHz with LC-circuit.	59
3.48	Dickson charge pump rectifier circuit operating at 2.4 GHz with LC-circuit.	60
3.49	Simulated S11 of Dickson charge pump rectifier circuit at 2.4 GHz with LC-circuit.	60
3.50	Vout (V) versus Pin (dBm) of Dickson charge pump rectifier circuit for different values of resistance load (R_L) at 2.4 GHz with LC-circuit.	61
3.51	Vout (V) versus Pin (dBm) of Dickson charge pump rectifier circuit for different Diodes at 2.4 GHz with LC-circuit.	62
3.52	Vout (V) versus Pin (dBm) of Dickson charge pump rectifier circuit for different ϵ_r at 2.4 GHz with LC-circuit.	62
3.53	Efficiency (η) versus Pin (dBm) of Dickson charge pump rectifier circuit for different values of resistance load (R_L) at 2.4 GHz with LC-circuit.	63
3.54	Efficiency (η) versus Pin (dBm) of Dickson charge	64

	pump rectifier circuit for different Diodes at 2.4 GHz with LC-circuit.	
3.55	Efficiency (η) versus Pin (dBm) of Dickson charge pump rectifier circuit for different ϵ_r at 2.4 GHz with LC-circuit.	64
3.56	Vout (V) versus Pin (dBm) of different rectifier circuits at 2.4 GHz with LC-circuit.	65
3.57	Efficiency (η) versus Pin (dBm) of different rectifier circuits at 2.4 GHz with LC-circuit.	66
4.1	Tools of Smith chart.	69
4.2	Window of the Smith chart in ADS.	70
4.3	Block diagram of Transmission Lines.	70
4.4	Window of the LineCalc to compute Width and Length.	71
4.5	Simulated Block diagram of Transmission Lines (TL) at 2.4 GHz.	71
4.6	Half-wave rectifier circuit operating at 2.4 GHz with TL-circuit.	72
4.7	Simulated S11 of half-wave rectifier circuit at 2.4 GHz with TL-circuit.	73
4.8	Vin (V) of half-wave rectifier circuit at 2.4 GHz with TL-circuit.	73
4.9	Vout (V) of half-wave rectifier circuit at 2.4 GHz with TL-circuit.	74
4.10	Output current of half-wave rectifier circuit at 2.4 GHz with TL-circuit.	74
4.11	Vout versus Pin of comparison between a half-wave rectifier circuit with an LC-circuit and a TL-circuit at 2.4 GHz.	75
4.12	Efficiency (η) versus Pin of comparison between a half-wave rectifier circuit with an LC-circuit and a TL-circuit at 2.4 GHz.	76
4.13	Full-wave rectifier circuit operating at 2.4 GHz with TL-circuit.	77
4.14	Simulated S11 of full-wave rectifier circuit at 2.4 GHz with TL-circuit.	77

4.15	Vout versus Pin of comparison between a full-wave rectifier circuit with an LC-circuit and a TL-circuit at 2.4 GHz.	78
4.16	Efficiency (η) versus Pin of comparison between a full-wave rectifier circuit with an LC-circuit and a TL-circuit at 2.4 GHz.	79
4.17	Voltage doubler rectifier circuit operating at 2.4 GHz with TL-circuit.	80
4.18	Simulated S11 of voltage doubler rectifier circuit at 2.4 GHz with TL-circuit.	80
4.19	Vout versus Pin of comparison between a voltage doubler rectifier circuit with an LC-circuit and a TL-circuit at 2.4 GHz.	81
4.20	Efficiency (η) versus Pin of comparison between a voltage doubler rectifier circuit with an LC-circuit and a TL-circuit at 2.4 GHz.	82
4.21	Villard charge pump rectifier circuit operating at 2.4 GHz with TL-circuit.	83
4.22	Simulated S11 of Villard charge pump rectifier circuit at 2.4 GHz with TL-circuit.	83
4.23	Vout versus Pin of comparison between a Villard charge pump rectifier circuit with an LC-circuit and a TL-circuit at 2.4 GHz.	84
4.24	Efficiency (η) versus Pin of comparison between a Villard charge pump rectifier circuit with an LC-circuit and a TL-circuit at 2.4 GHz.	85
4.25	Graetz charge pump rectifier circuit operating at 2.4 GHz with TL-circuit.	86
4.26	Simulated S11 of Graetz charge pump rectifier circuit at 2.4 GHz with TL-circuit.	86
4.27	Vout versus Pin of comparison between a Graetz charge pump rectifier circuit with an LC-circuit and a TL-circuit at 2.4 GHz.	87
4.28	Efficiency (η) versus Pin of comparison between a Graetz charge pump rectifier circuit with an LC-circuit and a TL-circuit at 2.4 GHz.	88

4.29	Dickson charge pump rectifier circuit operating at 2.4 GHz with TL-circuit.	89
4.30	Simulated S11 of Dickson charge pump rectifier circuit at 2.4 GHz with TL-circuit.	89
4.31	Vout versus Pin of comparison between a Dickson charge pump rectifier circuit with an LC-circuit and a TL-circuit at 2.4 GHz.	90
4.32	Efficiency (η) versus Pin of comparison between a dickson charge pump rectifier circuit with an LC-circuit and a TL-circuit at 2.4 GHz.	91
4.33	Vout (V) versus Pin (dBm) of different rectifier circuits at 2.4 GHz with TL-circuit.	92
4.34	Efficiency (η) versus Pin (dBm) of different rectifier circuits at 2.4 GHz with TL-circuit.	93
4.35	Efficiency (η) versus Pin (dBm) of Graetz charge pump rectifier circuit for different values of resistance load (R_L) at 2.4 GHz with TL-circuit.	94

List of tables

No.	Subject	Page
3.1	Show the Efficiency (η) for different Rectifier circuits at 10 and 30 dBm of input power (Pin).	67

List of Abbreviation	
AC	Alternative Current
ADS	Advanced Design System
BLE	Bluetooth low-energy
ETSI	European Telecommunications Standards Institute
EM	Electromagnetic Wave
FCC	Federal Communications Commission
GSM	Global System Mobile
IMD	Implantable Medical Device
ISM	Industrial Scientific & Medical
LTE	Long Term Evolution
MICS	Medical Implant Communication Service
RFEH	Radio Frequency Energy Harvesting
RF	Radio Frequency
RX	Receiver
TX	Transmitter
UMTS	Universal Mobile Telecommunication System
WPT	Wireless Power Transfer
WMTS	Wireless Medical Telemetry Service
PCE	Power Conversion Efficiency

List of Symbols

Symbol	Explanation	Unit
ϵ_r	Dielectric permittivity	[Farad/ Meter]
P_{RX}	Receiver Power	[Watt]
P_{TX}	Transmitted Power	[Watt]
P_{in}	Input power	[Decibel]
$V_{out.}$	Output Voltage	[Volt]
R_L	Load Resistance	[Ohm]
Q_s	Serial Q Factor	
Q_p	Parallel Q Factor	
R_+	Load Resistance	[Ohm]
R_-	Source Resistance	[Ohm]
Z_{in}	Input Impedance	[Ohm]
X_C	Capacitive Reactance	[Ohm]
X_L	Inductive Reactance	[Ohm]

CHAPTER ONE

INTRODUCTION

1.1 Introduction

Not only are fifth-generation (5G) technologies providing the groundwork for a sophisticated, high-performance wireless communication infrastructure, but also they additionally provide possibilities for swift socio-economic growth and the transformation of digital technology. With the advent of 5G technology, there is now greater possibility to connect a number of handheld devices with sensing and communication capabilities and to establish a secure, quick connection between them [1].

In the next years, thousand millions of electronic gadgets are predicted to be capable of connection; thanks to 5G and information technology networks [2].

Therefore, with the potential of 5G and information technology in mind, scientists are greatly concentrating on creating novel communication protocols as well as apparatus [3].

To ensure that the sensor appliances continue to operate sustainably, technicians must continue to provide these devices with perpetual electricity. One option is to use a rectenna system to charge these devices wirelessly, which might also save money by minimizing the need to replace batteries and hard wires. WPT, or wireless power transfer, and RFEH, or radio frequency energy harvesting provides an alternative method of recharging the sensing components. These methods allow for simple mobility and lower maintenance costs. [4].

The literature review has extensively researched only single-band, wide-band and multiple-band rectenna technology for energy harvesting since communication networks employ several frequency bands [5]-[9].

A key component of antennas that greatly affects power conversion efficiency (PCE) is the rectifying circuit. Additionally, the Schottky diode affects rectifier performance [10].

Therefore, the design of an efficient rectifier has great promise.

The basic principle of RF energy harvesting is based on the conversion of electromagnetic waves into electrical energy using a device called an RF energy harvester. The harvester typically consists of an antenna, a rectifier, and a power management unit as shown in Fig.1.1 [11].

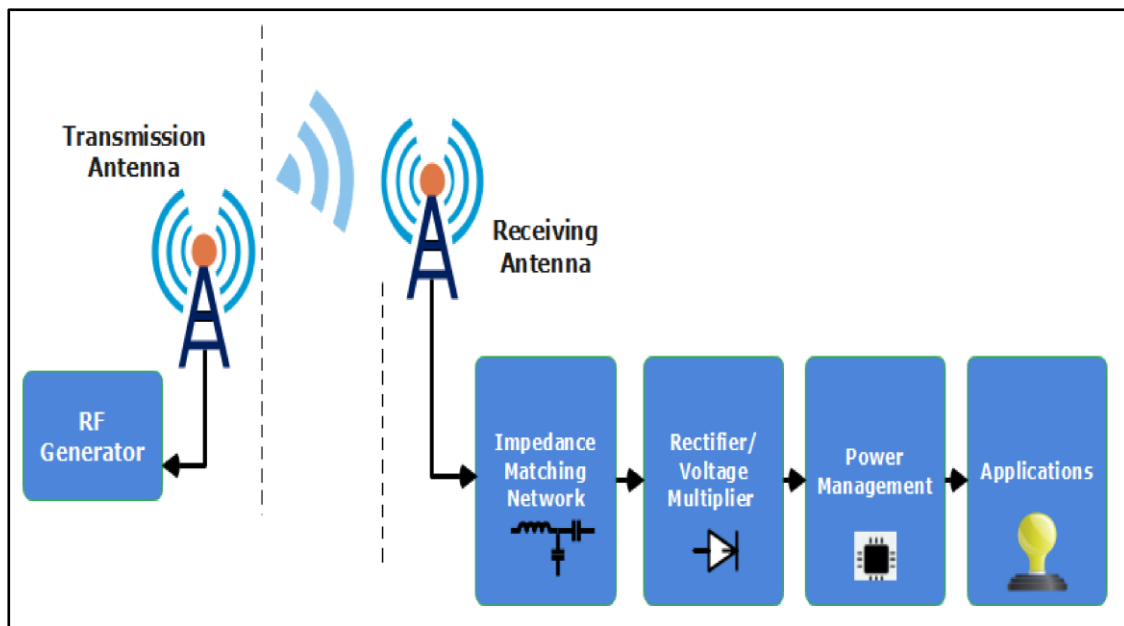


Fig.1.1: Schematic block diagram of RF energy harvesting [11].

It is becoming more possible to achieve battery less function for medical applications by collecting energy from sound wave, renewable energy, heating, and radio-frequency (RF) sources, When it comes to biomedical devices, RF energy harvesting is one of these methods that

demonstrates the most promise when other sources are insufficient. Additional uses for RF energy harvesting are in Internet of Things applications and the Radio Frequency Identification (RFID) system. Many of these applications take advantage of the widely-used Bluetooth low-energy (BLE) and WiFi connection protocols. Improvements in the design of very low power circuits and systems, together with wirelessly driven neural medical implants for nerve recording and stimulation, further enable these applications [12]-[15].

For radio frequency (RF) energy harvesting applications, one of the integrated circuit, or IC, design aims is to create highly efficient energy harvesting circuits throughout a wide input power scale in order to maximize the output power. Often, it also has to sustain the minimum desired input level of power in order to keep the system functioning correctly. New design techniques and analysis for underlying circuit designs have been made possible by these circuit and system design approaches [16]-[18].

The majority of the aforementioned applications make use of RF to rectifier characteristics; however, they frequently additionally need to solve issues specific to their application. Higher levels of on-chip integration are needed for a number of applications, such as n-IMD, in order to maintain compact device sizes for reduced costs, less invasiveness, and longer lifespans [19]-[21].

The ideal powering frequency rises as the energy harvester and matching network's sizes decrease. This work compares the performance of compact single-stage rectifiers for ambient RF energy harvesting, shows the tradeoffs so the user can find out the best choice of rectifier circuit based on his own application, and conditions [22].

1.2 Literature review

In 2016, Choi S. et al., A conventional rectifier's band-pass filter (BPF) is substituted with an open-ended composite right/left-handed (CRLH) transmission line (TL) stub that is used to create metamaterials. This stub is smaller than the standard BPF and is meant to match the fundamental frequency to a 50-ohm impedance while suppressing second and third order harmonics. The electronic device's implementation employs lumped components and a microstrip line. At 50 mW of input power and 1.8 kV of load, the rectifier suggested can achieve a maximum RF-to-DC conversion efficiency of 69.9% [23].

In 2017, Hsu C. et al., created a quad-band rectifier with the ability to capture 1.8 GHz Global System Mobile (GSM), 2.4 GHz Wi-Fi, 3.6 GHz Long Term Evolution (LTE), and 1.3 GHz L-band frequencies [24].

In 2018, Gozel MA et al. presented a 180-degree hybrid ring (rat-race) coupler where the passive RF/microwave circuit was coupled with the Greinacher full-wave rectifier circuit design. The rectifier circuit designed using a rat-race coupler and featuring a 125 MHz bandwidth at 1850 MHz Centre frequency, provided a power conversion efficiency (PCE) of 71% at 4.7 dBm input power. Furthermore, a 40% PCE value was attained with this investigation at -15 dBm input power, which was a quite low power level [25].

In 2018, Chandravanshi S. et al, a triple-band rectifier operating at 2.1 GHz Universal Mobile Telecommunication System (UMTS), 2.45 GHz WirelessLAN (WLAN), and 3.5 GHz WiMAX was suggested in [26].

In 2019, Wu P. et al., The suggested structure has a broad stopband DC-pass filter and a compact broadband low-loss matching network that

together provide a high conversion efficiency across a large frequency range. The matching network's three transmission line segments were carefully chosen and designed to have low loss and compact dimensions. The suggested DC-pass filter is also small and efficient in blocking broadband radio frequency signals and their high order harmonics within the band. A simulations and theoretical study of the suggested structure is performed. A working prototype was created, showing a broadband bandwidth of 41.5% (2.0-3.05 GHz) with an input power of 10 dBm and an RF-DC power conversion efficiency greater than 70%. When the input power drops to 0 dBm, the observed efficiency stays over 45% within the frequency range of 1.9-3.05 GHz. At 14 dBm input power, the maximum measured efficiency is 75.8% [27].

In 2020, Wu S. et al., In this study, a unique low-input power single-branch wideband rectifier architecture is proposed. Wideband impedance matching makes use of both an impedance-tuning component and a dual-band matching network. The suggested wideband rectifier is theoretically analyzed, and its closed-form design equations are obtained. A wideband rectifier is developed and constructed as an example. According to experimental findings, the manufactured rectifier has a low input power level of between -5.0 dBm and 5 dBm and a broad operating fractional bandwidth of more than 50% [28].

In 2020, He Z. and Liu C., to achieve high radio frequency (RF) to dc conversion efficiency, a unique broadband impedance-matching network is used in the suggested structure. Impedance transformation from three microstrip line segments reduces mismatching loss over a large bandwidth and input power range, resulting in a compact design to provide broadband impedance matching. The suggested rectifier is

examined theoretically and is simulated. A broadband rectifier that operates between 2.1 and 3.3 GHz is put into practice and evaluated for validation. With an input power of 14 dBm, the suggested rectifier demonstrates a bandwidth of 44.4% and an efficiency of over 70%. From 2 to 3.3 GHz, the observed efficiency stays over 50% when the input power is between 4 and 16 dBm [29].

In 2020, Muhammad et al. proposed a transmission line rectifier using an HSMS2850 diode and operating at 0.9 GHz. For 0 dBm input power, the suggested RFEH rectifier achieves simulated and measured RF-to-dc (RF to direct current) power conversion efficiency (PCE) of 43.6% and 44.3%, respectively. Furthermore, the rectifier is able to detect low input power at -20 dBm and achieved 3.1 V DC output voltage across a 2 k Ω load terminal for 14 dBm [30].

In 2021, Surender D. et al., A Schottky diode with two frequency bands selected for rectification is the HSMS2860. Rectangular stubs associated to the rectifier circuit and microstrip transmission lines allow for adequate impedance matching. For 5 dBm input power, the suggested rectifier circuit provides a maximum power conversion efficiency (PCE) of 54.53% and 41.26% for 3.5 and 5.8 GHz frequencies, respectively. At two frequencies, the output voltages are 1.31 V and 1.16 V, respectively [31].

In 2021, Muhammad S. et al., at 1.8 GHz Global System Mobile (GSM), 2.1 GHz Universal Mobile Telecommunication System (UMTS), 2.4 GHz Wi-Fi, and 2.6 GHz Long Term Evolution (LTE) bands, another quad-band rectifier is in operation [32].

In 2021, Ismail and Abd proposed an approach to increase the power conversion efficiency (PCE) and attained 42% efficiency at -10 dBm input power using a reversed L-type matching impedance approach. The rectifier circuit uses a voltage doubler-type architecture and only has two circuit components: a Schottky diode and a capacitor. These components can both receive a 2.45 GHz Wi-Fi input signal from a harvester antenna. Based on a coplanar waveguide feed, the antenna design is a rectangular patch antenna [33].

In 2021, Pinto et al. described a 2.45 GHz rectifier with a 7-stage Villard voltage doubler and a boost circuit. The output voltage was 0.204 V before the boost circuit. The boost circuit generated an output value of 3.3 V. The design and performance assessment of a Wi-Fi energy harvester are the main topics of this research. The technique of absorbing and transforming ambient energy into useful electrical energy is known as energy harvesting. Here, the purpose of the Wi-Fi energy harvester is to extract energy from Wi-Fi signals and transform it into electrical energy so that low-power gadgets may be powered [34].

In 2021, Narayanan and Thangavel proposed a 2.45 GHz rectenna with a rectifier created by a Cockcroft-Walton voltage doubler. The circuit for the Cockcroft-Waltons voltage doubler rectifier is developed and constructed using an L-type microstrip line impedance matching network. The measured findings show that at 2.45 GHz and 2 K load resistance, the suggested rectifier circuit obtained the highest RF to DC conversion efficiency of 45%. With an input power of +10 dBm, the rectenna's DC output voltage is 1.5 V [35].

In 2021, Coskuner et al. achieved a 45% conversion efficiency at 10 dBm input power. Using a metamaterial matching impedance circuit (IMN)

operating at 2.4 GHz and 5 GHz, they presented a rectifier with an input power of -30 dBm and an efficiency of 22% and 12% at corresponding frequencies. They draw the conclusion that metamaterial transmission lines provide for more design flexibility and enable matching of impedance over several bands. [36].

In 2021, Yusoff et al.'s have used Advanced Design System (ADS) software for the GSM 900 and 1800 MHz bands was presented. An impedance-matching network (IMN) and a voltage multiplier circuit (double rectifier) make up the RFEH system. Inductors and capacitors are examples of passive parts found in conventional IMNs. However, because of the peculiar behavior of their material, these components deteriorate at high RF. The voltage multiplier circuit's output DC power is maximized by the IMN based distributed element arrangement, often referred to as stubbing configuration, which improves the overall performance of the RFEH circuit. With an optimal load of 25 k Ω and a low input RF power of -10 dBm, the proposed RFEH circuit achieves maximum efficiency for RF-DC conversion at 43.514% and 25.985% for the 950 MHz and 1850 MHz bands, respectively [37].

In 2021, Li et al claimed power conversion efficiencies (PCEs) of 43.51% and 25.98% for the 950 MHz and 1850 MHz bands, respectively. A stepping impedance stub-matched network is used to increase circuit efficiency in rectifiers that operate at 2.45 GHz and 915 MHz. The suggested rectifier, according to the author, has the benefits of a high frequency ratio, a straightforward design, and a small dimension [38].

In 2022, a new study presents a rectifier circuit for RFEH applications that is based on a tuned matching circuit. By adjusting the inductor's value in the matching network, the rectifier circuit's design may be used

to pick a broad variety of operating frequency bands. A rectifier has been constructed, tested, and designed at 2.45 GHz for validation purposes. Peak power conversion efficiency (PCE) of 64.5% was attained by the rectifier at 0 dBm. In the range of -8.5–2 dBm input power, the PCE is more than 50% [39].

In 2022, a rectifier circuit with a shunt-diode rectifier is used. At an input power level of 5.75 dBm, the power conversion efficiency attained at the frequency of operation is 72.5% [40].

In 2022, Surender D. et al., with a minimum conversion efficiency of 60% inside the operational bands at 0 dBm input power, a single diode series-connected rectifier has been chosen to perform efficiently throughout a wide range of input power levels from -10 dBm to 5 dBm. The output voltage of the rectenna system is 1.123 V when tested experimentally at 2.45 GHz frequency [41].

In 2022, Halimi MA. et al., A rectenna system's essential component, the rectifier, transforms radiofrequency radiation into direct current (dc). A unique matching approach and single series diode architecture for a suggested triple-band rectifier presented. In order to concurrently convert multiple RF signals into dc, at first a single band rectifier constructed then modified it into a dual- and triple-band rectifier by adding the required transmission line and shorted stub, respectively. Using a single impedance matching circuit, the suggested rectifier runs in the popular frequency bands of 1.95, 2.7, and 5.8 GHz with power conversion efficiency (PCE) of 65.5%, 62%, and 57.1%, respectively [42].

In 2022, Surender D. et al., This article presents a broadband rectenna that is circularly polarized (CP) so that radio frequency (RF) energy may

be harvested from the surrounding environment by sensing nodes connected in smart cities. At 11 dBm input power, the highest predicted and observed conversion efficiencies are 65.2% and 66.6%, respectively [43].

In 2022, Mansour I. et al., This paper proposes a broadband RF-rectifier with a wide range of RF input power levels using FR-4 substrate. The two sections of the RF-rectifier circuit are configured using a modified L-section matching network (MN) through a series impedance transformer. A wideband resistance compression network (RCN) is utilized to accomplish the distinct RF-rectifier design approach. The method enhances the matching capability of the circuit over a broader range of the available input RF signals and frequency. From 1.780 to 2.620 GHz and 1.780 to 2.610 GHz, respectively, the suggested RF-rectifier attained a fractional percentage bandwidth (FBW) of 38.5% and 38% in simulation and measurement, respectively. The suggested RF harvester may achieve maximum measured RF-to-DC PCE and output DC voltage (V_{dc}) of 75.5% and 3.2 V, respectively [44].

In 2023, Halimi MA. et al., For use in microwave power transmission and radiofrequency energy harvesting, a dual-band rectifier is proposed. Beginning with a single-band rectifier, the matching network's half-wavelength transmission line is used to add the second band. Power conversion is accomplished by utilizing an HSMS-2860 Schottky diode in a series diode architecture. With power conversion efficiency (PCE) of 54.9% and 42.3%, respectively, and output voltages of 1.4 and 1.242 V at 0-dBm input power for the 3.5-GHz 5G band and the 5.8-GHz Wi-Fi band, the rectifier concurrently harvests the RF energy [45].

In 2023, Wang C. et al., a quad-band rectifier with Global System Mobile dual (GSM) (0.9, 1.8 GHz) and Industrial Scientific Medical dual (ISM) (2.45, 5.8 GHz) bands of operation was suggested in [46].

In 2023, Surender D. et al., For the aim of RF-to-DC conversion, a broadband rectifier circuit (4.67-7.0 GHz) with a staircase-type multiple-stage transmission line matching circuit spanning all resonant frequencies in different facet-loaded antenna topologies is suggested. At 13.5 dBm input power level, the rectifier achieves a maximum power conversion efficiency (PCE) of 77.3%, with a matching output voltage of 4.92V [47].

In 2023, Muhammad S. et al, This study presents a large DC voltage radio frequency (RF) voltage doubler rectifier for energy harvesting (EH) systems using ROG4003C material and Schottky diode, together with a wideband, considerable RF-DC conversion efficiency. A series resonance circuit and the π network are used in the construction of the input matching network. There are two designed wideband rectifiers. In the first design, distributed rectangular inductors are used, whereas lumped inductors in the π network are used in the second. A rectifier prototype based on HSMS2852 is evaluated for verification. The results show that the rectifier prototype has an input power of 3 dBm, a peak saturated DC voltage of 3.6 V, an input return loss (S11) of under -10 dB, and a bandwidth of 31.6% from 720 to 1050 MHz with $68 \pm 2\%$ [48].

1.3 Aims of the thesis

The aim of this work is to investigate the performance comparison between different rectifier circuits for RF energy harvesting systems. The primary objective is to design and optimize the rectifier circuits using various types of rectifier circuits for different resistance loads, HSMS282X diodes, and standard substrate materials that represent ϵ_r .

The thesis will also explore the potential applications of the proposed energy harvesting system, including wireless sensor networks. The research will involve theoretical analysis and simulation.

Ultimately, the goal of this thesis is to contribute to the development of efficient and reliable energy harvesting technologies for wireless applications. These aims will be achieved by:

- 1- Conducting comparative study of the output voltage and conversion efficiency of different rectifier circuits with varying input power.
- 2- Compare the rectifier circuits at frequency 2.4 GHz by examining the output voltage efficiency to determine which circuit has the highest efficiency and select the best one among them.
- 3- Designing a suitable matching network consists of both the LC-match method and the TL-match method between the source and the rectifier circuit to improve the system performance and reduce the reflections that lead to losses in power.

1.4 Thesis Layout

The chapters of the thesis are presented as follows:

- The first chapter discussed the introduction and literature review of RF energy harvesting devices in terms of rectifier circuits.
- The second chapter included reviews on introduction to Rectifier Circuits for RF Energy Harvesting, discussion on Wireless Power Transfer (WPT) and highlights on the characteristics of rectifier.
- The third chapter discussed the simulation methodology of different rectifier circuits where the efficiency and output voltage

with varying input power are recorded for all circuits at operating frequency of 2.4 GHz with LC- match circuit.

- The fourth chapter focused on a comparison between all the rectifier circuits at 2.4 GHz with LC-match method and TL-match method.
- The fifth chapter presented the conclusion of this work and the suggested future works.

CHAPTER TWO

THEORETICAL BACKGROUND

2.1 Introduction

Rectifier circuits play a crucial role in the field of RF energy harvesting, enabling the conversion of radio frequency (RF) signals into usable direct current (DC) power. These circuits are essential for powering low-power electronic devices and sensors in various applications, including wireless sensor networks, Internet of Things (IOT) devices, and wearable electronics. In RF energy harvesting, rectifier circuits extract energy from ambient RF signals, which are omnipresent in our environment due to the proliferation of wireless communication systems [61].

Fig.2.1 illustrates the three broad kinds of RF power sources surrounding us: internal sources, predicted ambient sources, and unknown ambient sources [49].

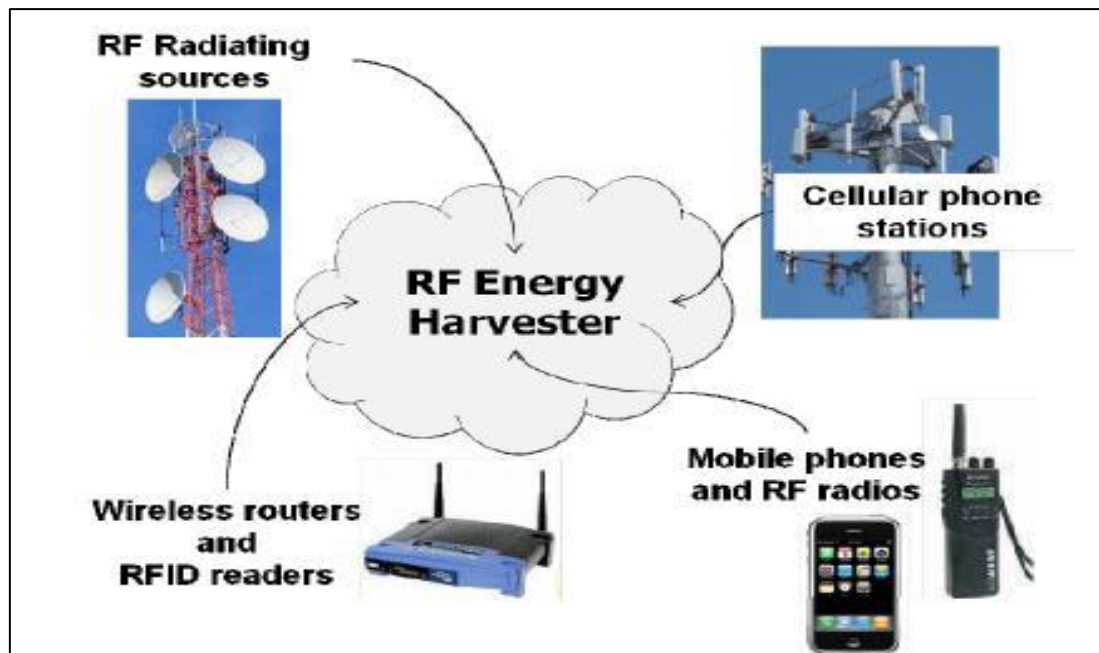


Fig.2.1: RF Energy Sources [49].

There are several types of rectifier circuits commonly used in RF energy harvesting, each with its own advantages and limitations. Each of these rectifier circuits possesses unique characteristics and performance trade-offs, making them suitable for different RF energy harvesting scenarios. The choice of rectifier circuit depends on factors such as the available RF power, desired output voltage, efficiency requirements, and cost considerations.

2.2 Wireless Power Transfer (WPT)

Wireless Power Transfer (WPT) is a revolutionary technology that enables the transmission of electrical power from a power source to an electronic device or system without the need for physical connections. It is a solution to the challenges that offer a promise posed by traditional wired power transmission, providing convenience, flexibility, and improved safety in various applications. This technology is widely used in many different applications, including powerful electric vehicles [50]-[51].

WPT operates on the principle of electromagnetic induction or electromagnetic resonance. The power transfer process involves two main components: a transmitter and a receiver. The transmitter generates an alternating current (AC) or radio frequency (RF) signal, which is then converted into an electromagnetic field. The receiver, equipped with a compatible receiver coil, captures the electromagnetic field and converts it back into electrical energy to power the device [52]-[53].

2.3 Rectifier Characteristics

Rectifiers, regardless of their specific type or configuration, exhibit certain common characteristics. These characteristics define their behavior and performance in converting AC (alternating current) input to DC (direct current) output. Here are some key characteristics of rectifiers:

1- Rectification: The primary function of a rectifier is to convert AC voltage into DC voltage. Rectification is the process by which the rectifier allows the flow of current in only one direction, blocking the opposite direction.

2- Ripple Voltage: Ripple voltage refers to the fluctuation or variation in the DC output voltage of a rectifier. It is caused by the residual AC component present in the rectified output. Ripple voltage is typically expressed as a percentage of the peak-to-peak voltage or as a fraction of the DC output voltage. Lower ripple voltage indicates a smoother and more stable DC output.

3- Efficiency: Rectifier efficiency is a measure of how effectively the rectifier converts AC power to DC power. It is defined as the ratio of DC output power to the AC input power, typically expressed as a percentage. Higher efficiency indicates less power loss during the rectification process, resulting in more efficient utilization of the input power.

Moreover, the Power Conversion Efficiency is calculated from Eq. (1).

$$\text{PCE} = \frac{P_{out}}{P_{in}} \times 100(\%) \quad (2.1)$$

Where the V_{out} refers to output voltage, R_L represents the load resistance and P_{in} stand for the input power in dBm (Decibel milliwatts).

2.4 Rectifier Circuits

Rectifier circuits are essential components in converting (AC) to (DC) in various electronic applications. This section provides an overview of different rectifier circuits, including half-wave rectifiers, full-wave rectifiers, voltage doublers, Villard charge pumps, Graetz charge pumps, and Dickson charge pumps. The review discusses their topology, working principles, advantages, and limitations.

2.4.1. Half-Wave Rectifiers:

Half-wave rectifiers utilize a single diode to convert the positive or negative half-cycle of an AC input into a pulsating DC output. While they are simple and cost-effective, half-wave rectifiers suffer from low efficiency and produce high ripple voltage. Although a full-wave rectifier requires more diodes than a half-wave rectifier, it performs better than the latter [50]. Fig.2.2, depict circuit for half-wave rectifier.

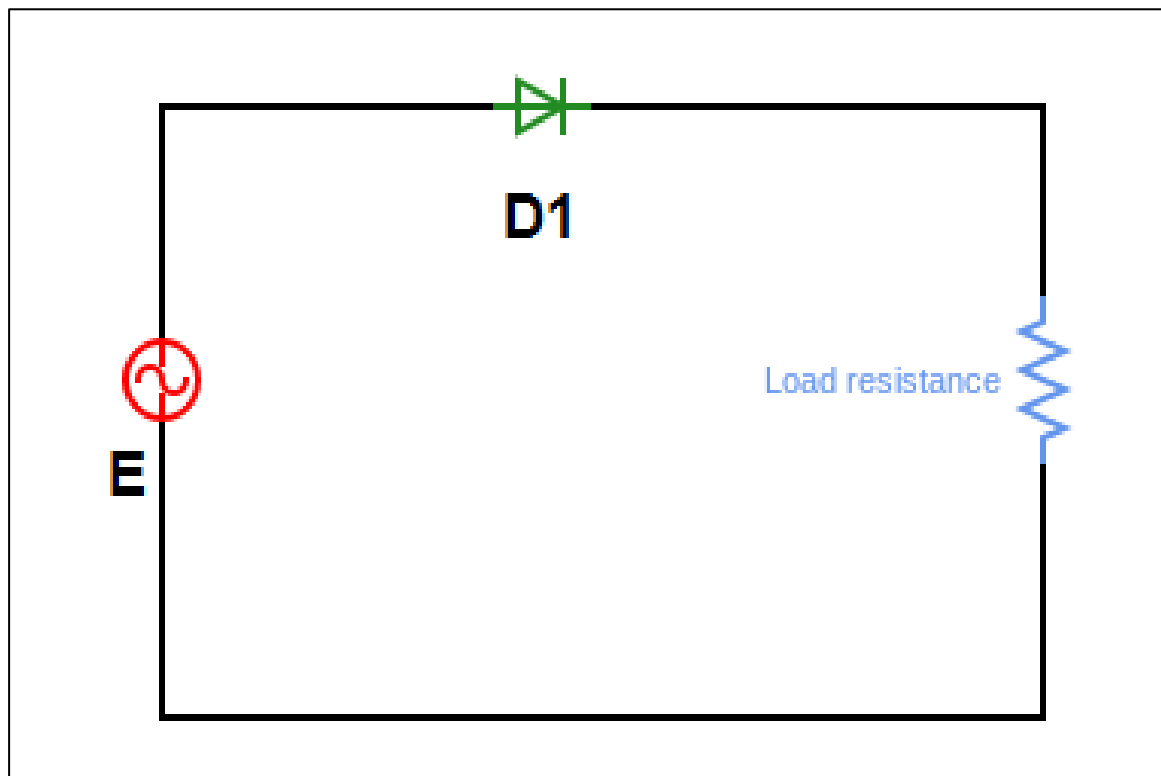


Fig.2.2: Half-Wave Rectifier circuit [54].

2.4.2. Full-Wave Rectifiers:

Full-wave rectifiers are further classified into center-tapped and bridge rectifiers. Fig.2.3, depicts circuit for full-wave rectifier [54].

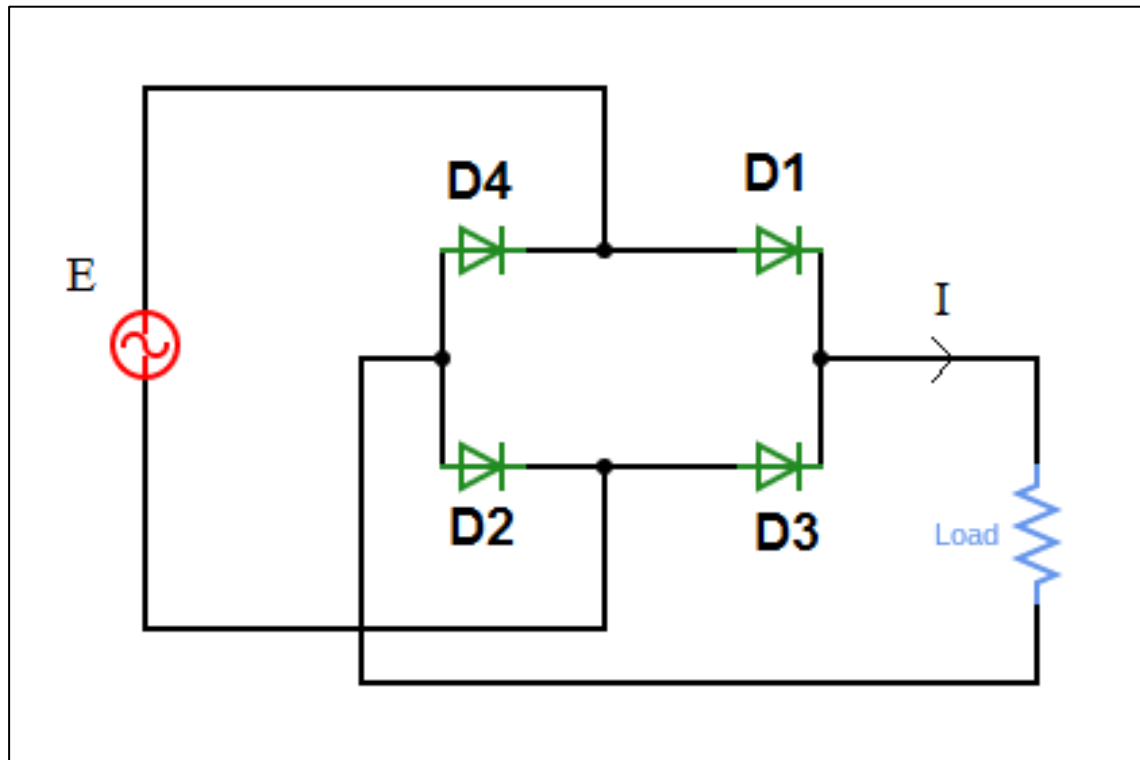


Fig.2.3: Full-Wave Rectifier circuit [54].

2.4.2.1 Center-Tapped Rectifiers:

Center-tapped rectifiers use a center-tapped transformer and two diodes to convert both positive and negative half-cycles of the AC input. These rectifiers provide improved efficiency compared to half-wave rectifiers but still exhibit ripple voltage.

2.4.2.2 Bridge Rectifiers:

Bridge rectifiers employ a bridge configuration consisting of four diodes to convert the complete AC input waveform into DC. They offer better efficiency and lower ripple voltage compared to half-wave and center-tapped rectifiers. The bridge rectifier topology is widely used due to its simplicity and effectiveness.

2.4.3. Voltage Doubler:

Voltage doublers are rectifier circuits that double the peak voltage of the AC input. They use capacitors and diodes to achieve this voltage multiplication. Voltage doublers are commonly used in low-power applications where a higher DC voltage is required. This circuit consists of two diodes, a charging capacitor, and a smoothing capacitor, as shown in Fig. 2.4 [55] [56].

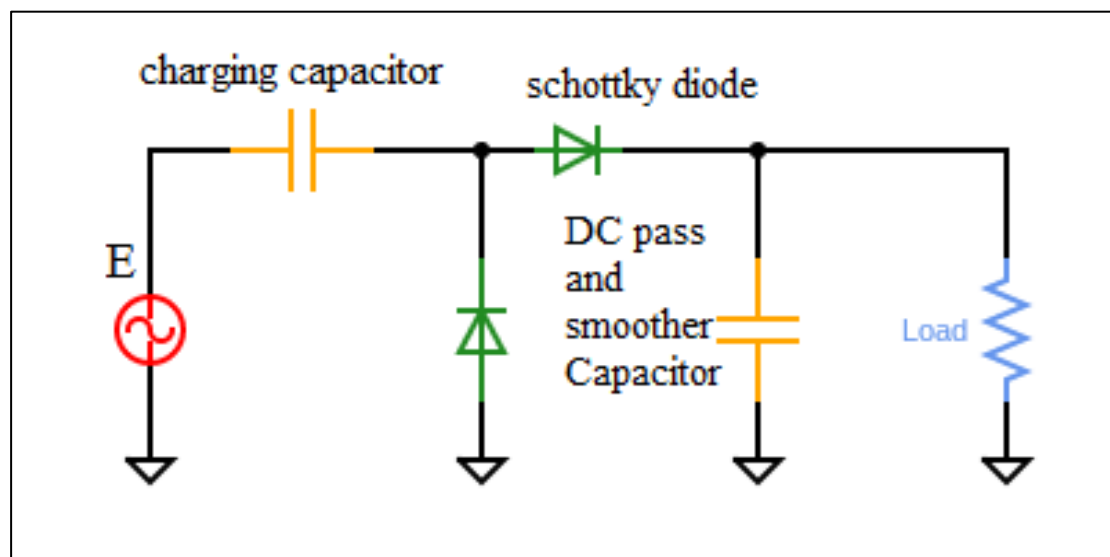


Fig. 2.4: Voltage doubler rectifier circuit diagram [55] [56].

2.4.4. Villard Charge Pump:

At this time, the Villard charge pump rectifier is employed, also known as the Villard cascade or Villard doubler. It is an electrical circuit used for rectifying and multiplying the voltage of an alternating current (AC) input signal. It was named after Paul Ulrich Villard. The Villard charge pump rectifier is a type of voltage multiplier circuit that can generate a DC voltage that is several times higher than the peak value of the AC input voltage. It is primarily used in applications where high-voltage DC is required, such as in certain types of power supplies, electrostatic generators, and X-ray machines. The basic configuration of the Villard charge pump rectifier consists of a series of diodes and capacitors connected in a cascade arrangement.

The Villard charge pump is a voltage multiplier circuit that uses a combination of capacitors and diodes to generate a higher DC voltage. It is an extension of the voltage doubler circuit and can achieve higher voltage multiplication factors. The Villard charge pump rectifier circuit diagram, as shown in Fig. 2.5 [57].

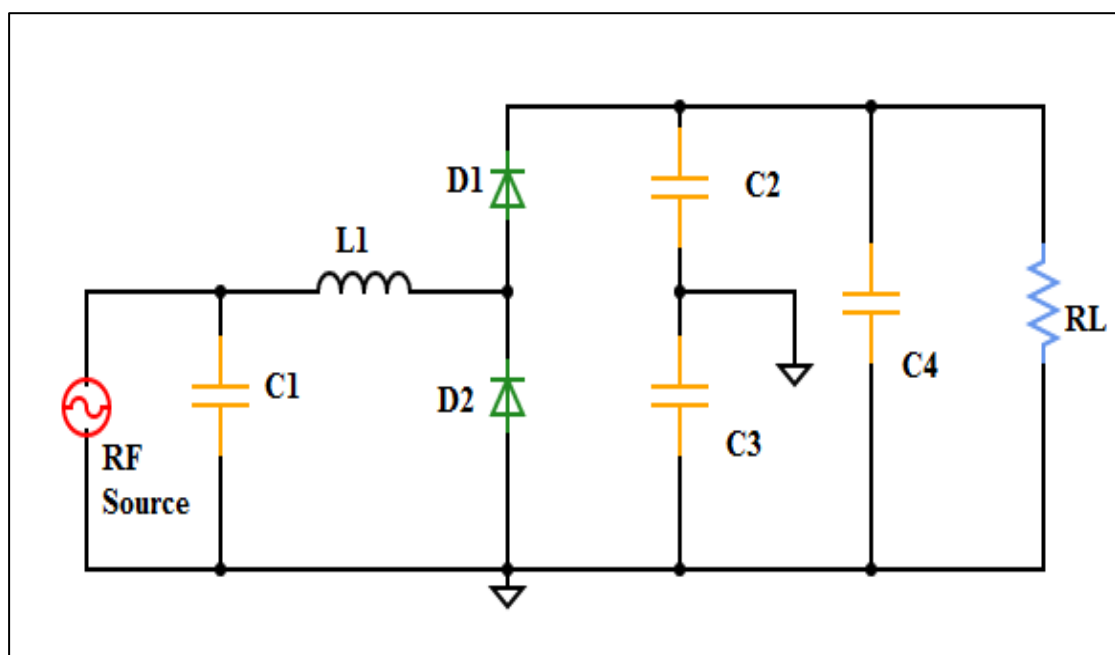


Fig. 2.5: Villard charge pump rectifier circuit diagram [57].

2.4.5. Graetz Charge Pump:

The Graetz charge pump, also known as a voltage doubler, is an electronic circuit used to generate a higher DC voltage from a lower DC voltage source. It is named after its inventor, Leo Graetz. The charge pump is a type of voltage multiplier circuit that utilizes diodes and capacitors to achieve voltage doubling. The basic configuration of a Graetz charge pump consists of four diodes and two capacitors arranged in a bridge-like structure. The input voltage is applied across the input terminals of the charge pump circuit. During the charging phase, the capacitors are charged in parallel with the input voltage. Then, during the pumping phase, the charge stored in the capacitors is pumped to the output terminals in series, effectively doubling the voltage.

The Graetz charge pump is a rectifier circuit that utilizes a combination of diodes and capacitors to convert AC input to DC voltage. It offers improved efficiency compared to traditional rectifiers by reducing diode conduction losses. Fig.2.6, demonstrates the circuit diagram of the Graetz charge pump rectifier [58].

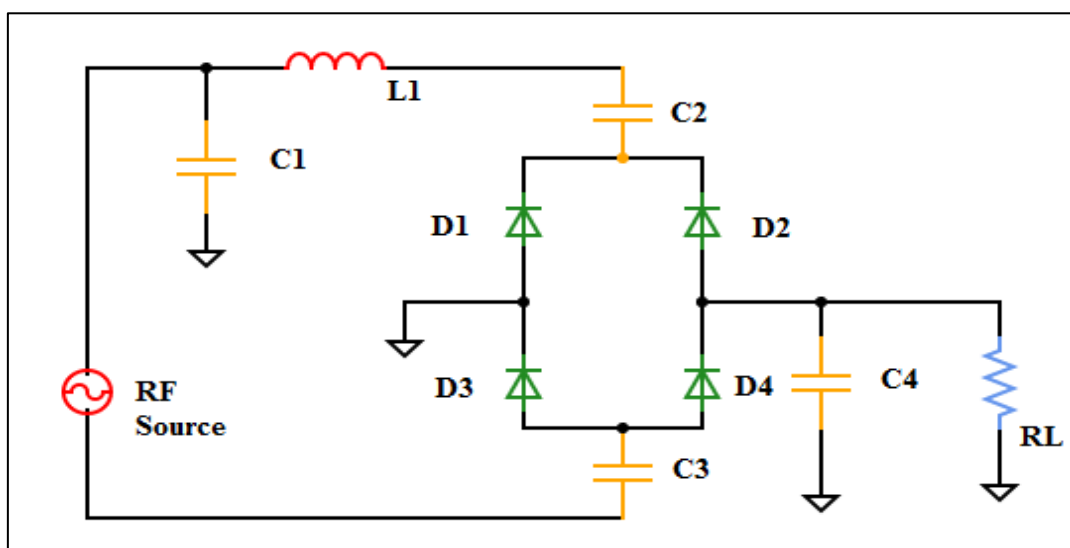


Fig. 2.6: Graetz charge pump rectifier circuit diagram [58].

Here is a step-by-step explanation of the operation of a Graetz charge pump:

1. **Charging Phase:** Initially, all the diodes in the circuit are reverse-biased, preventing any current flow. During this phase, the capacitors C1 and C2 get charged to the input voltage level through the diodes D1 and D2, respectively. The voltage across each capacitor is equal to the input voltage.

2. **Pumping Phase:** In this phase, the input voltage is removed, and the capacitors are connected in series with the help of the diodes D3 and D4. The diodes D1 and D2 are now forward-biased, while D3 and D4 are reverse-biased. The voltage across C1 and C2 adds up, resulting in a doubled voltage at the output terminals.

3. **Voltage Regulation:** The output voltage of the charge pump is dependent on the capacitance values and the load connected to it. The voltage across the capacitors decreases as the charge is pumped into the load. To maintain a stable output voltage, a feedback control mechanism or regulation circuitry may be employed.

2.4.6. Dickson Charge Pump:

The Dickson charge pump rectifier is another type of voltage multiplier circuit that is commonly used to generate a higher DC voltage from a lower AC voltage source. It is named after its inventor, J. M. Dickson. The Dickson charge pump rectifier is particularly useful in applications where a higher voltage is needed, such as in power management circuits and low-power electronics. The Dickson charge pump rectifier is based on the concept of cascading multiple stages of diode-capacitor voltage doublers. Each stage consists of a diode and a capacitor connected in

series. The output of one stage is connected to the input of the next stage, creating a cascaded arrangement.

One advantage of the Dickson charge pump rectifier is its scalability; by cascading multiple stages, the voltage multiplication factor can be increased. However, it is important to note that as the number of stages increases, the voltage drop across each diode also increases, leading to higher losses and decreased efficiency.

The Dickson charge pump, also known as a voltage multiplier, is a cascaded rectifier circuit that uses multiple capacitors and diodes to generate a higher DC voltage. It provides a compact and efficient solution for voltage multiplication.

The Fig.2.7, demonstrates the circuit diagram of the Dickson charge pump rectifier [59].

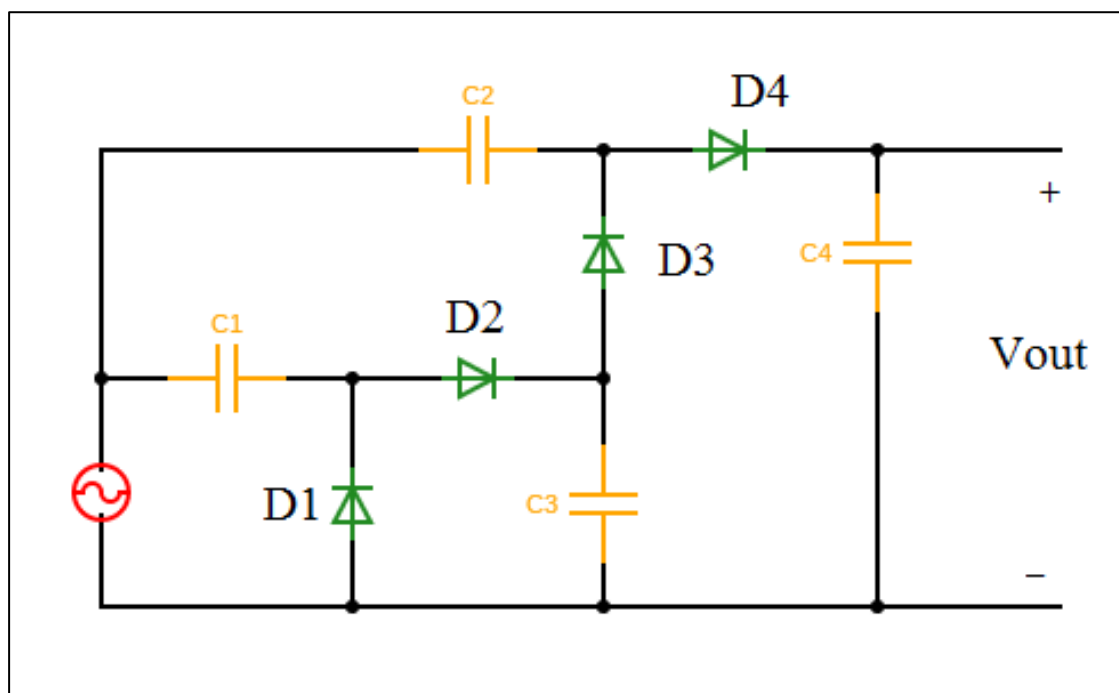


Fig. 2.7: Dickson charge pump rectifier circuit diagram [59].

CHAPTER THREE

Performance Analysis of Various Rectifier Circuits with the LC-Match Method

Half-wave, full-wave, voltage doubler, Villard charge pump, Graetz charge pump, and Dickson charge pump design and simulation are carried out at 2.4 GHz, using Advanced Design System (ADS) Software. Wireless Power Transfer (WPT) is a reliable method of transferring power from a source to an end system without the need of cables or connections. This task is performed by rectennas, which are antennas coupled with rectifiers. Undoubtedly, the rectifier which converts RF power received into DC power is the most important component of the rectenna. RF energy is taken in by the antenna and transferred to the matching circuit.

The antenna and rectifier's impedances will be matched using a LC-matching circuit, while the Schottky is utilized for rectification. It is worth mentioning that choosing the right diode is one of the most vital factors in designing rectifier circuits. The resistance load (R_L) is varied from 1 k Ω to 5 k Ω to investigate the impact of the load on the rectifier performance. Furthermore, the substrate dielectric constant (ϵ_r) variation was also studied as a case parameter. Several materials such as Rogers R04725JXR, Rogers R04534, FR-4, Porcelain, Rogers R03006 and Rubber with a 2.64, 3, 3.55, 4.3, 6 and 6.5, respectively, are used for comparison purposes with keeping the thickness of these substrates at 1.57 mm for all six types of rectifier circuits. Using the 2.4 GHz frequency range, the simulation results are recorded. These include DC output voltage in relation to input power and efficiency in relation to input power at various resistance loads, diodes, and substrate epsilon.

3.1 Impedance Matching Circuit using LC-match method

LC (Inductance and Capacitance)-Matching Method is employed in this work. This approach has four circuit configurations from which to choose, based on factors such as whether DC current passing is required or not, and which is higher the input or load resistance, as seen in Fig. 3.1 [60].

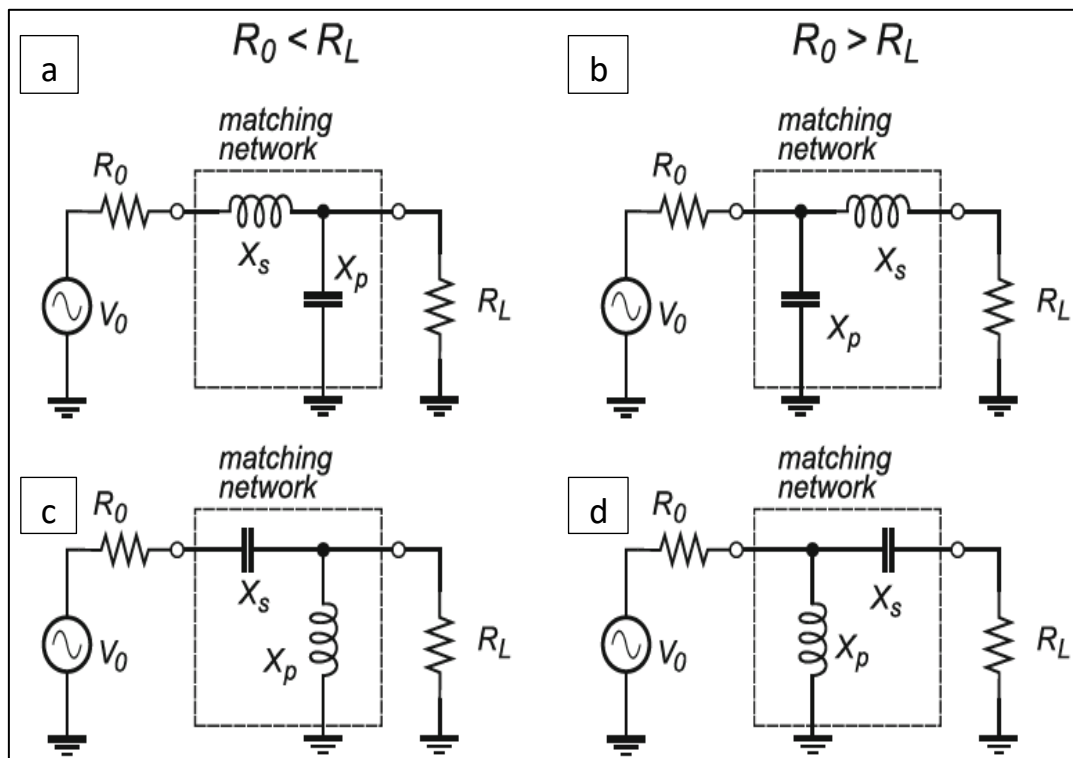


Fig.3.1: LC-Matching Method.

The common features of the LC-matching Method are:

- Q matching technique is employed to determine the LC-matching network.
- One of the drawbacks of this technique is its use of reactive components, meaning that the matching is possible at only one frequency.
- An LC section placed between two resistive terminations creates a serial subnetwork and a parallel subnetwork as shown in Fig.3.2.

When the two subnetworks are conjugate matched to each other, their Q factors are equal.

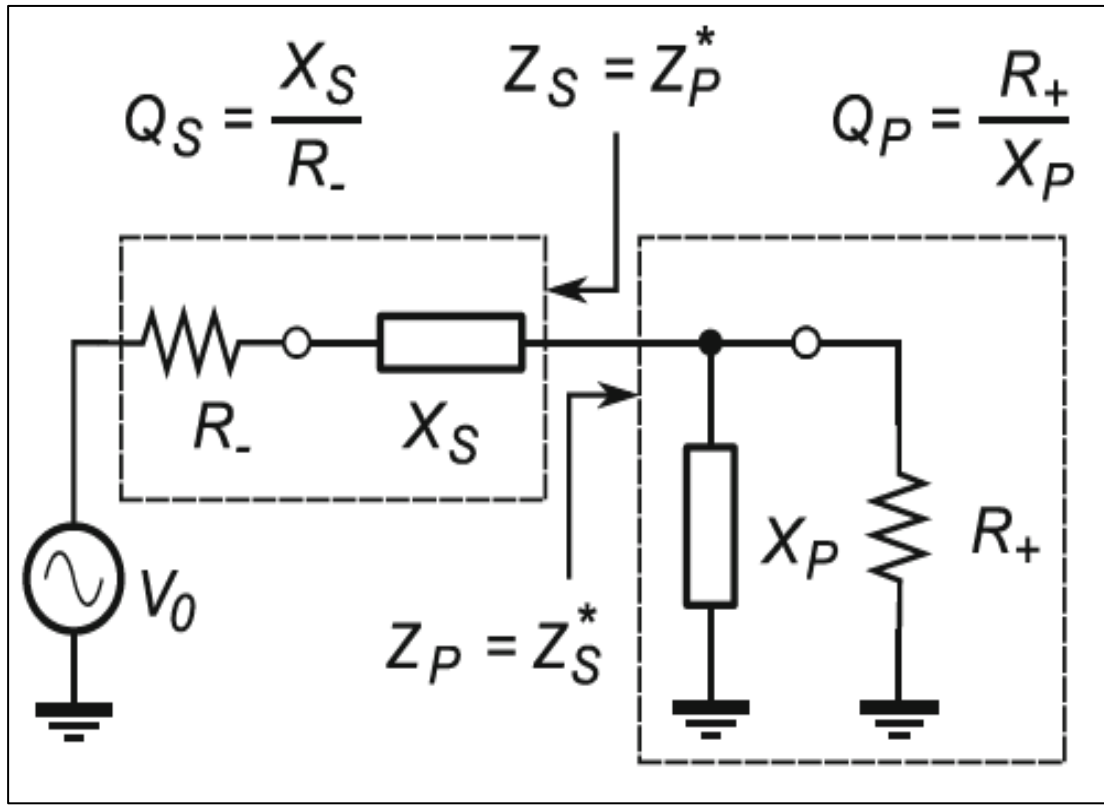


Fig.3.2: Equivalent Circuit for LC-Circuit [60].

Now, we will try to calculate the L and C values of the matching for the Half-wave rectifier at 2.4 GHz for a 50Ω source (R_+) representing the antenna. The first step is to calculate the input impedance using ADS software. The Half-wave circuit in Fig. 3.3 is simulated in ADS without using any matching method and the input impedance (Z_{in}) versus frequency is plotted as illustrated in Fig.3.4. The input impedance is recorded over the frequency range 2.34 GHz to 2.5 GHz and it is found that Z_{in} at 2.4 GHz is equal to $(6.391 - j64.235 \Omega)$.

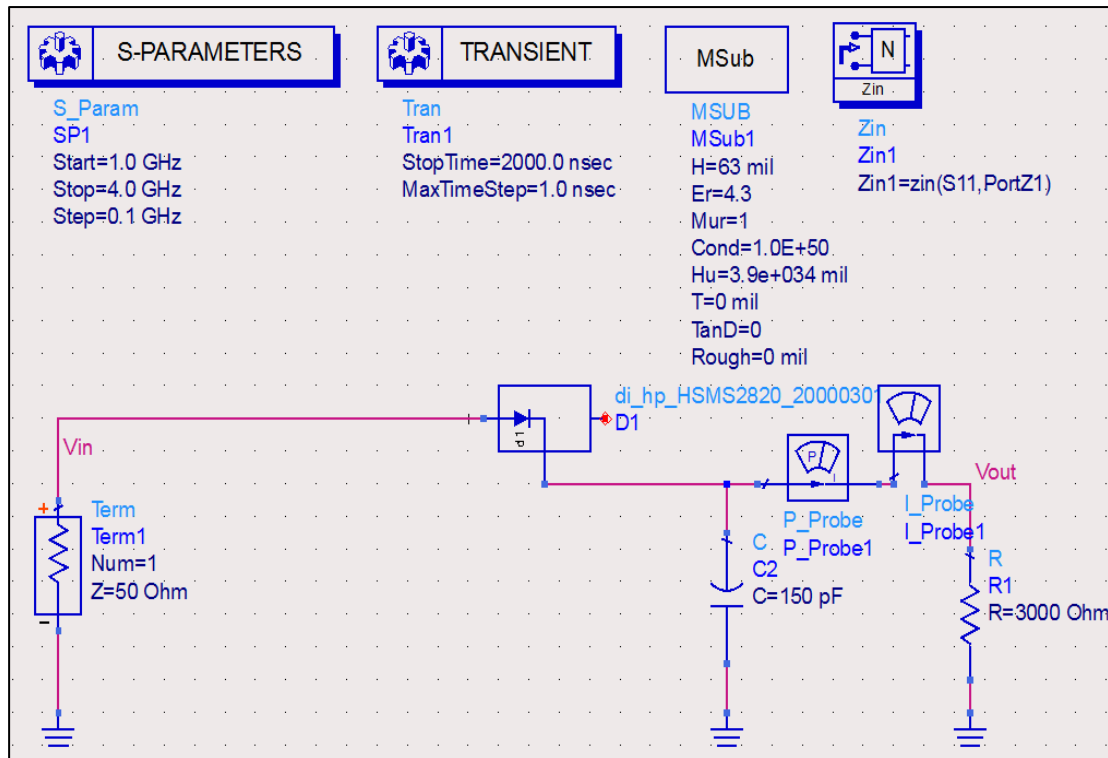


Fig. 3.3: Simulated circuit to find Zin for half-wave rectifier at frequency band 2.4 GHz.

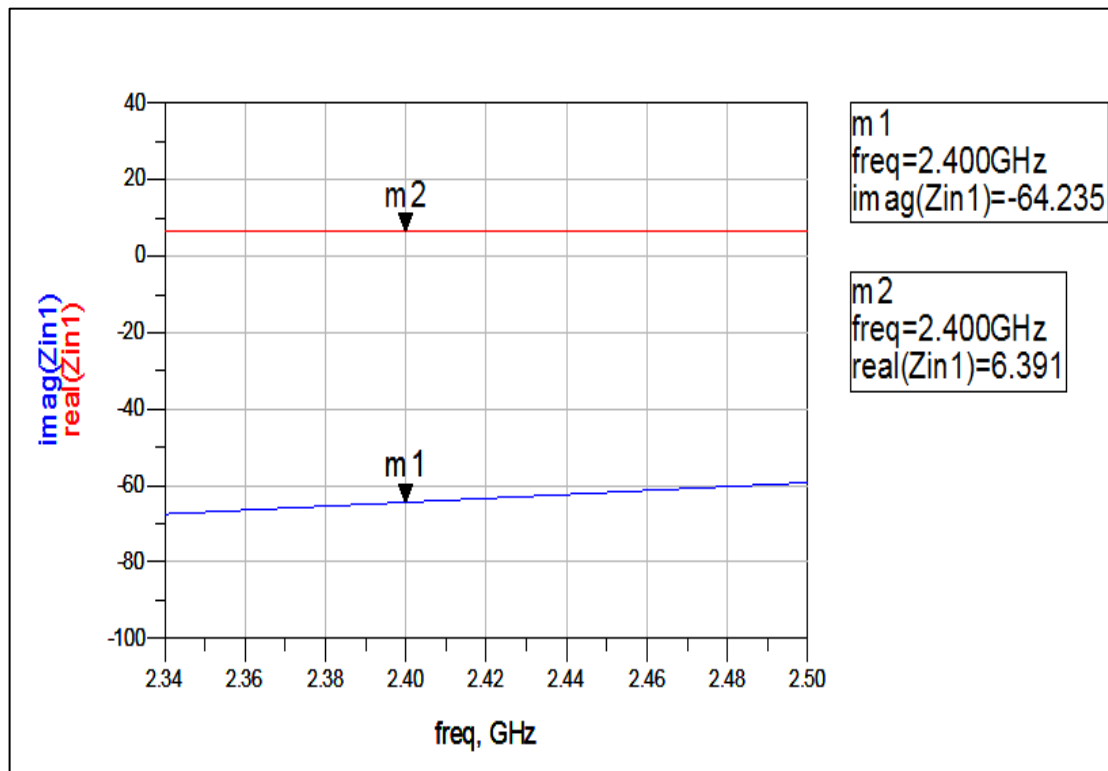


Fig. 3.4: Simulated value of Zin.

Fig.3.1-b will be adopted as a matching method in this thesis since it fulfills the conditions of the Half-wave rectifier used in this work.

Now, to compute the values of L and C of the matching method, use the following equations [60]:

$$Q_s = Q_p = \sqrt{\frac{R_+}{R_-} - 1} \quad (3.1)$$

And then:

$$Q_s = \frac{X_s}{R_-} \quad (3.2)$$

$$Q_p = \frac{R_+}{X_p} \quad (3.3)$$

where R_- is the source resistance, R_+ is the load resistance, Q_s is the Serial Q Factor and Q_p is the parallel Q Factor.

From the Eq. 3.2 and 3.3, the values of Q_s and Q_p can be calculated to be:

$$Q_s = Q_p = 2.612$$

$$Q_s = \frac{X_s}{R_-}$$

$$X_s = 2.612 \times 6.391 = 13.548$$

$$X_s = X_L = 2\pi fL \rightarrow 2 \times \pi \times 2.4 \times 10^9 \times L$$

$$L = \frac{13.548}{2 \times \pi \times 2.4 \times 10^9} = 0.89 \text{ nH}$$

$$Q_p = \frac{R_+}{X_p}$$

$$X_p = \frac{50}{2.612} = 19.142$$

$$X_p = X_C = \frac{1}{2\pi fC} \rightarrow 19.142 = \frac{1}{2 \times \pi \times 2.4 \times 10^9 \times C}$$

$$C = \frac{1}{2 \times \pi \times 2.4 \times 10^9 \times 19.142} = 3.4 \text{ pF}$$

The source impedance is pure resistance (50Ω) with no reactive component; hence, the parallel capacitance will have an additional value of 3.4 pF. Conversely, the series inductor's computed value for the load side is 0.89 nH. On the other hand, it is evident that the load, which is comparable to the rectifier's impedance ($6.391-j64.235 \Omega$), has a reactive portion ($+j64.235$) that has to be resonated out. An inductor with a value of $L=4.41$ nH can help achieve this. $L=0.89\text{nH}+4.41\text{nH}=5.3$ nH must be the total additional inductor provided to the circuit as a result.

3.2 Half-wave rectifier circuit using LC-match method

The calculated values of the matching network is implanted as shown in Fig. 3.5, where a single-stage half-wave rectifier is simulated using Advanced Design System (ADS). A power source, which in such systems is anticipated as the antenna component, is found in the employed circuit. The power source has an internal impedance of 50Ω and transmits RF power from 0 to 30 dBm at 2.4 GHz. The matching network circuit for the rectifier circuit, which consists of an LC-circuit, is chosen to match between the antenna and the rectifier.

Furthermore, HSMS-2820, HSMS-282B, and HSMS-282C diodes were used while keeping the resistance load at $3 \text{ k}\Omega$ and ϵ_r equals to 4.3, which contributes to rectifying the coming RF signal and transforming it from (AC) to (DC). In the next step, the resistance load is set to 1, 2, 3, 4, and 5 $\text{k}\Omega$, respectively, while keeping HSMS2820 diodes and ϵ_r equal to 4.3. Additionally, the output has a capacitance to smooth the DC output before it is fed to the load as DC power or stored in a battery, as illustrated in Fig. 3.5. In another simulation step, the FR-4 substrate was replaced another substrates having a dielectric constant of 2.64, 3, 3.55, 4.3, 6, and 6.5 that are set in the ϵ_r MSub block in ADS software and a

thickness of 1.6 mm that is set in the H MSub block, where 63 mil equals to 1.6 mm. The matching network has done the job perfectly, where excellent matching is achieved, as shown in the S-parameters curve in Fig. 3.6.

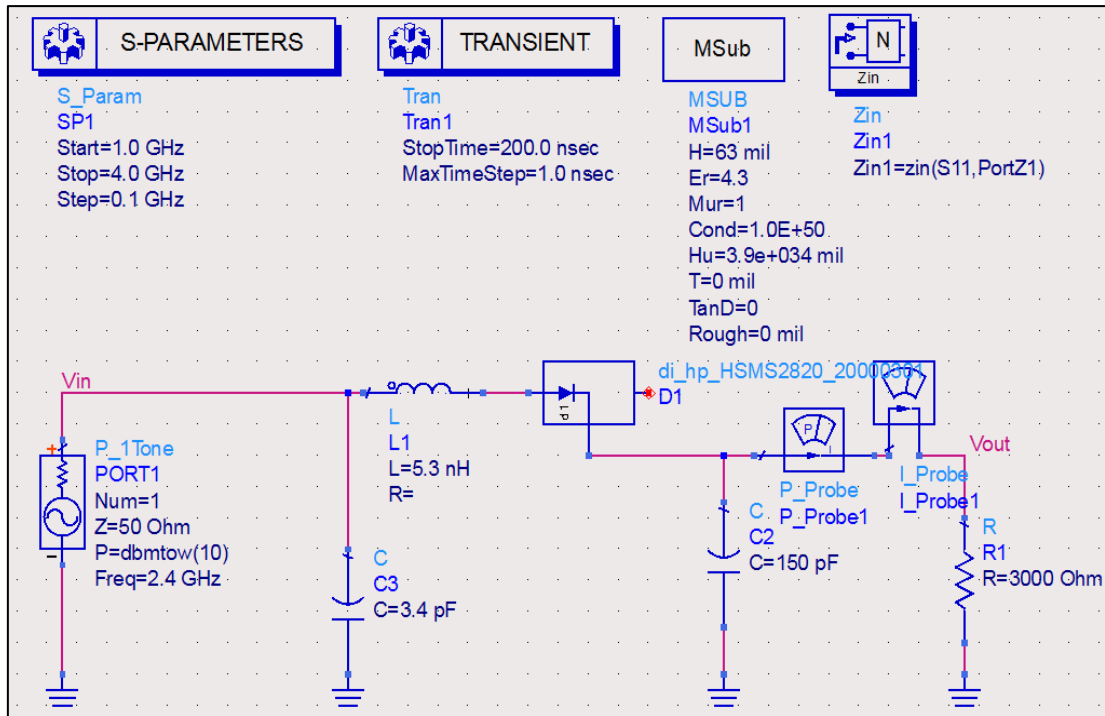


Fig. 3.5: Half-wave rectifier circuit operating at 2.4 GHz with LC-circuit.

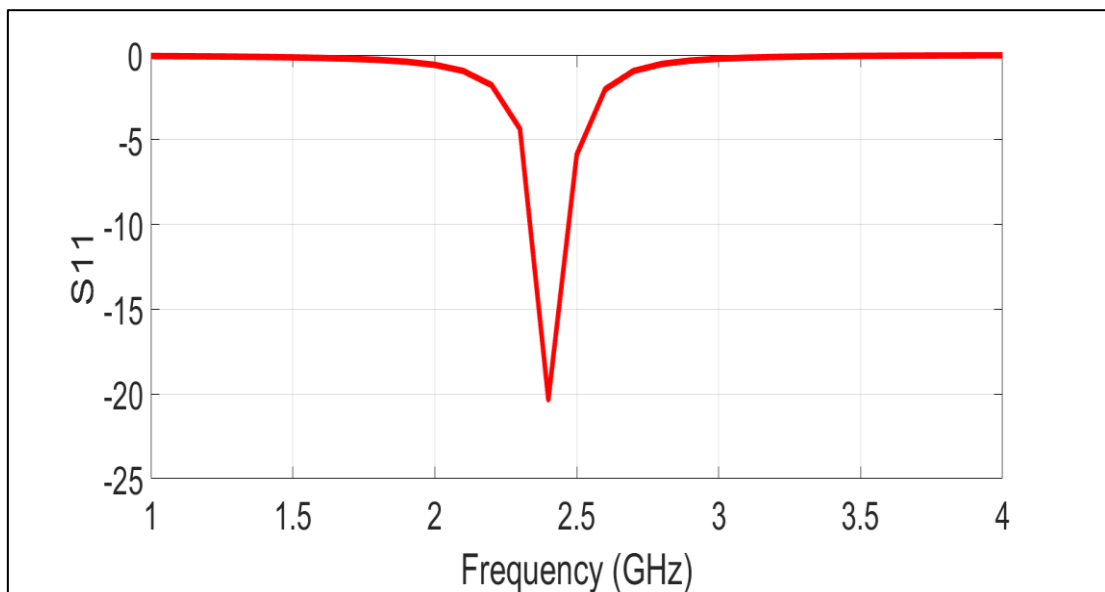


Fig. 3.6: Simulated S11 of half-wave rectifier circuit at 2.4 GHz with LC-circuit.

Fig. 3.7 displays the input voltage waveform that is fed to the half-wave rectifier circuit in the 2.4 GHz frequency band with an LC-circuit, which is simulated by ADS Software.

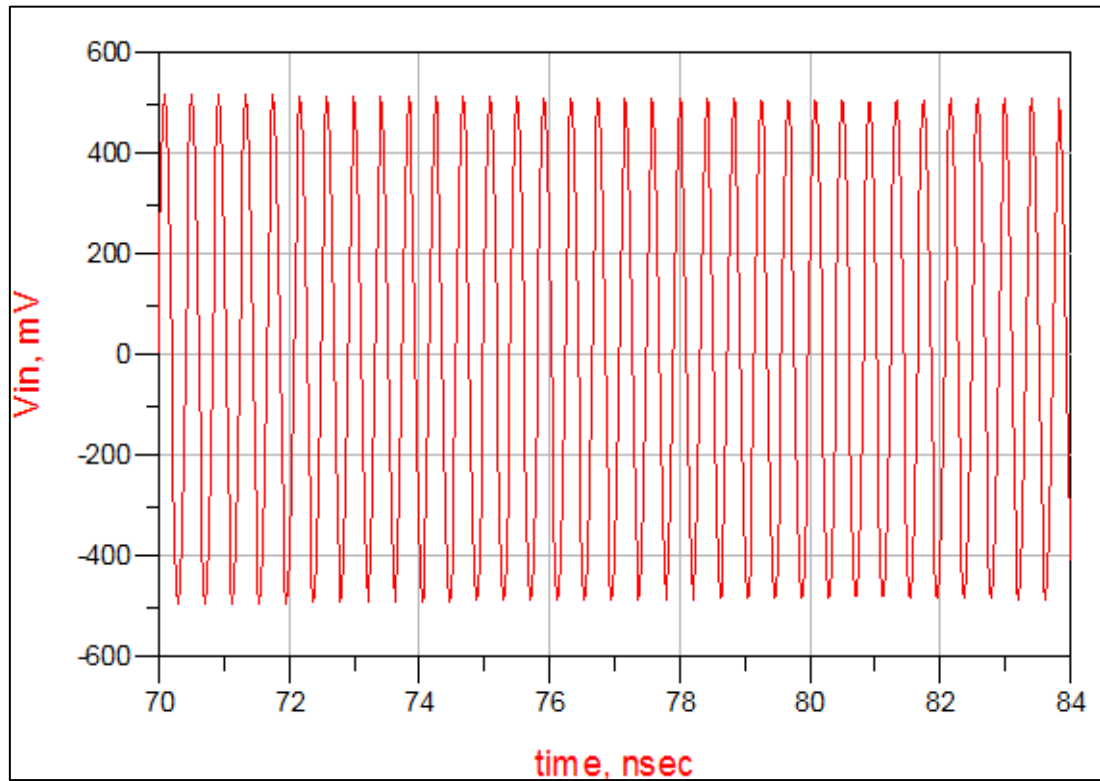


Fig. 3.7: V_{in} (V) of half-wave rectifier circuit at 2.4 GHz with LC-circuit.

Fig. 3.8 illustrates the output voltage waveform for a half-wave rectifier circuit at 2.4 GHz. The achieved DC output voltage is around 1.2 V, as shown in Fig. 3.8.

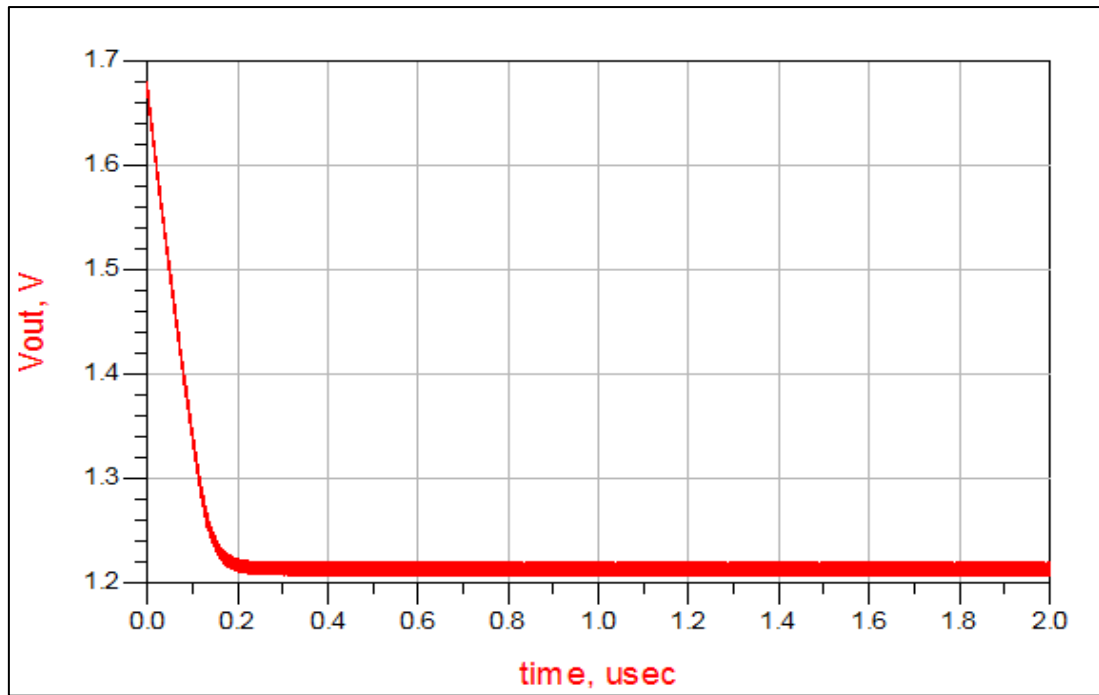


Fig. 3.8: V_{out} (V) of half-wave rectifier circuit at 2.4 GHz with LC-circuit.

Fig. 3.9 displays the waveform of output current for the half-wave rectifier circuit at 2.4 GHz. The output current is about $400 \mu\text{A}$.

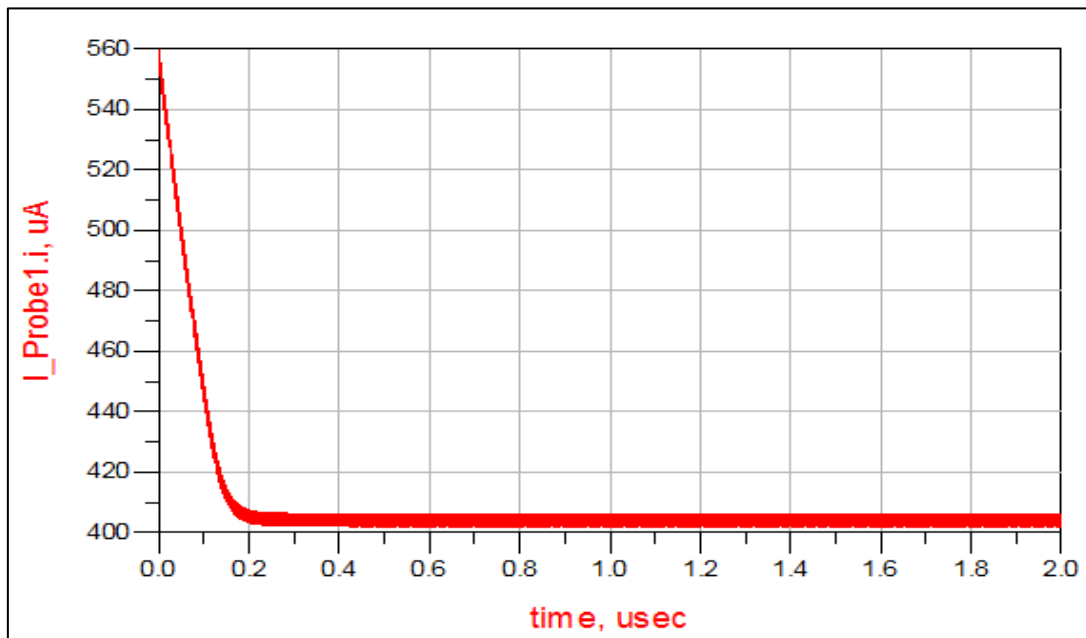


Fig. 3.9: Output current of half-wave rectifier circuit at 2.4 GHz with LC-circuit.

Fig. 3.10 shows the comparison in V_{out} of the rectifier's performance when changing the resistance load from 1 to 5 $k\Omega$ with a step of 1 $k\Omega$. It has been investigated that there is little impact on the V_{out} at low input power (P_{in}) on the contrary at high input power (P_{in}).

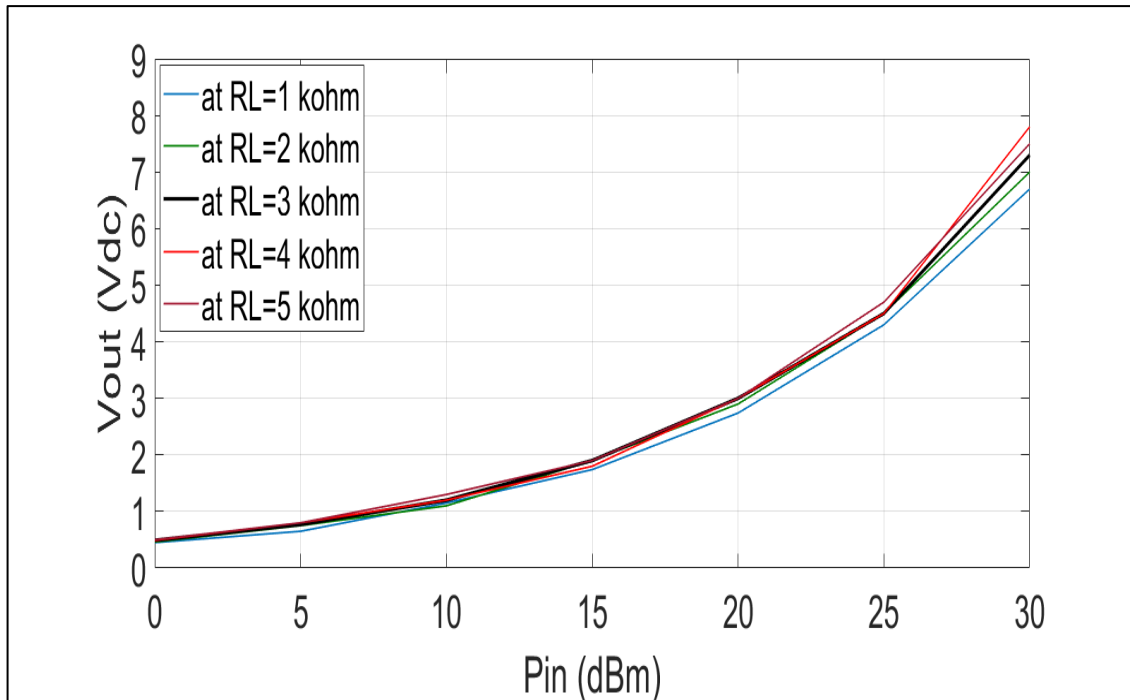


Fig. 3.10: V_{out} versus P_{in} of half-wave rectifier circuit for different resistance values of load (R_L) at 2.4 GHz with LC-circuit.

Fig. 3.11 shows the comparison in V_{out} of the rectifier's performance when changing diodes, where HSMS2820, HSMS282B, and HSMS282C diodes are used, respectively. It has been discovered that diodes have little effect on V_{out} .

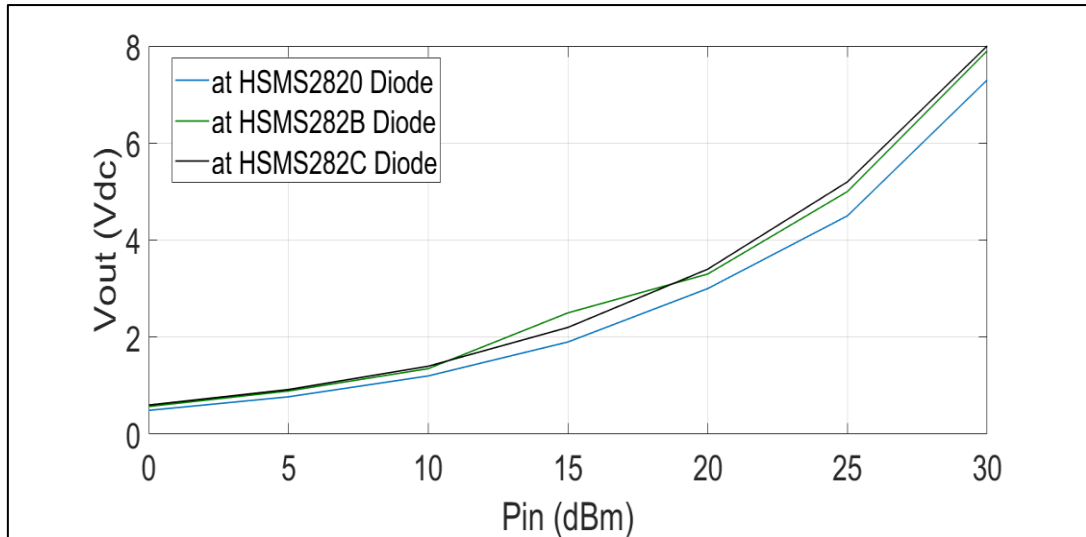


Fig. 3.11: V_{out} (V) versus P_{in} (dBm) of Half-wave rectifier circuit for different Diodes at 2.4 GHz with LC-circuit.

Fig. 3.12 shows the comparison in V_{out} of the rectifier's performance when changing in ϵ_r , where 2.64, 3, 3.55, 4.3, 6, and 6.5 are utilized, respectively. It is seen that there is no impact on the V_{out} at low input power (P_{in}) with a change in ϵ_r on the contrary at high input power (P_{in}).

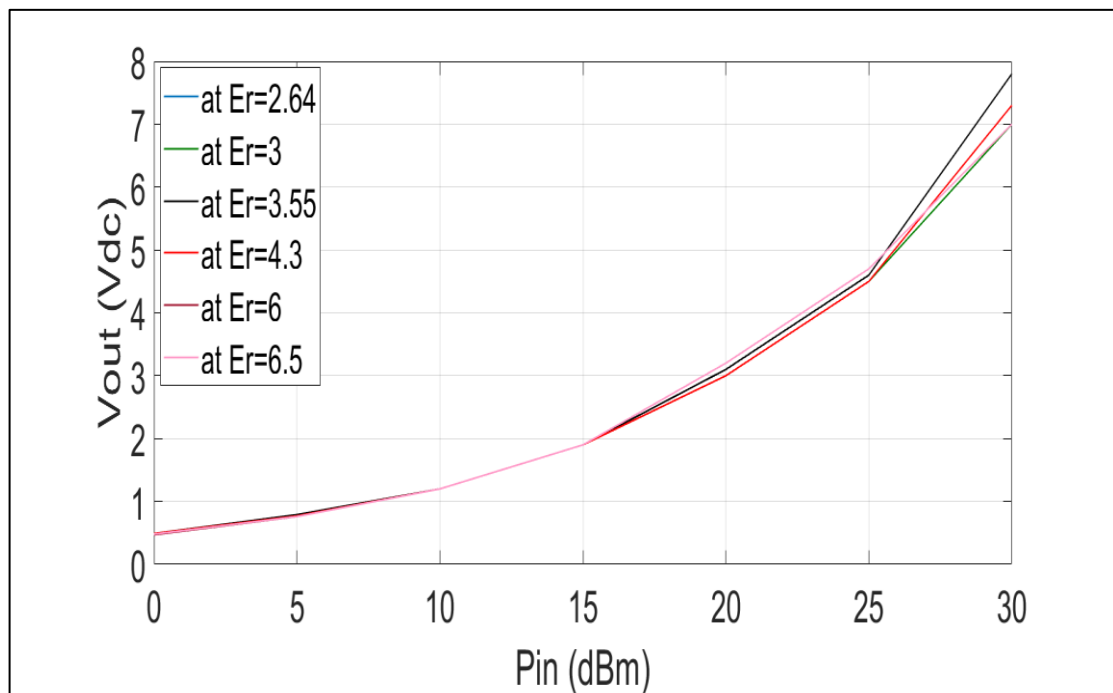


Fig. 3.12: V_{out} (V) versus P_{in} (dBm) of half-wave rectifier circuit for different ϵ_r at 2.4 GHz with LC-circuit.

Fig. 3.13 shows the comparison in efficiency (η) of the rectifier's performance when changing the load resistance from 1 to 5 k Ω . It has been found that the efficiency (η) decreases with an increasing (R_L).

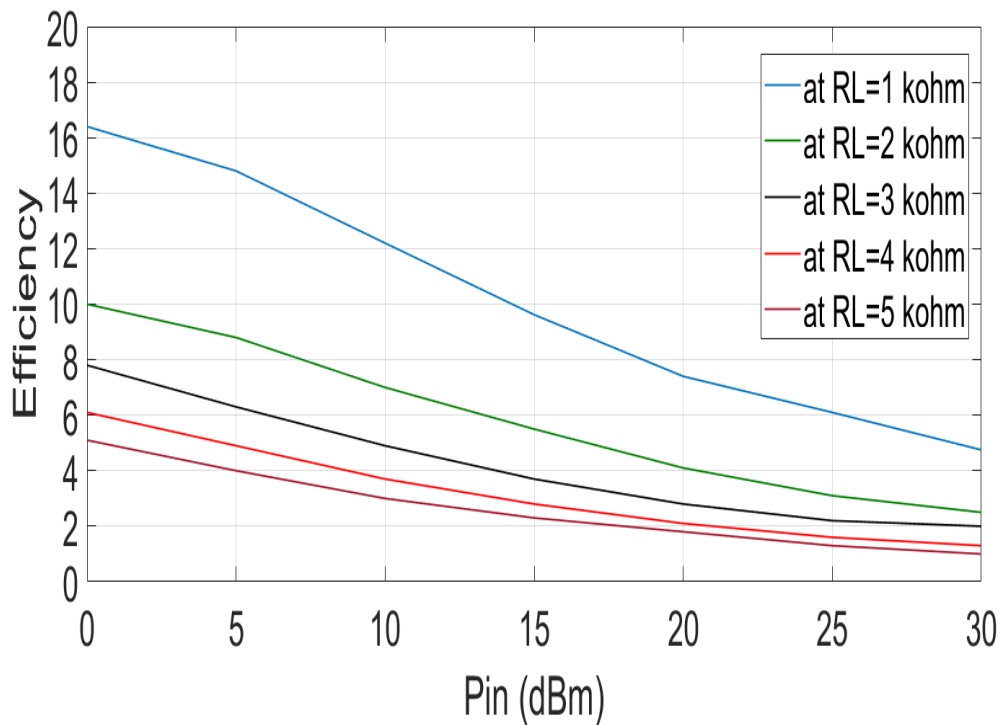


Fig. 3.13: Efficiency (η) versus Pin (dBm) of half-wave rectifier circuit for different values of resistance load (R_L) at 2.4 GHz with LC-circuit.

Fig. 3.14 shows the comparison in efficiency (η) of the rectifier's performance when changing diodes. It has been investigated that the best efficiency (η) was with the use of HSMS282C Diode.

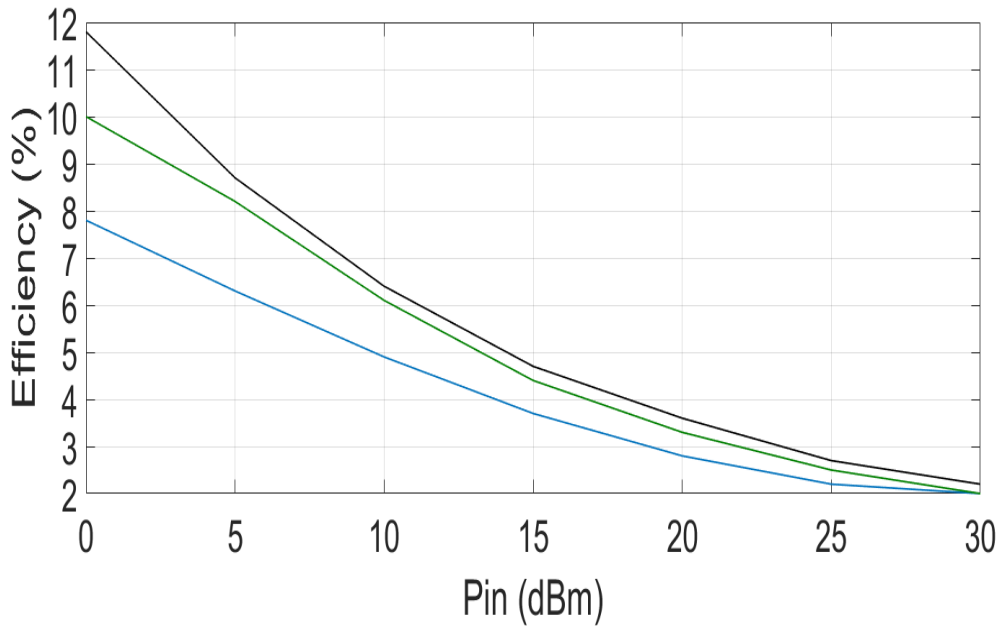


Fig. 3.14: Efficiency (η) versus Pin (dBm) of half-wave rectifier circuit for different Diodes at 2.4 GHz with LC-circuit.

Fig. 3.15 shows the comparison in efficiency (η) of the rectifier's performance when changes in ϵ_r are made. It has been observed that there is only a little impact on the efficiency (η) at high input power (Pin) on the contrary at low input power (Pin).

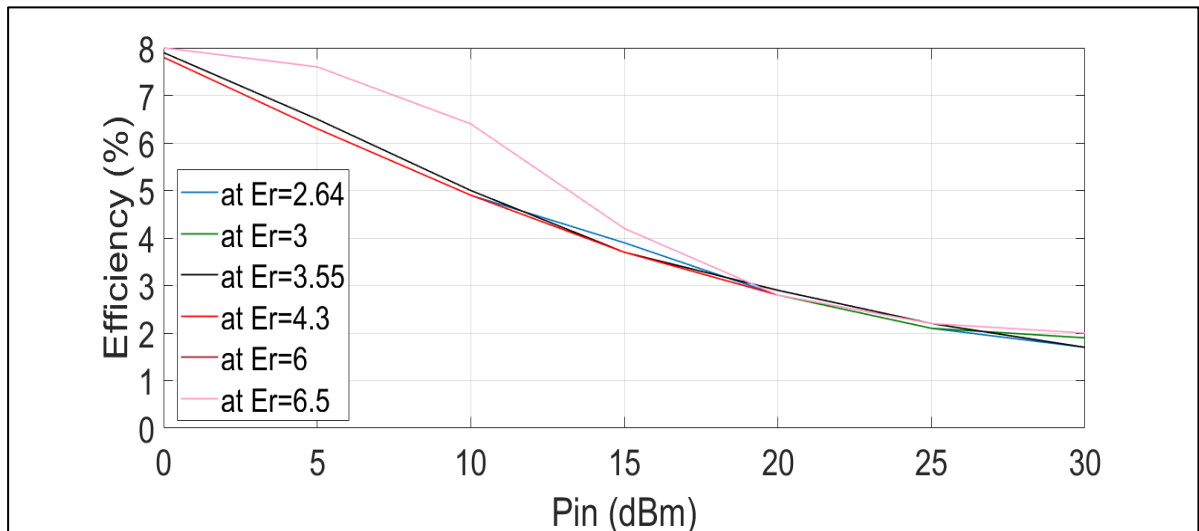


Fig. 3.15: Efficiency (η) versus Pin (dBm) of half-wave rectifier circuit for different ϵ_r at 2.4 GHz with LC-circuit.

3.3 Full-wave rectifier circuit using LC-match method

Another rectifier circuit is implemented by using the full-wave topology. In this way, an inductance (L) and capacitance (C) are employed at the input part of the circuit to match the source to the rectifier circuit as illustrated in Fig.3.16. Fig.3.17 shows the simulated S11 of full-wave rectifier circuit at 2.4 GHz with LC-circuit, where the return loss value went below -34 dB.

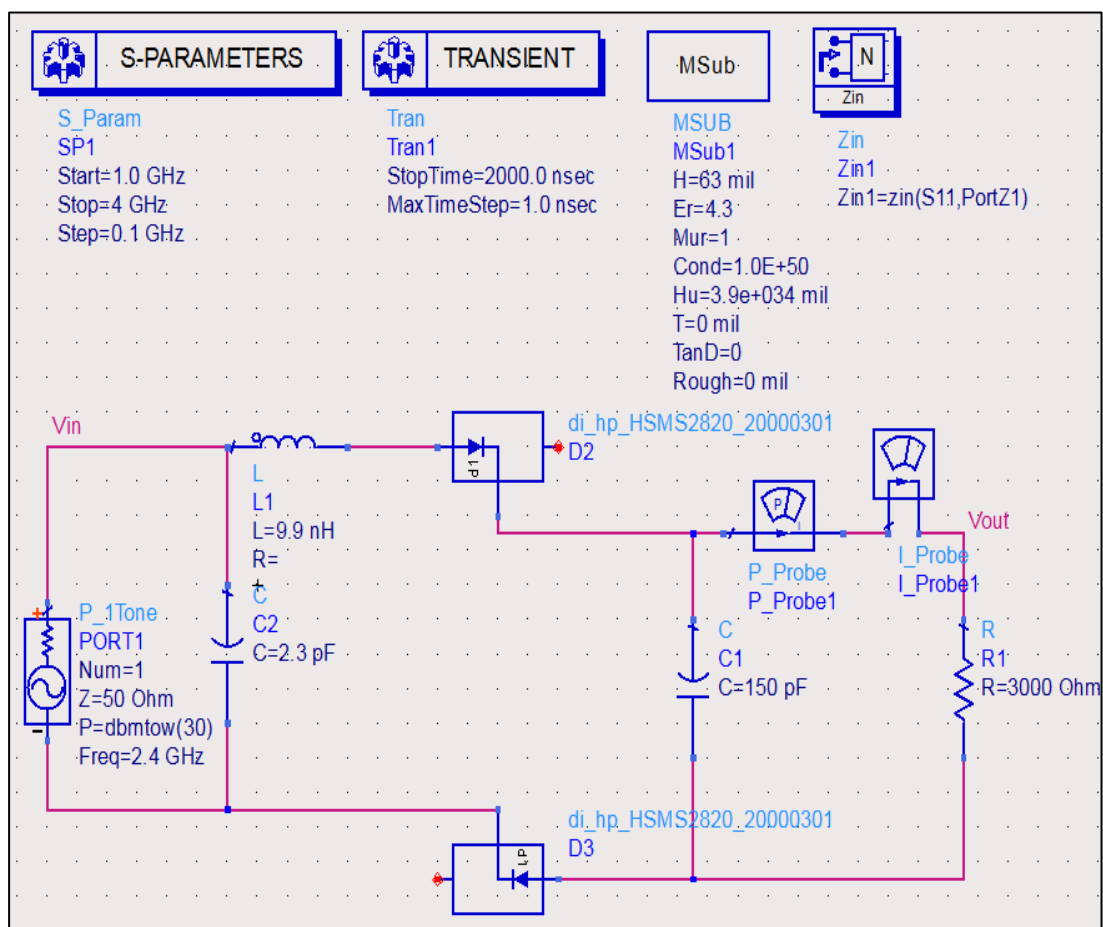


Fig. 3.16: Full-wave rectifier circuit operating at 2.4 GHz with LC circuit.

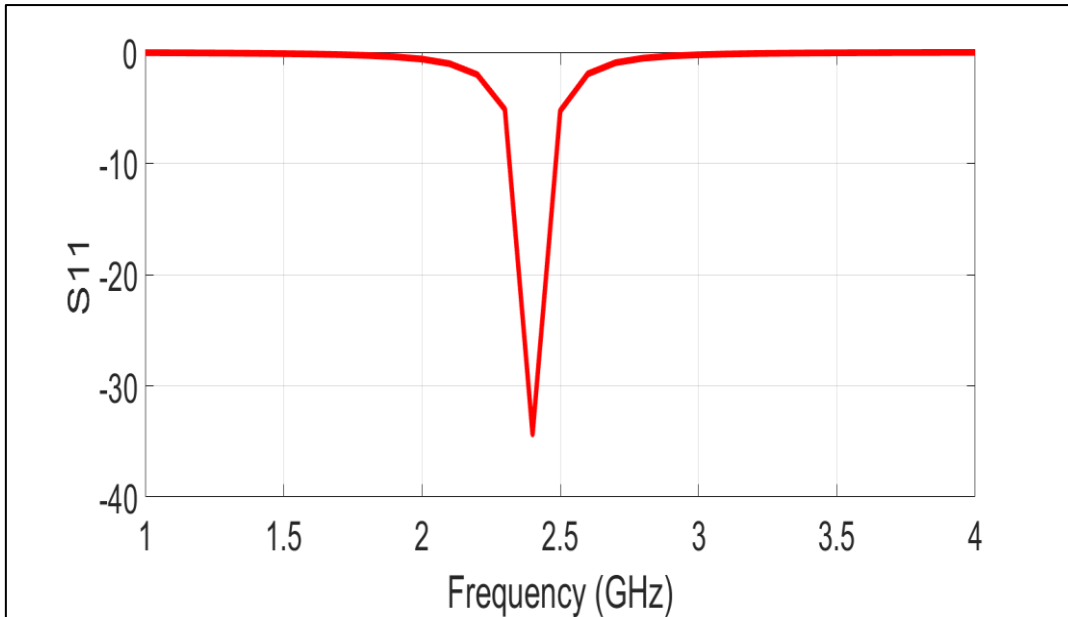


Fig. 3.17: Simulated S11 of full-wave rectifier circuit at 2.4 GHz with LC-circuit.

Fig. 3.18 shows the comparison in V_{out} of the rectifier's performance when changing the resistance load from 1 to 5 k Ω with a step of 1 k Ω . It has been noticed that there is little impact on the V_{out} at low input power (P_{in}) on the contrary at high input power (P_{in}).

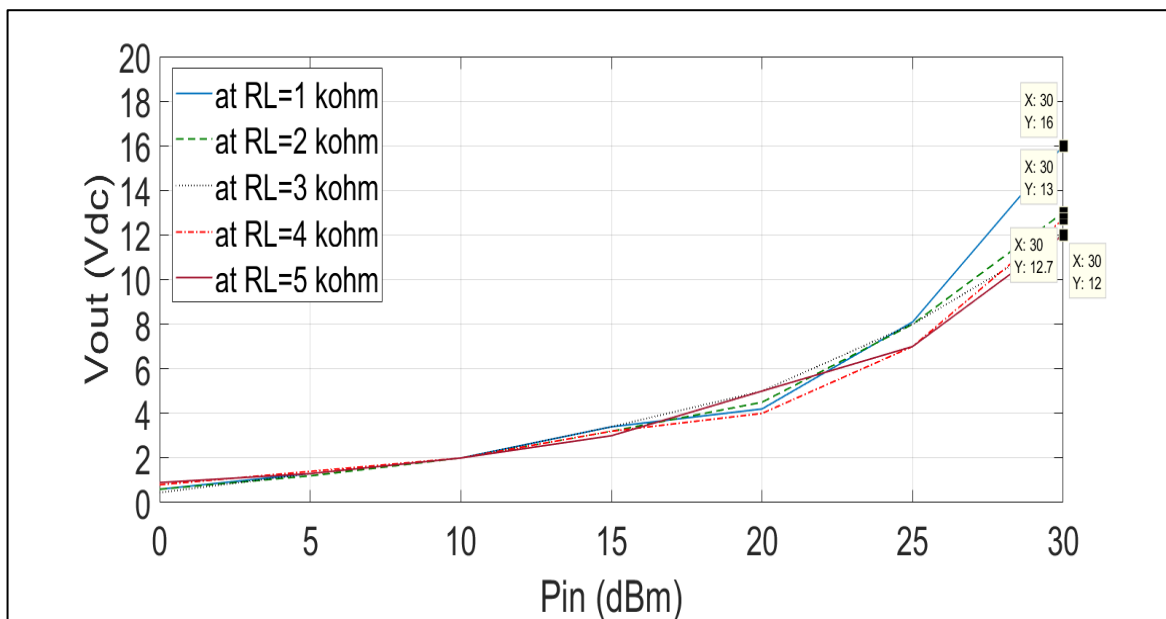


Fig. 3.18: V_{out} (V) versus P_{in} (dBm) of full-wave rectifier circuit for different resistance load (R_L) at 2.4 GHz with LC-circuit.

Fig. 3.19 shows the comparison in V_{out} of the rectifier's performance when changing diodes, where HSMS2820, HSMS282B, and HSMS282C diodes are used. It has been discovered that the diode HSMS2820 exhibits better performance compared to other types.

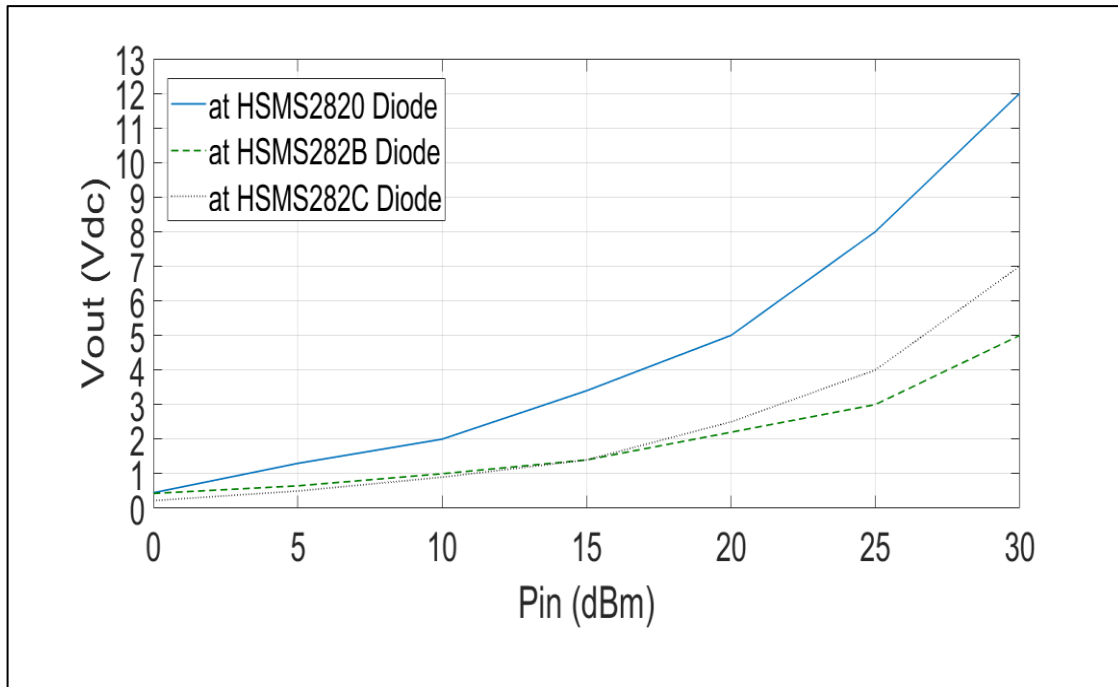


Fig. 3.19: V_{out} (V) versus P_{in} (dBm) of full-wave rectifier circuit for different diodes at 2.4 GHz with LC-circuit.

Fig. 3.20 shows the comparison in V_{out} of the rectifier's performance when changing the value of ϵ_r , where 2.64, 3, 3.55, 4.3, 6, and 6.5 are used. It has been noted that there is no impact on the V_{out} at low input power (P_{in}) and high input power (P_{in}), but there is a difference when using a value of 6.5 of ϵ_r , especially at the middle value of P_{in} .

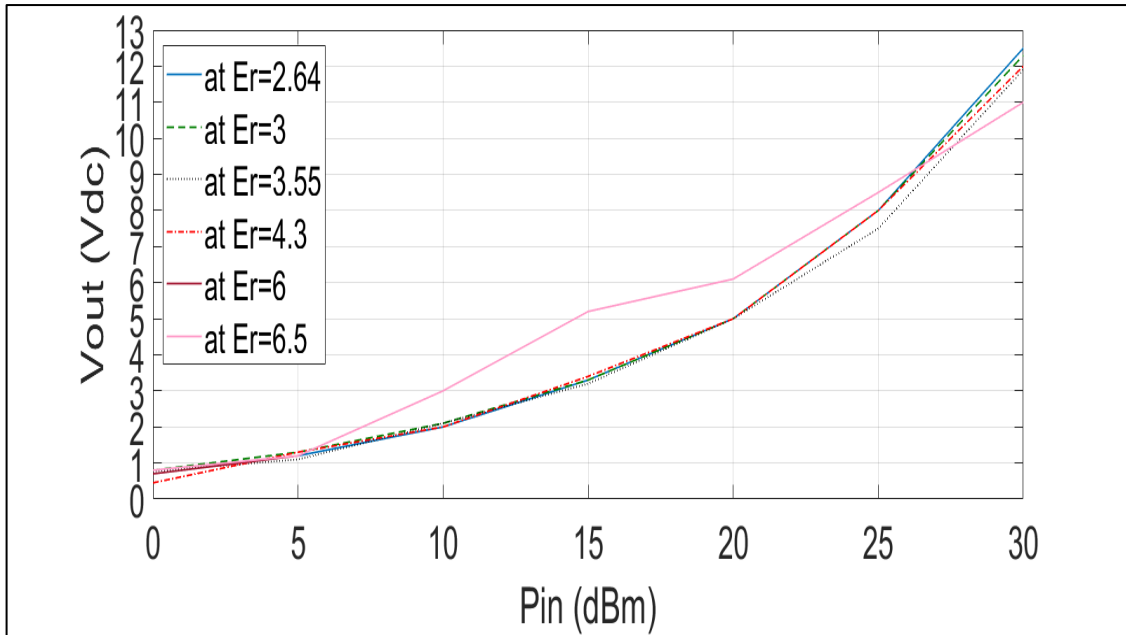


Fig. 3.20: V_{out} (V) versus P_{in} (dBm) of full-wave rectifier circuit for different ϵ_r at 2.4 GHz with LC-circuit.

Fig. 3.21 shows the comparison in efficiency (η) of the rectifier's performance when changes in resistance load (from 1 to 5 k Ω) are used. It has been found that the efficiency (η) decreases with an increase (R_L) in a way that is different from the case of half wave rectifier especially at low input powers.

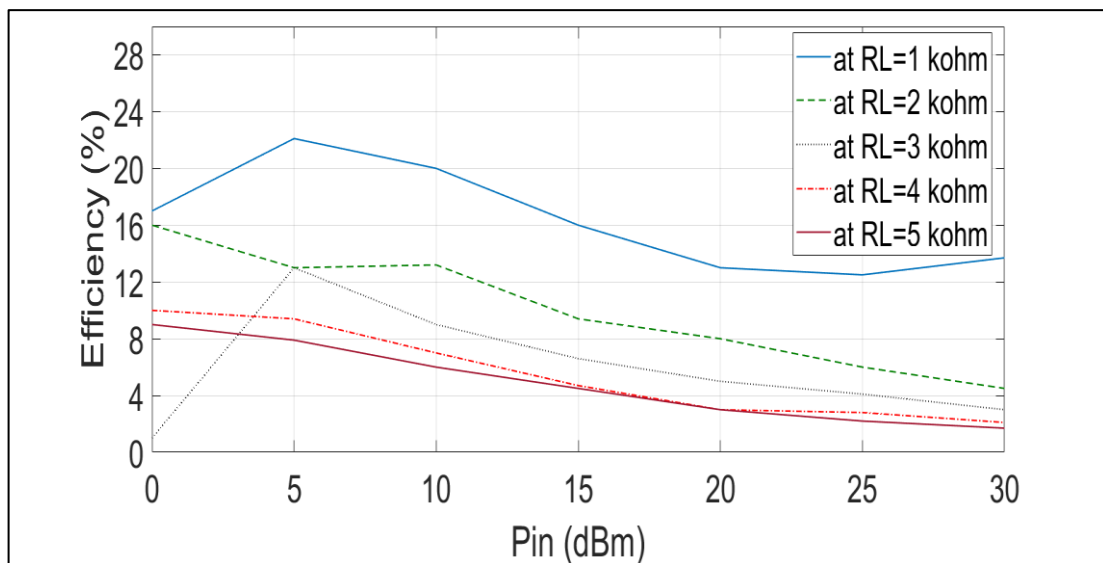


Fig. 3.21: Efficiency (η) versus P_{in} (dBm) of full-wave rectifier circuit for different values of resistance load (R_L) at 2.4 GHz with LC-circuit.

Fig. 3.22 shows the comparison in efficiency (η) of the rectifier's performance when changes in diodes are made. It has been investigated that the best efficiency (η) was with the use of the HSMS2820 diode and the worst with the HSMS282C diode.

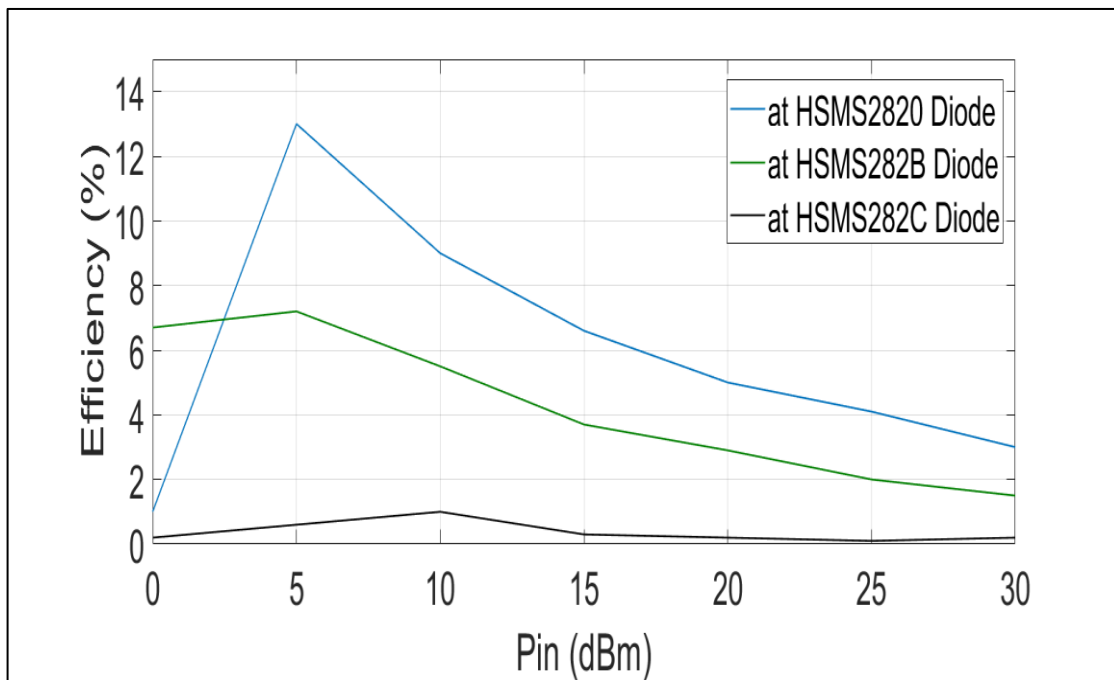


Fig. 3.22: Efficiency (η) versus Pin (dBm) of full-wave rectifier circuit for different Diodes at 2.4 GHz with LC-circuit.

Fig. 3.23 shows the comparison in efficiency (η) of the rectifier's performance when changes in ϵ_r are made. It has been seen that the best efficiency (η) with an ϵ_r of 4.3 represents the FR-4 substrate.

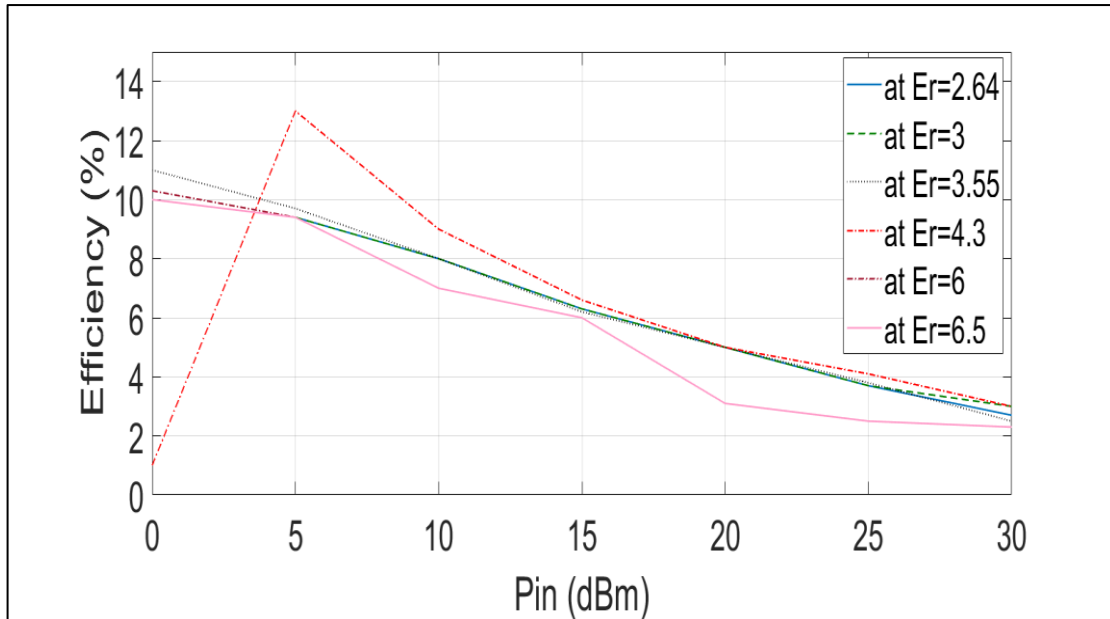


Fig. 3.23: Efficiency (η) versus Pin (dBm) of full-wave rectifier circuit for different ϵ_r at 2.4 GHz with LC-circuit.

3.4 Voltage Doubler rectifier circuit using LC-match method

Another rectifier circuit is applied by using the voltage doubler rectifier. At the input, the series capacitance acts as a voltage doubler. Additionally, the output has a capacitance to smooth the DC output before it is fed to the load as DC power or stored in a battery, as illustrated in Fig. 3.24. The matching network has done the job perfectly, where excellent matching is achieved, as shown in the S-parameters curve in Fig. 3.25.

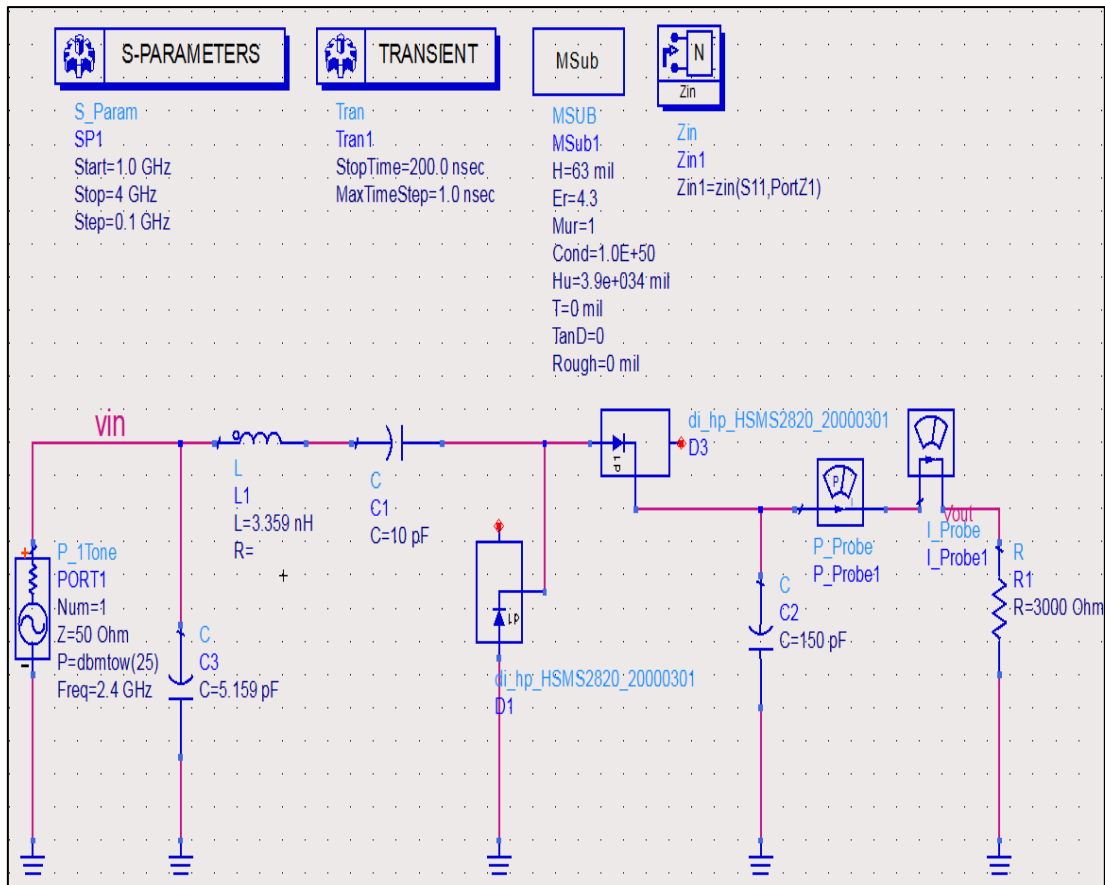


Fig. 3.24: Voltage doubler rectifier circuit operating at 2.4 GHz with LC-circuit.

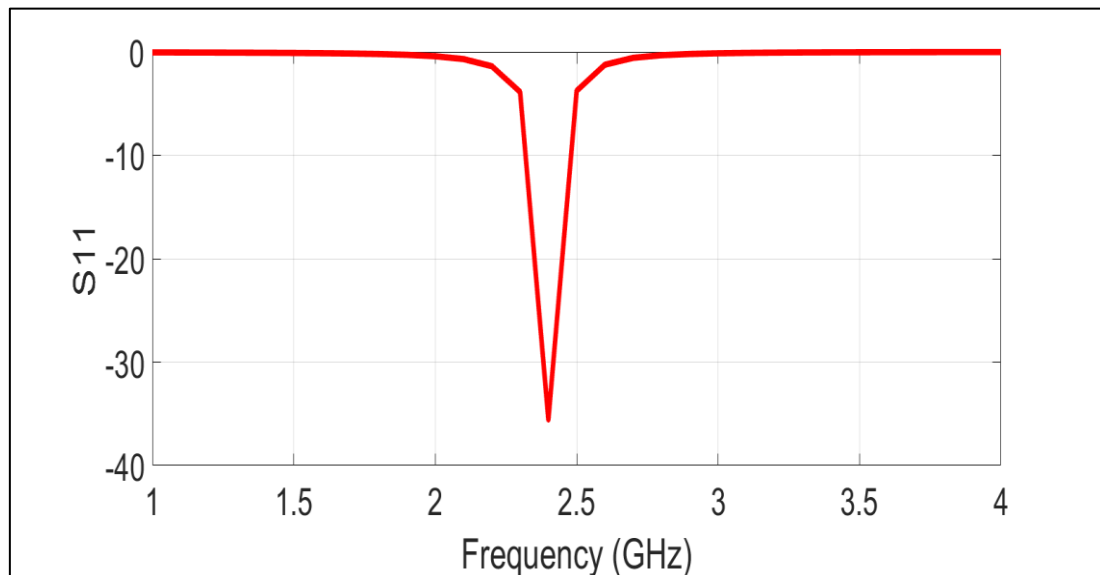


Fig. 3.25: Simulated S11 of voltage doubler rectifier circuit at 2.4 GHz with LC-circuit.

Fig. 3.26 shows the comparison in V_{out} of the rectifier's performance when changing the resistance load (R_L) (from 1 to 5 k Ω) with a step of 1 k Ω . It is seen that the highest of V_{out} is at high (R_L) with huge differences at higher input power.

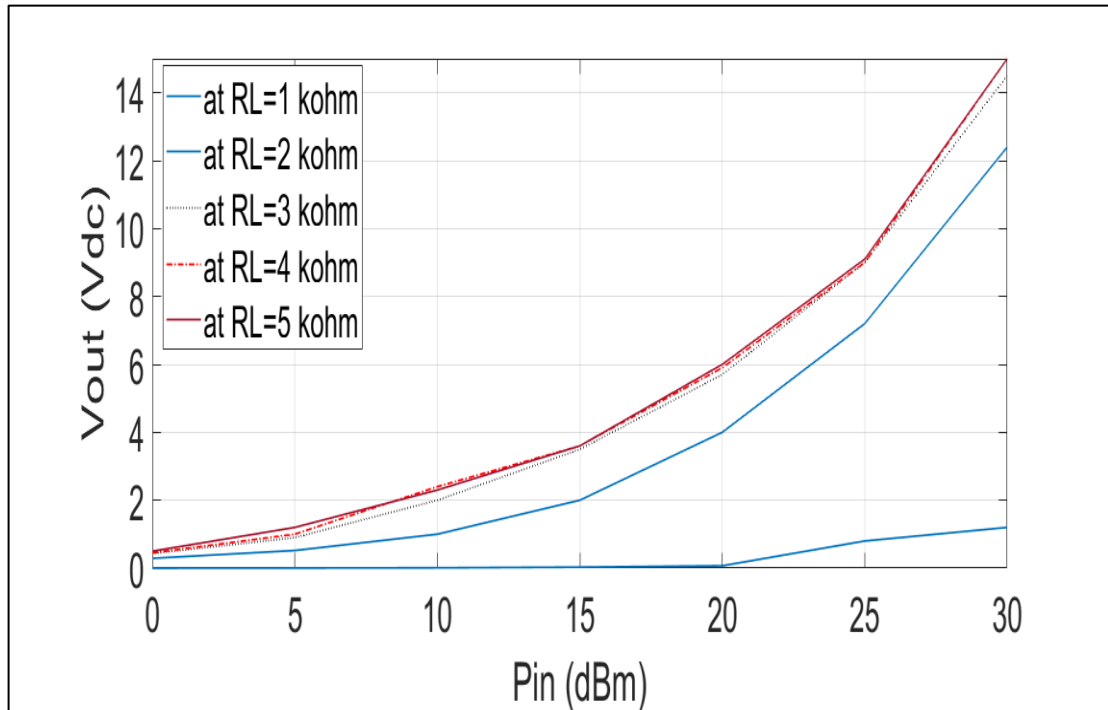


Fig. 3.26: V_{out} (V) versus P_{in} (dBm) of voltage doubler rectifier circuit for different values of resistance load (R_L) at 2.4 GHz with LC-circuit.

Fig. 3.27 shows the comparison in V_{out} of the rectifier's performance when changing diodes, where HSMS2820, HSMS282B, and HSMS282C diodes are employed. It has been discovered that the diode HSMS282B shows the best performance.

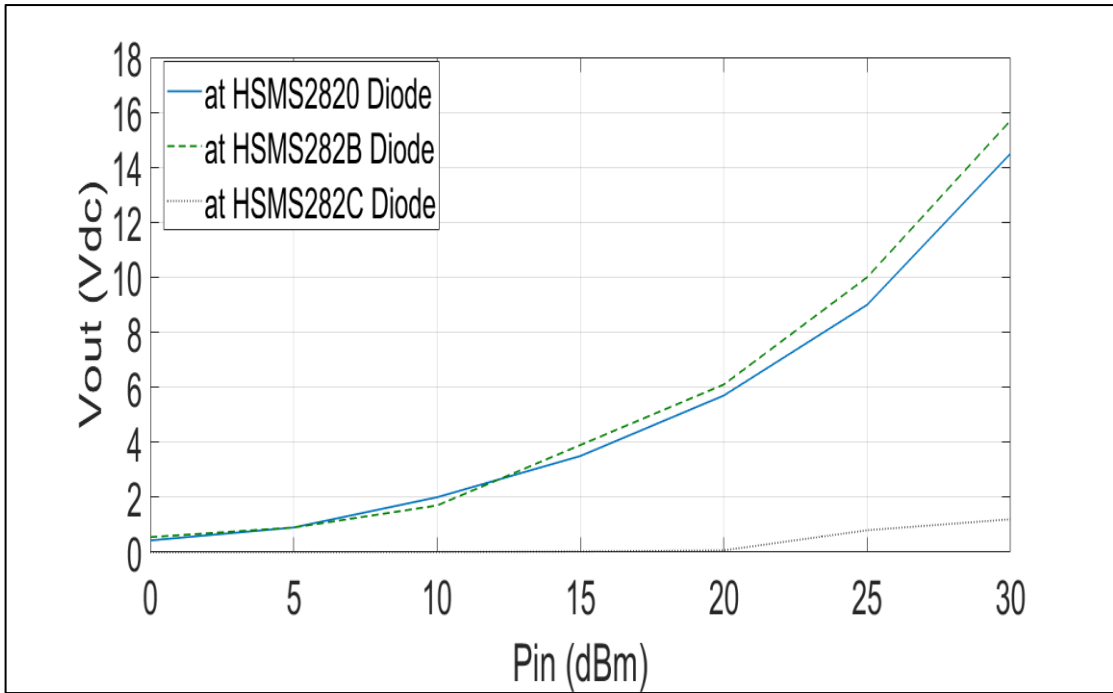


Fig. 3.27: V_{out} (V) versus P_{in} (dBm) of voltage doubler rectifier circuit for different Diodes at 2.4 GHz with LC-circuit.

Fig. 3.28 shows the comparison in V_{out} of the rectifier's performance when changing in ϵ_r , where 2.64, 3, 3.55, 4.3, 6, and 6.5 are used. It has been noticed that the differences are almost negligible.

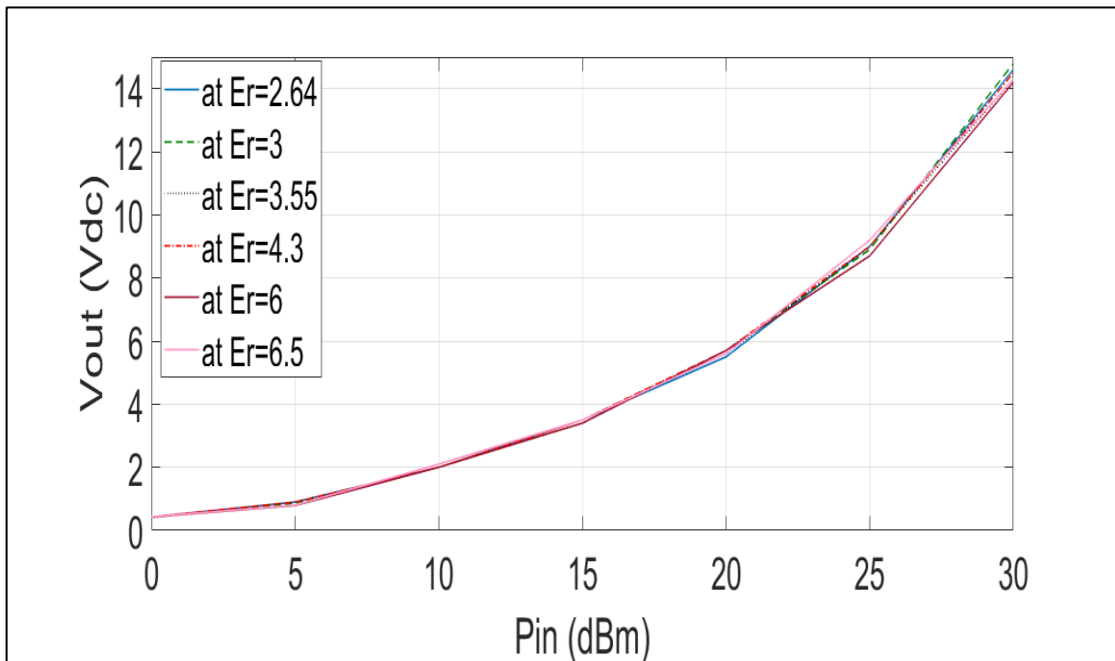


Fig. 3.28: V_{out} (V) versus P_{in} (dBm) of voltage doubler rectifier circuit for different ϵ_r at 2.4 GHz with LC-circuit.

Fig. 3.29 shows the comparison in efficiency (η) of the rectifier's performance when changes in resistance load (from 1 to 5 k Ω) are used. It has been found that the efficiency (η) decreases with an increase (R_L) at higher input powers.

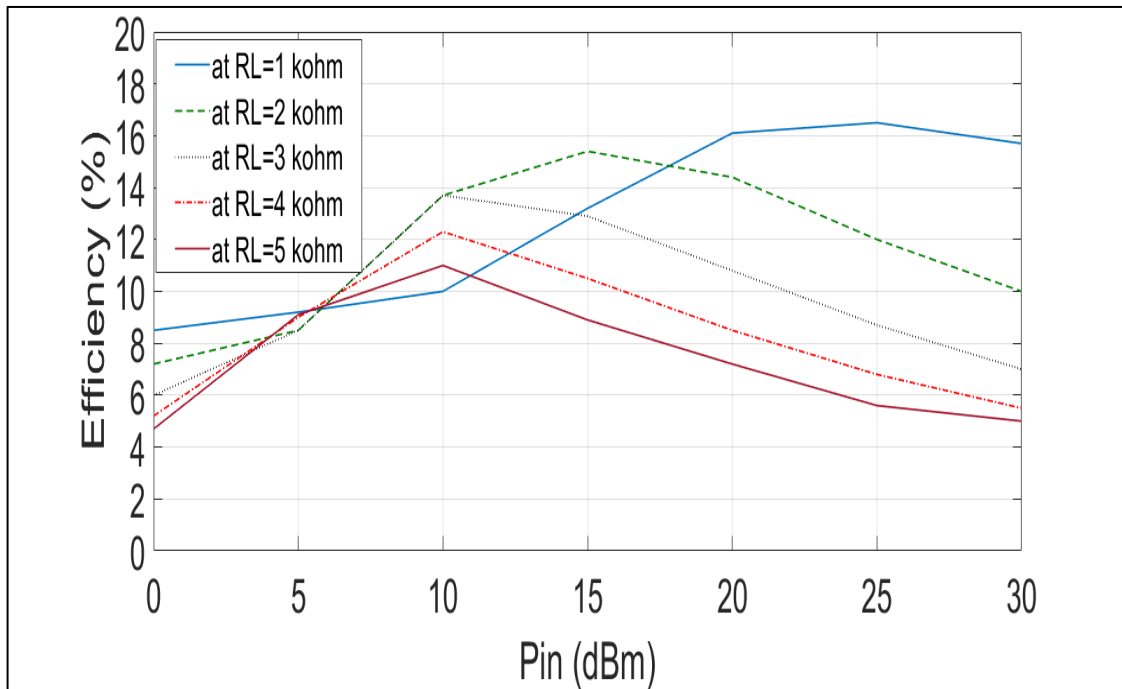


Fig. 3.29: Efficiency (η) versus Pin (dBm) of voltage doubler rectifier circuit for different values of resistance load (R_L) at 2.4 GHz with LC-circuit.

Fig. 3.30 shows the comparison in efficiency (η) of the rectifier's performance when changes in diodes are made. It is found that the best efficiency (η) was with the use of the HSMS2820 diode and the worst with the HSMS282C diode.

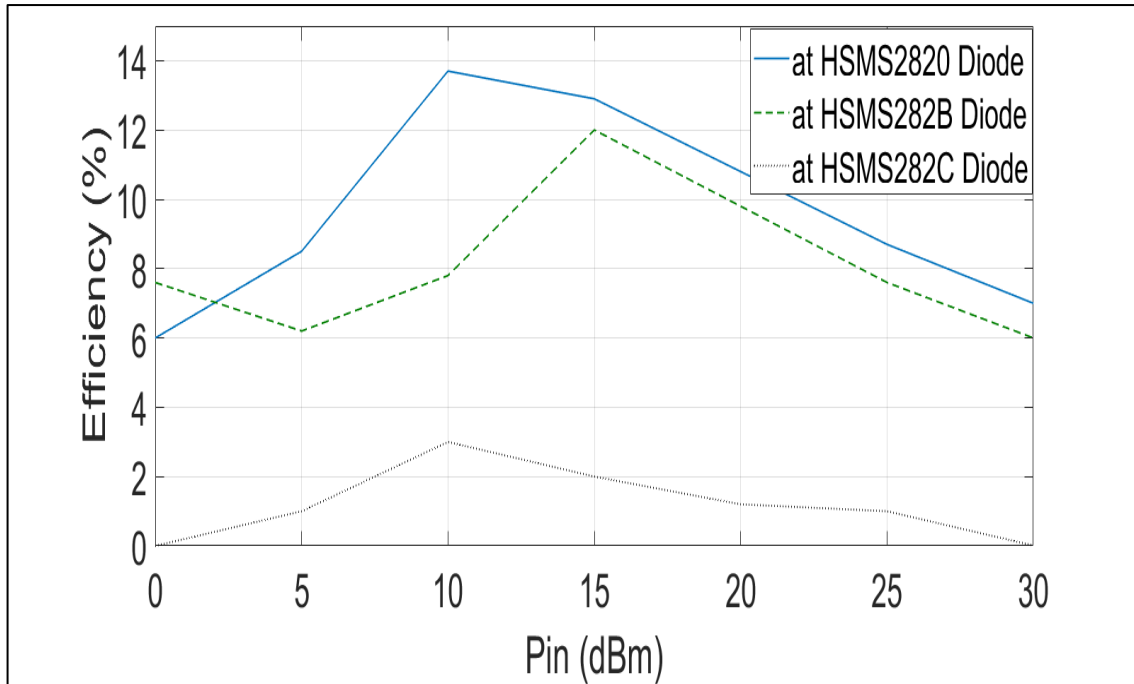


Fig. 3.30: Efficiency (η) versus Pin (dBm) of voltage doubler rectifier circuit for different Diodes at 2.4 GHz with LC-circuit.

Fig. 3.31 shows the comparison in efficiency (η) of the rectifier's performance when changes in ϵ_r are made. It is clear that the efficiency (η) almost kept the same with a different ϵ_r of substrate are used.

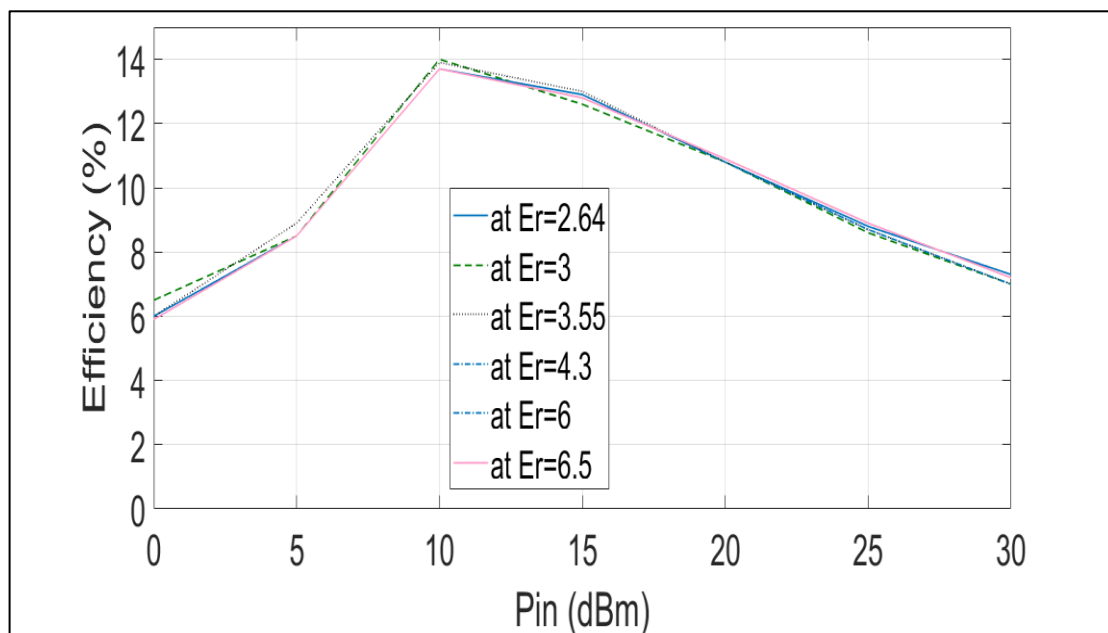


Fig. 3.31: Efficiency (η) versus Pin (dBm) of voltage doubler rectifier circuit for different ϵ_r at 2.4 GHz with LC-circuit.

3.5 Villard charge pump rectifier circuit using LC-match method

The basic configuration of the Villard charge pump rectifier consists of a series of diodes and capacitors connected in a cascade arrangement as illustrated in Fig. 3.32. The diodes are used to rectify the AC input voltage, allowing only the positive half-cycles to pass through, while the capacitors store and accumulate charge. The output voltage is taken across the capacitors. The matching network of parallel $C=5.075$ pF and series $L=2.933$ nH has done the job perfectly, where excellent matching is achieved, as shown in the S-parameters curve in Fig. 3.33.

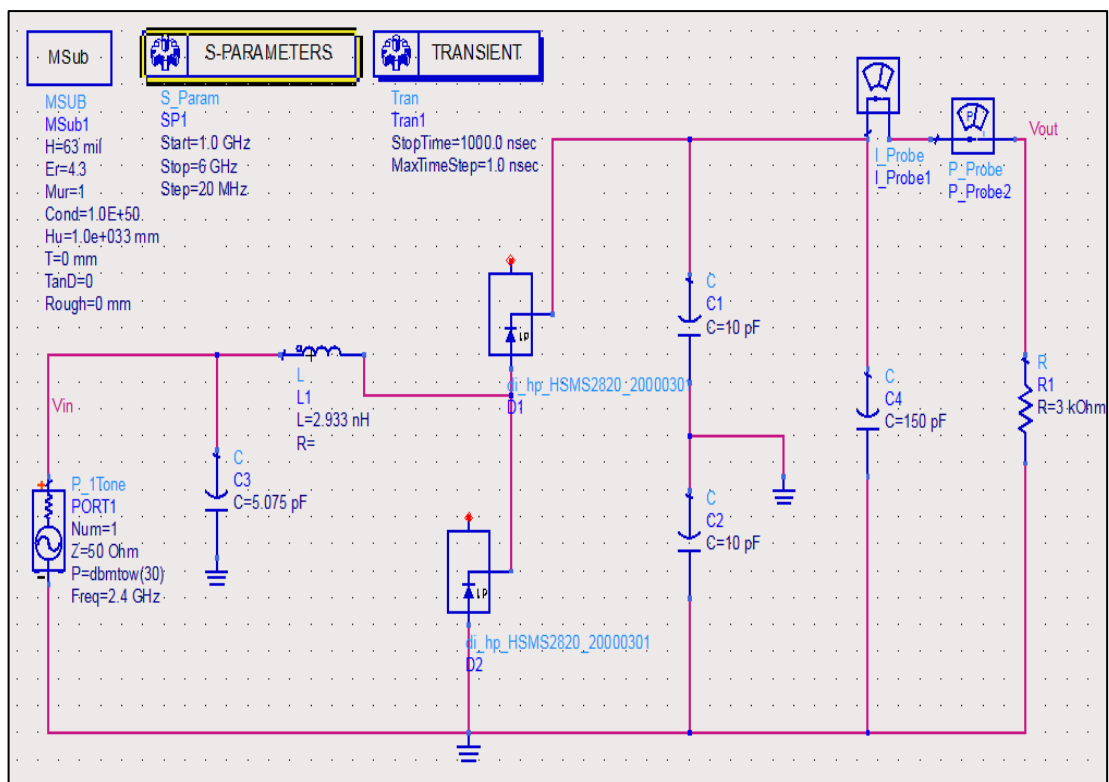


Fig. 3.32: Villard charge pump rectifier circuit operating at 2.4 GHz with LC-circuit.

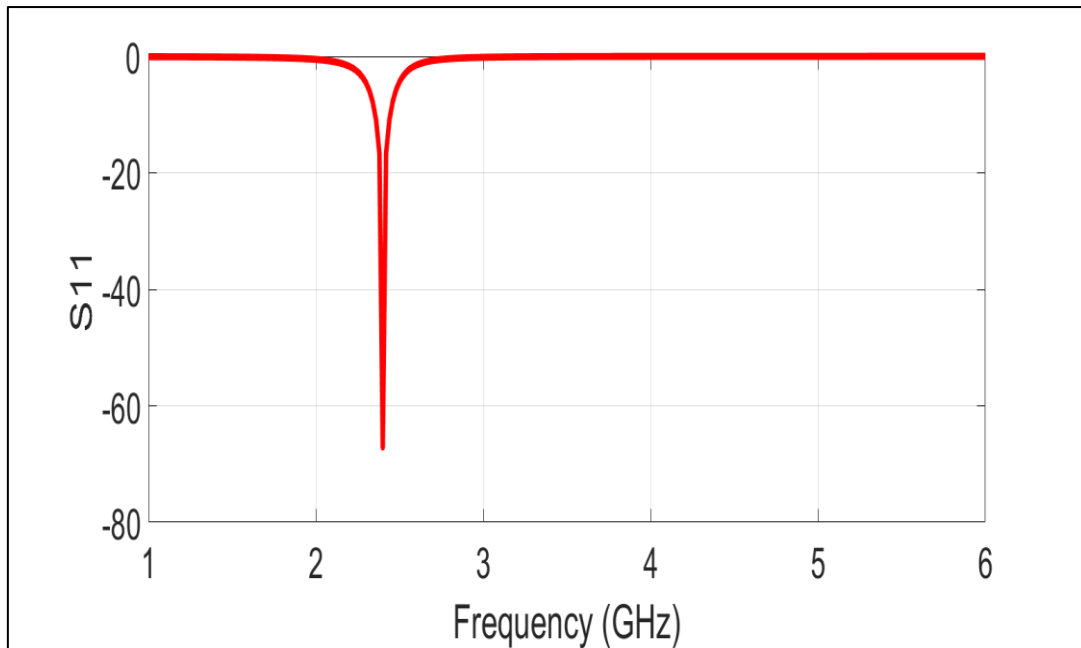


Fig. 3.33: Simulated S11 of Villard charge pump rectifier circuit at 2.4 GHz with LC-circuit.

Fig. 3.34 shows the comparison in V_{out} of the rectifier's performance when changing the resistance load (R_L) (from 1 to 5 k Ω) with a step of 1 k Ω . It has been found that there is little impact on the V_{out} at low input power (P_{in}) on the contrary at high input power (P_{in}).

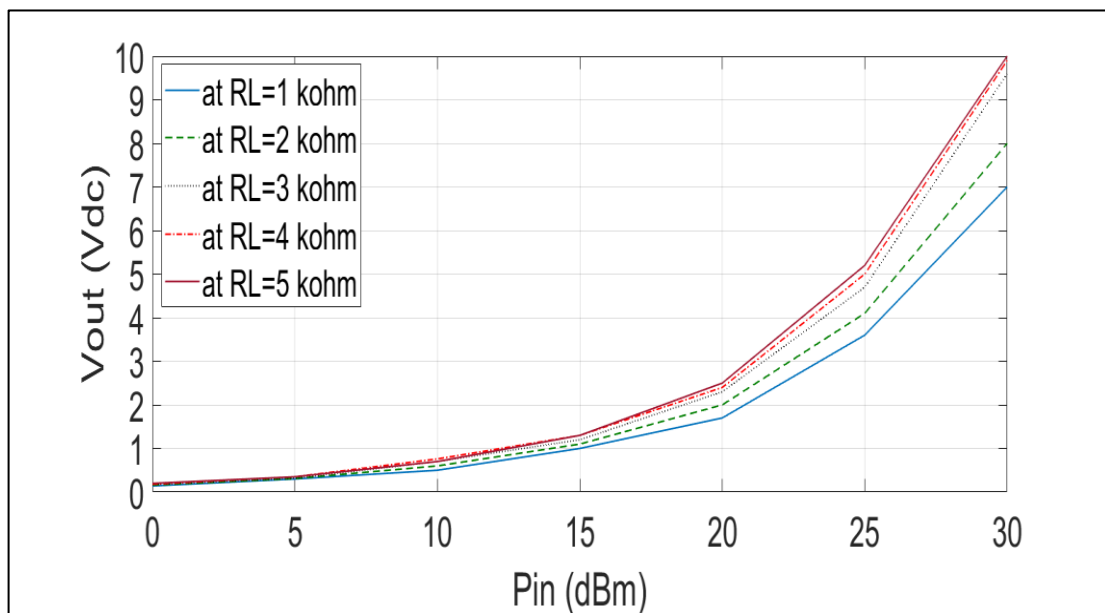


Fig. 3.34: V_{out} (V) vs. P_{in} (dBm) of Villard charge pump rectifier circuit for different values of resistance load (R_L) at 2.4 GHz with LC-circuit.

Fig. 3.35 shows the comparison in V_{out} of the rectifier's performance when changing diodes, where HSMS2820, HSMS282B, and HSMS282C diodes are used. It has been discovered that the diode HSMS2820 outperforms other types.

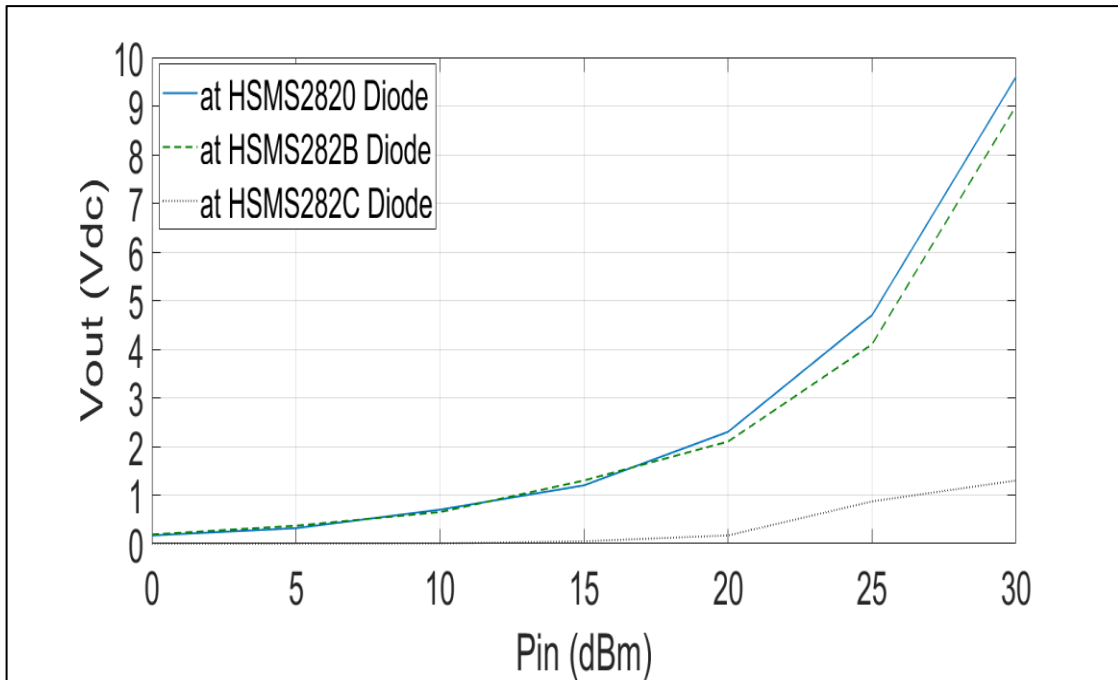


Fig. 3.35: V_{out} (V) versus P_{in} (dBm) of Villard charge pump rectifier circuit for different Diodes at 2.4 GHz with LC-circuit.

Fig. 3.36 shows the comparison in V_{out} of the rectifier's performance when changing ϵ_r , where 2.64, 3, 3.55, 4.3, 6, and 6.5 are used. It has been concluded that the differences are negligible.

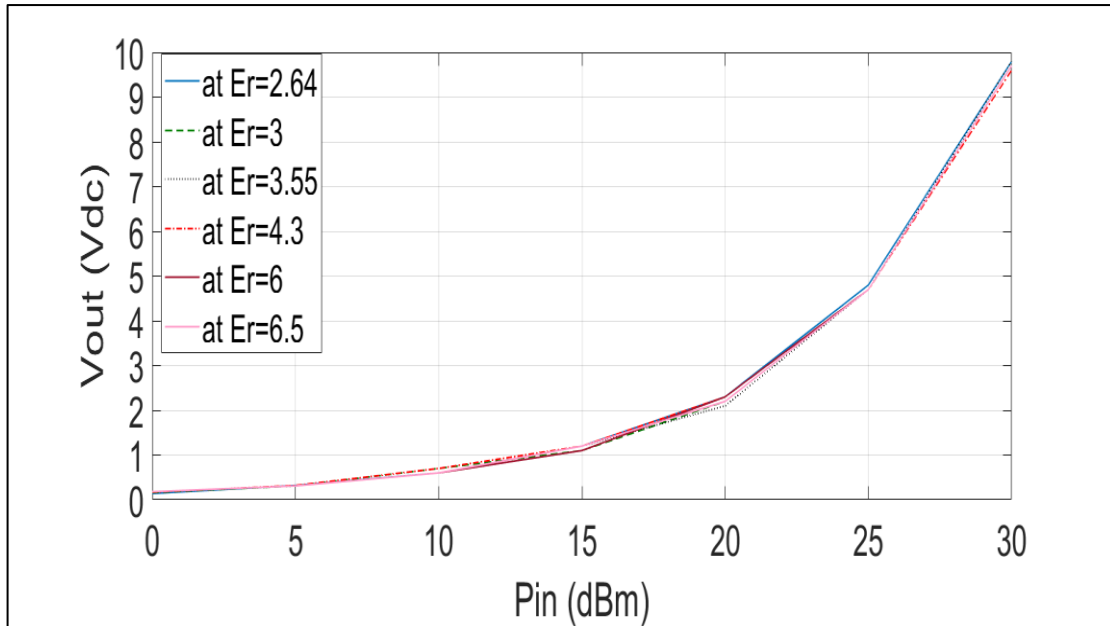


Fig. 3.36: Vout (V) versus Pin (dBm) of Villard charge pump rectifier circuit for different ϵ_r at 2.4 GHz with LC-circuit.

Fig. 3.37 shows the comparison in efficiency (η) of the rectifier's performance when changing the load resistance (from 1 to 5 k Ω). It has been found that the efficiency (η) decreases when increasing (R_L), with the highest (η) at (R_L) equals to 3 k Ω at 30 dBm of Pin.

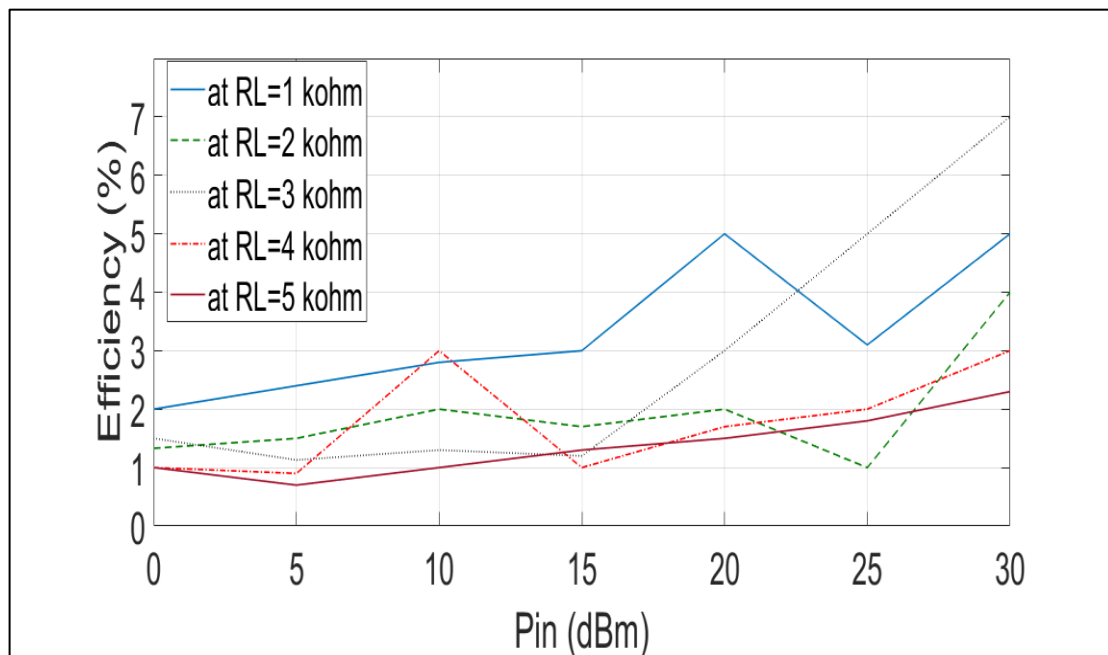


Fig. 3.37: Efficiency (η) vs. Pin (dBm) of Villard charge pump rectifier circuit for different values of load (R_L) at 2.4 GHz with LC-circuit.

Fig. 3.38 shows the comparison in efficiency (η) of the rectifier's performance when changes in diode's type are made. It has been seen that the best efficiency (η) was with the use of the HSMS2820 diode and the worst with the HSMS282C diode especially at high input power (P_{in}).

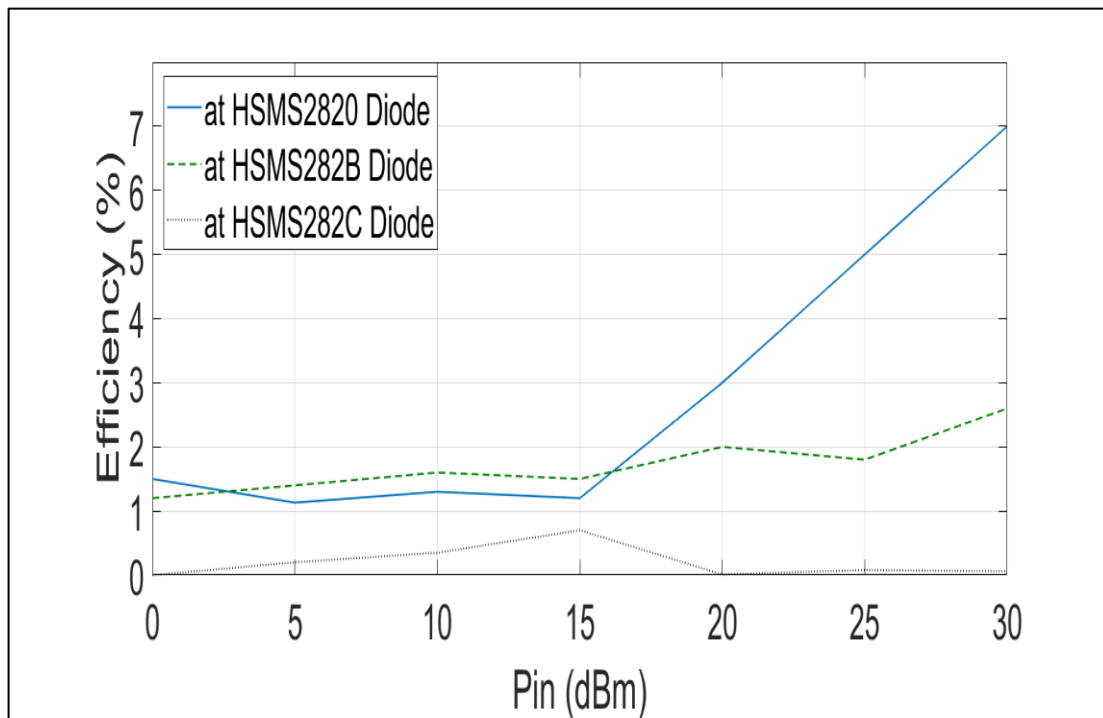


Fig. 3.38: Efficiency (η) versus P_{in} (dBm) of villard charge pump rectifier circuit for different Diodes at 2.4 GHz with LC-circuit.

Fig. 3.39 shows the comparison in efficiency (η) of the rectifier's performance when changes in ϵ_r are made. It has been noted that the efficiency (η) is almost matched when a different ϵ_r of substrate is used except at 4.3 especially at high input power (P_{in}).

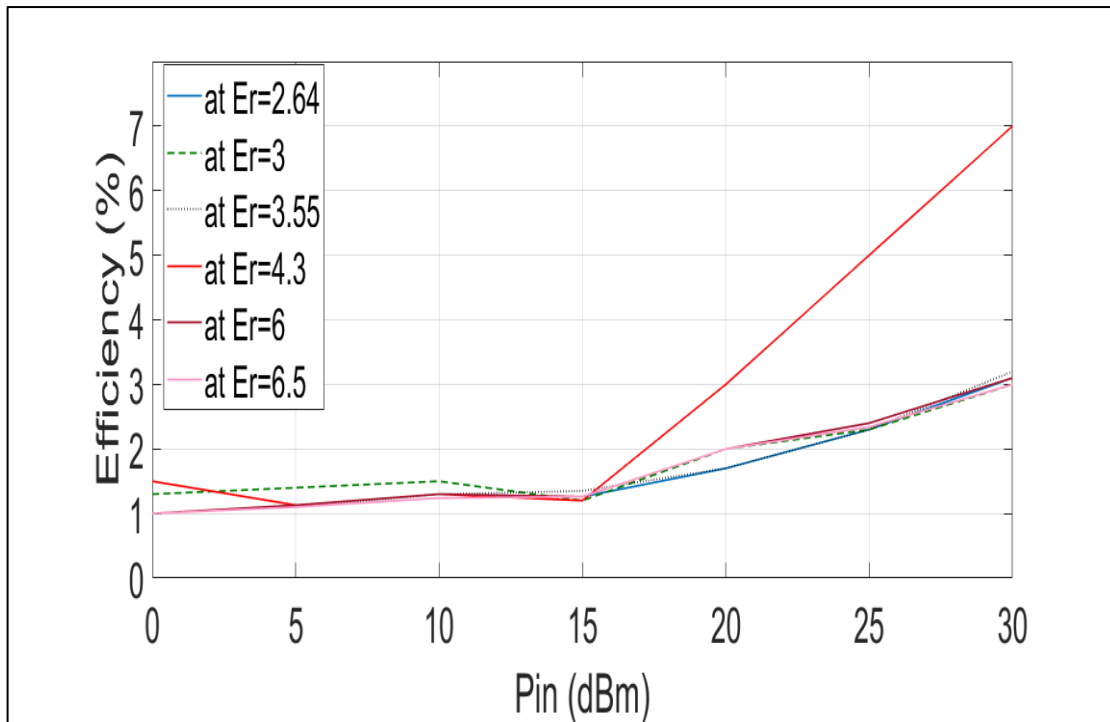


Fig. 3.39: Efficiency (η) versus Pin (dBm) of Villard charge pump rectifier circuit for different ϵ_r at 2.4 GHz with LC-circuit.

3.6 Graetz charge pump rectifier circuit using LC-match method

The basic configuration of a Graetz charge pump consists of four diodes and two capacitors arranged in a bridge-like structure, as shown in Fig. 3.40. The S-parameters curve is very good at 2.4 GHz, as shown in Fig. 3.41.

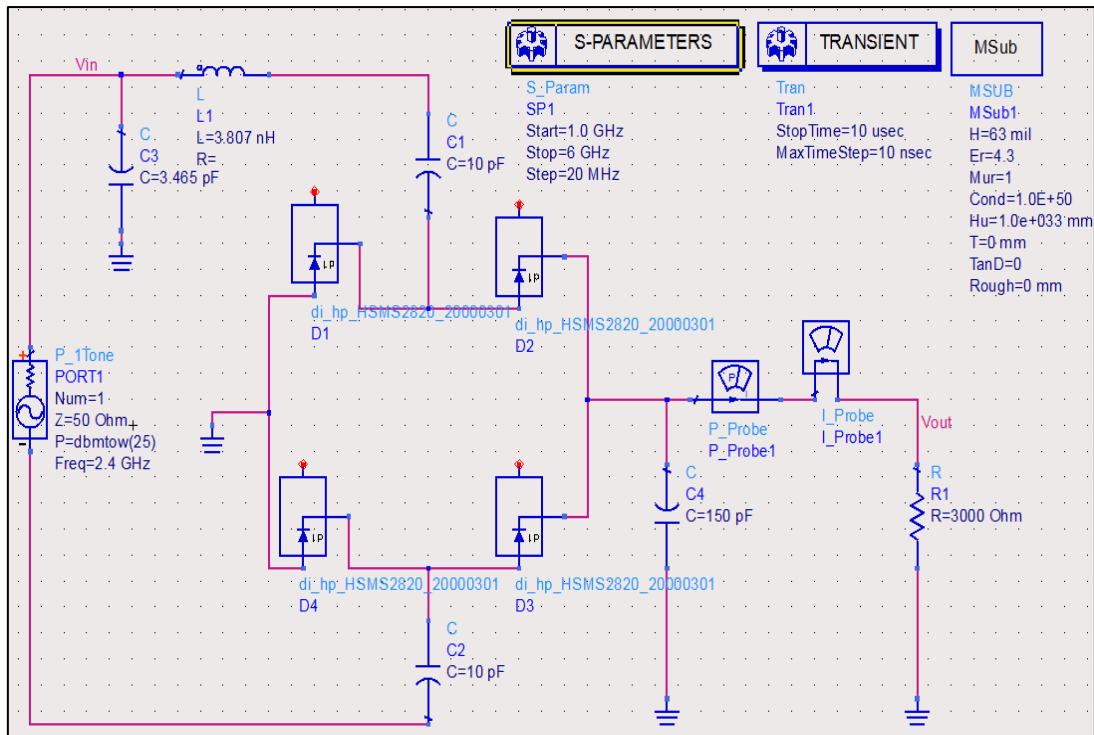


Fig. 3.40: Graetz charge pump rectifier circuit operating at 2.4 GHz with LC-circuit.

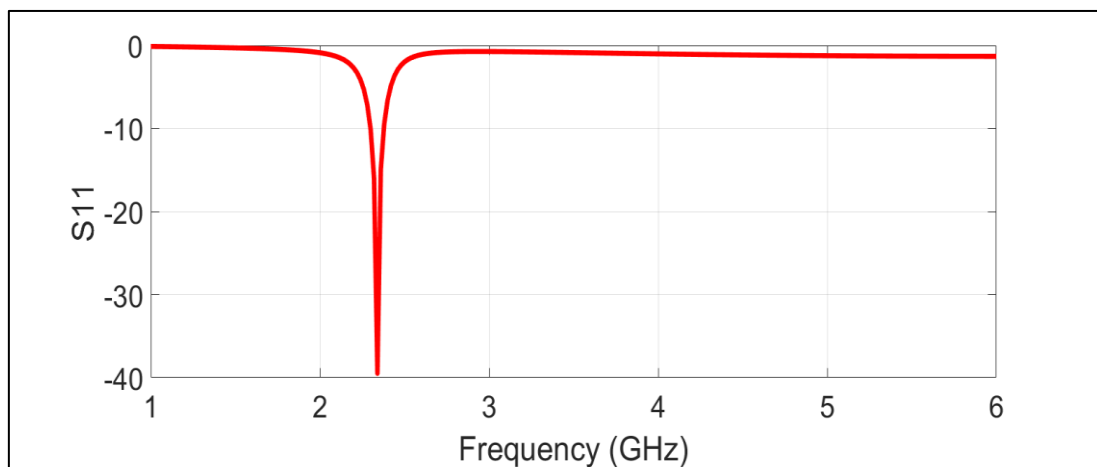


Fig. 41: Simulated S11 of Graetz charge pump rectifier circuit at 2.4 GHz with LC-circuit.

Fig. 3.42 shows the comparison in V_{out} of the rectifier's performance when changing the resistance load (R_L) (from 1 to 5 k Ω) with a step of 1 k Ω . It has been investigated that there is little impact on the V_{out} at low input power (P_{in}) on the contrary at high input power (P_{in}), and it is noticed that a higher V_{out} can be achieved at higher R_L .

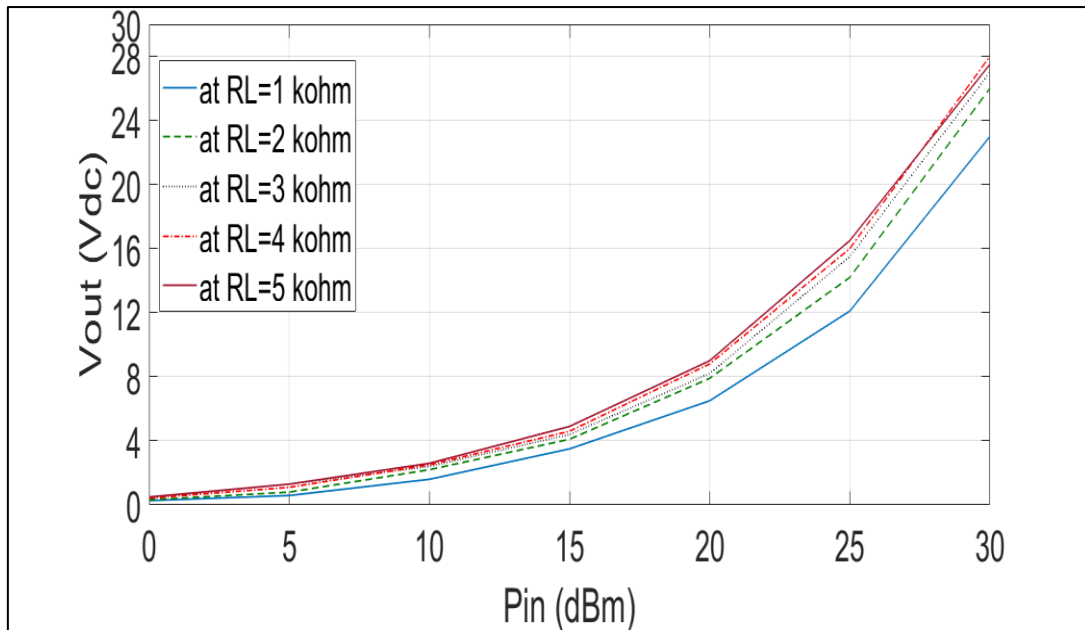


Fig. 3.42: V_{out} (V) versus P_{in} (dBm) of Graetz charge pump rectifier circuit for different values of resistance load (R_L) at 2.4 GHz with LC-circuit.

Fig. 3.43 shows the comparison in V_{out} of the rectifier's performance when changing diodes, where HSMS2820, HSMS282B, and HSMS282C diodes are employed. It has been discovered that the differences are almost negligible when changing the diodes for this type of rectifiers.

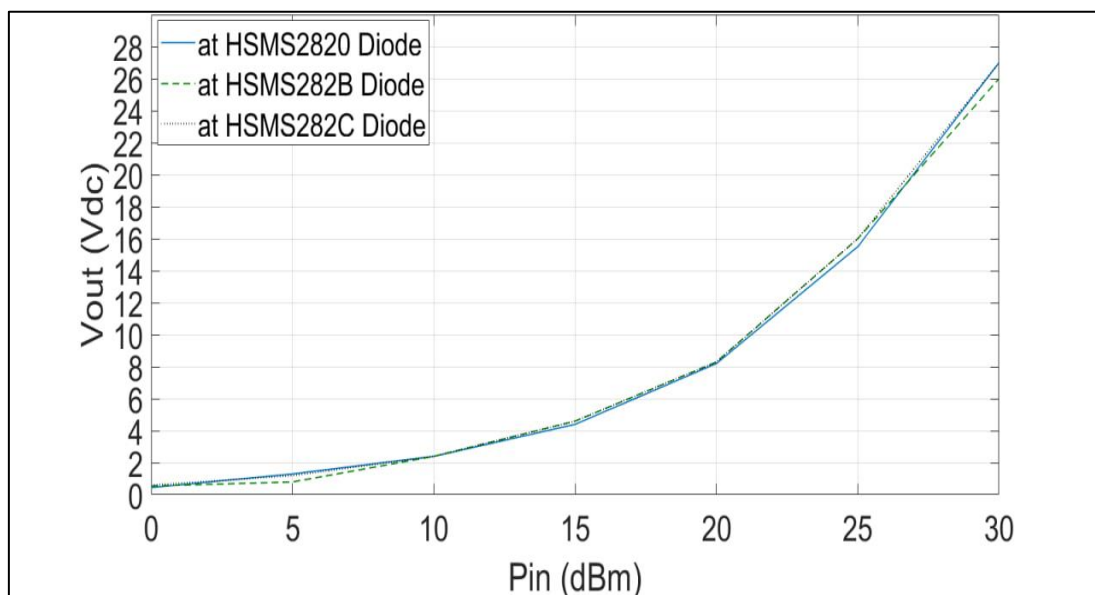


Fig. 3.43: V_{out} (V) versus P_{in} (dBm) of Graetz charge pump rectifier circuit for different Diodes at 2.4 GHz with LC-circuit.

Fig. 3.44 shows the comparison in V_{out} of the rectifier's performance when changing in ϵ_r , where 2.64, 3, 3.55, 4.3, 6, and 6.5 are utilized. It is obvious that the differences are almost negligible, except in the middle of P_{in} where there is only a slight difference noticed.

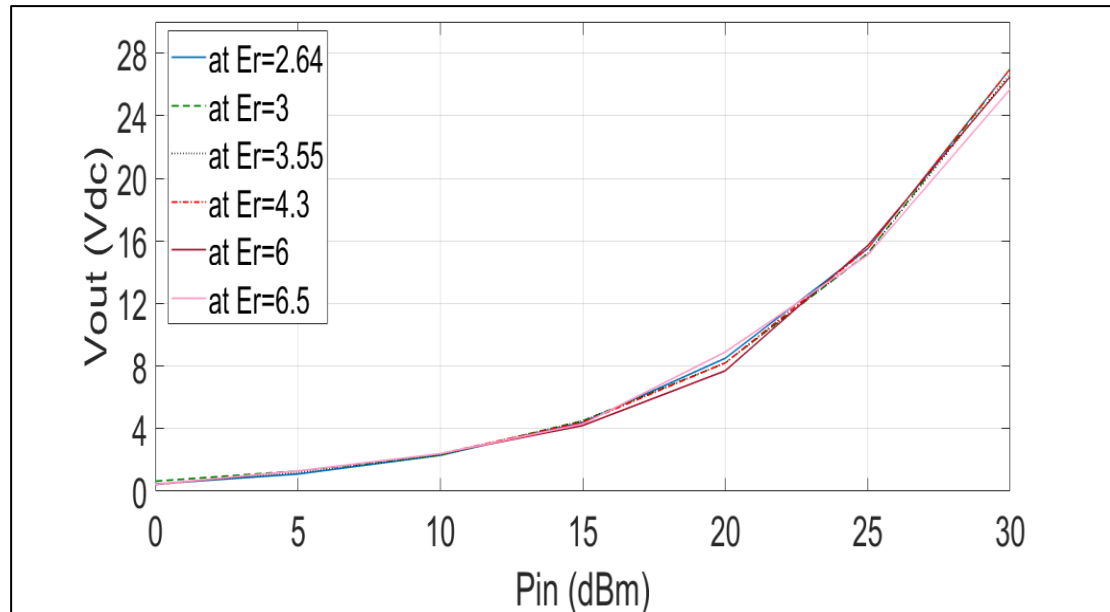


Fig. 3.44: V_{out} (V) versus P_{in} (dBm) of Graetz charge pump rectifier circuit for different ϵ_r at 2.4 GHz with LC-circuit.

Fig. 3.45 shows the comparison in efficiency (η) of the rectifier's performance when changing load resistance (from 1 to 5 k Ω). It has been found that the efficiency (η) decreases with an increase (R_L), with the highest (η) at (R_L) equal to 1 k Ω at 30 dBm of P_{in} , where the $\eta = 50\%$.

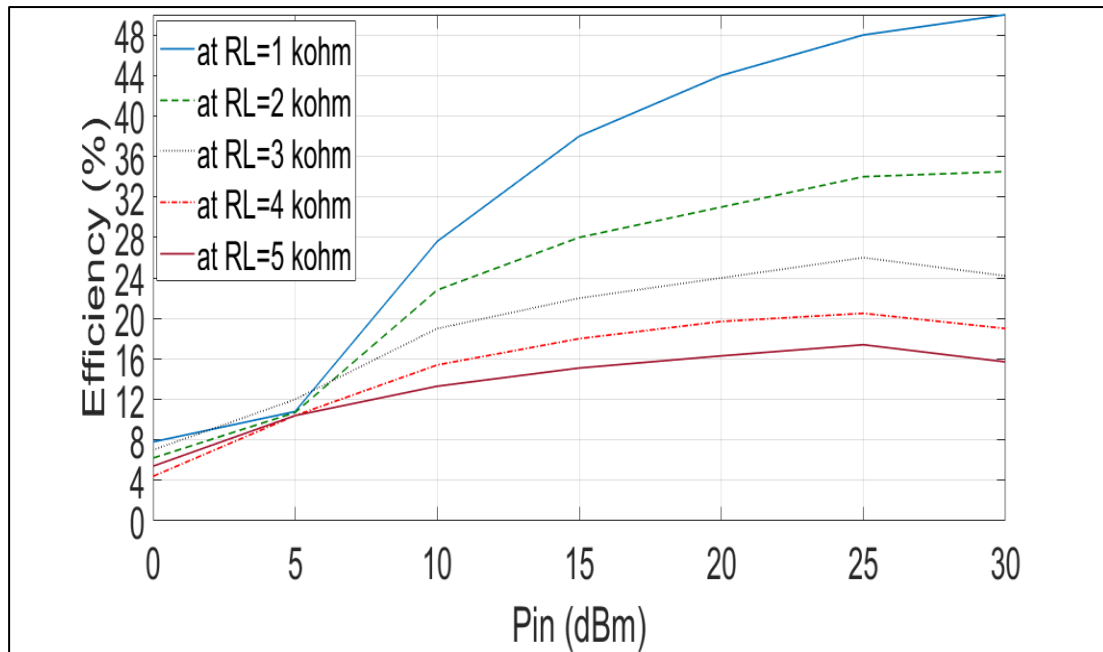


Fig. 3.45: Efficiency (η) vs. Pin (dBm) of Graetz charge pump rectifier circuit for different values of load (R_L) at 2.4 GHz with LC-circuit.

Fig. 3.46 shows the comparison in efficiency (η) of the rectifier's performance when changes in diodes are made, respectively. It has been investigated that the best efficiency (η) was with the use of the HSMS282B diode and the worst with the HSMS2820 diode especially at low input power (Pin).

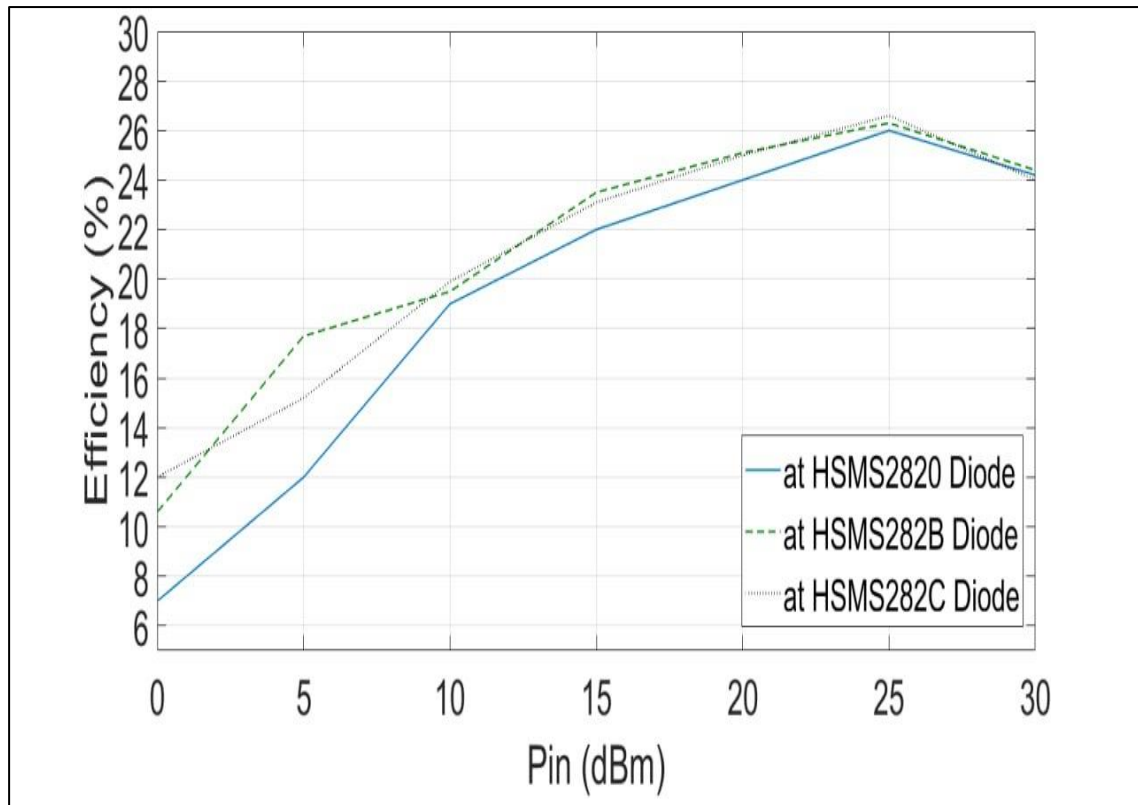


Fig. 3.46: Efficiency (η) versus Pin (dBm) of Graetz charge pump rectifier circuit for different Diodes at 2.4 GHz with LC-circuit.

Fig. 3.47 shows the comparison in efficiency (η) of the rectifier's performance when changes in ϵ_r are made. It has been clear that the efficiency (η) almost unchanged at different ϵ_r of substrate.

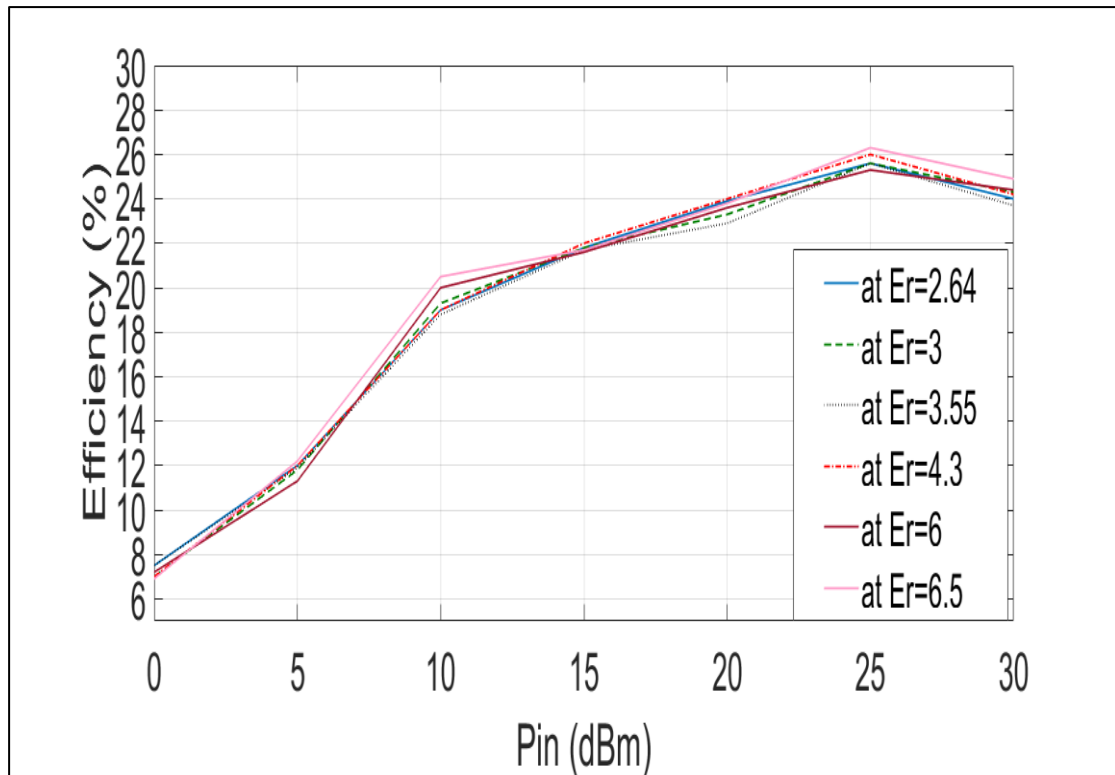


Fig. 3.47: Efficiency (η) versus Pin (dBm) of Graetz charge pump rectifier circuit for different ϵ_r at 2.4 GHz with LC-circuit.

3.7 Dickson charge pump rectifier circuit using LC-match method

The Dickson charge pump rectifier is based on the concept of cascading multiple stages of diode-capacitor voltage doublers. Each stage consists of a diode and a capacitor connected in series, as shown in Fig. 3.48. The S11 curve is excellent at 2.4 GHz, as shown in Fig. 3.49.

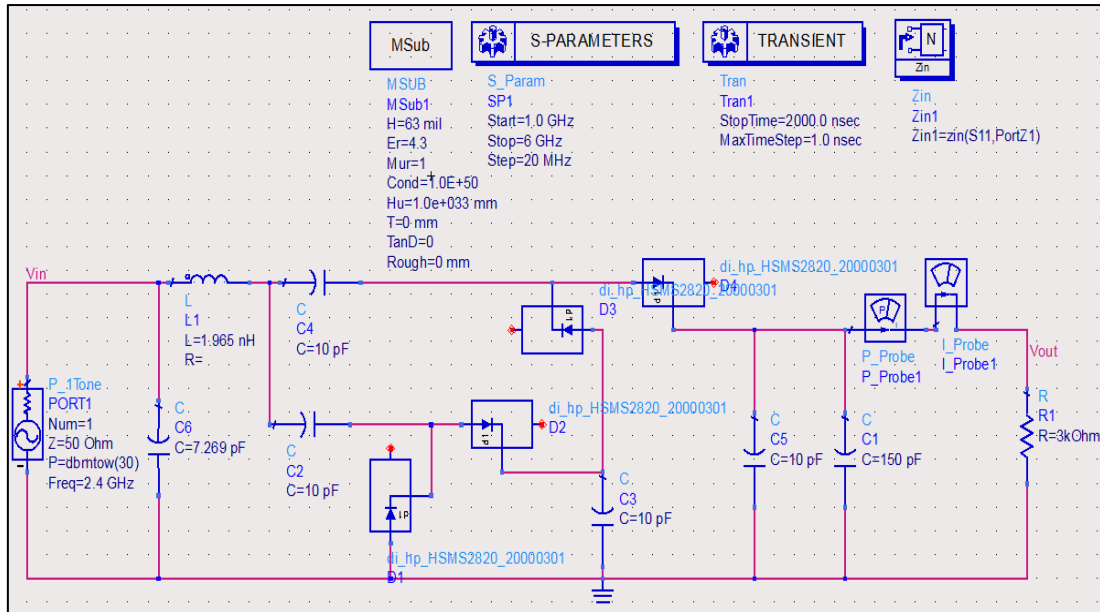


Fig. 3.48: Dickson charge pump rectifier circuit operating at 2.4 GHz with LC-circuit.

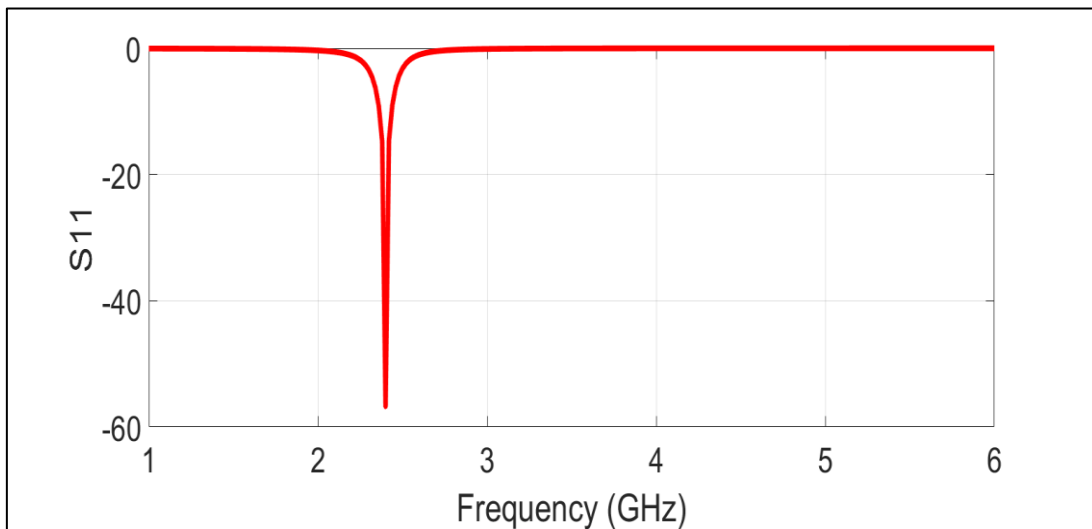


Fig. 3.49: Simulated S11 of Dickson charge pump rectifier circuit at 2.4 GHz with LC-circuit.

Fig. 3.50 shows the comparison in V_{out} of the rectifier's performance when changing the resistance load (R_L) (from 1 to 5 k Ω) with a step of 1 k Ω . It has been noticed that there is little impact on the V_{out} at low input power (P_{in}) while the impact is higher at higher input power (P_{in}), and a better V_{out} at higher R_L .

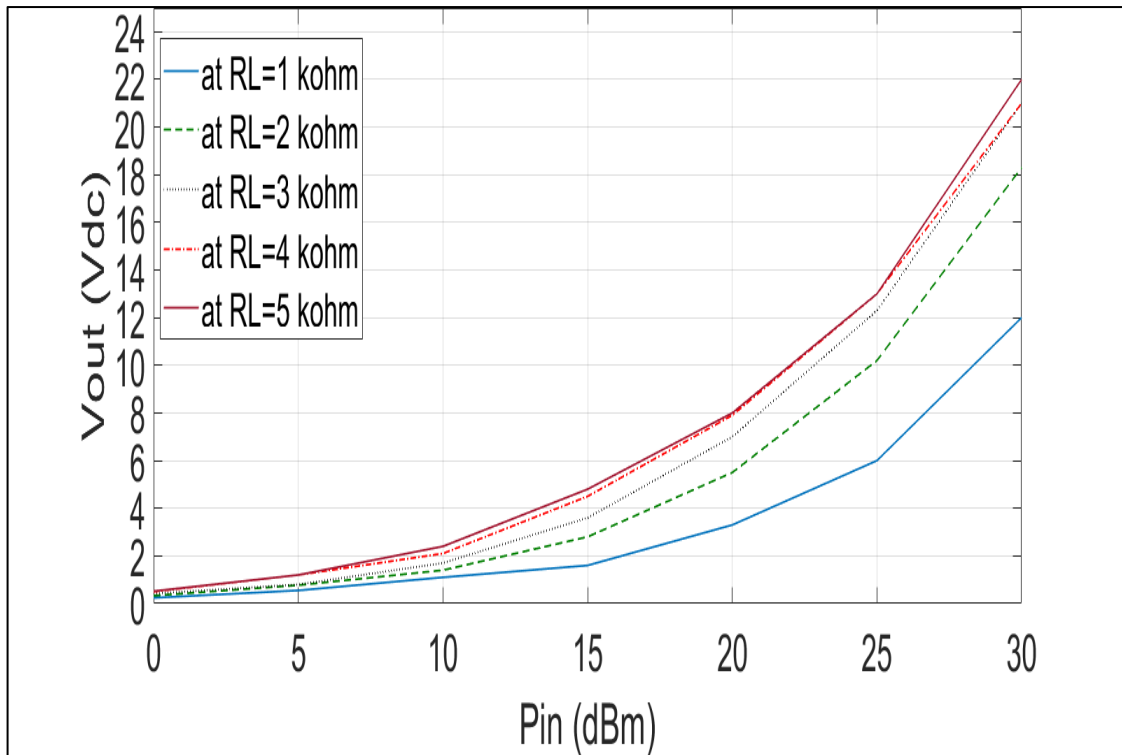


Fig. 3.50: V_{out} (V) versus P_{in} (dBm) of Dickson charge pump rectifier circuit for different values of resistance load (R_L) at 2.4 GHz with LC-circuit.

Fig. 3.51 shows the comparison in V_{out} of the rectifier's performance when changing diodes, where HSMS2820, HSMS282B, and HSMS282C diodes are used. It has been discovered that the diodes HSMS2820 and HSMS282B have similar performance while HSMS282C showed a very poor performance at this type of rectifiers.

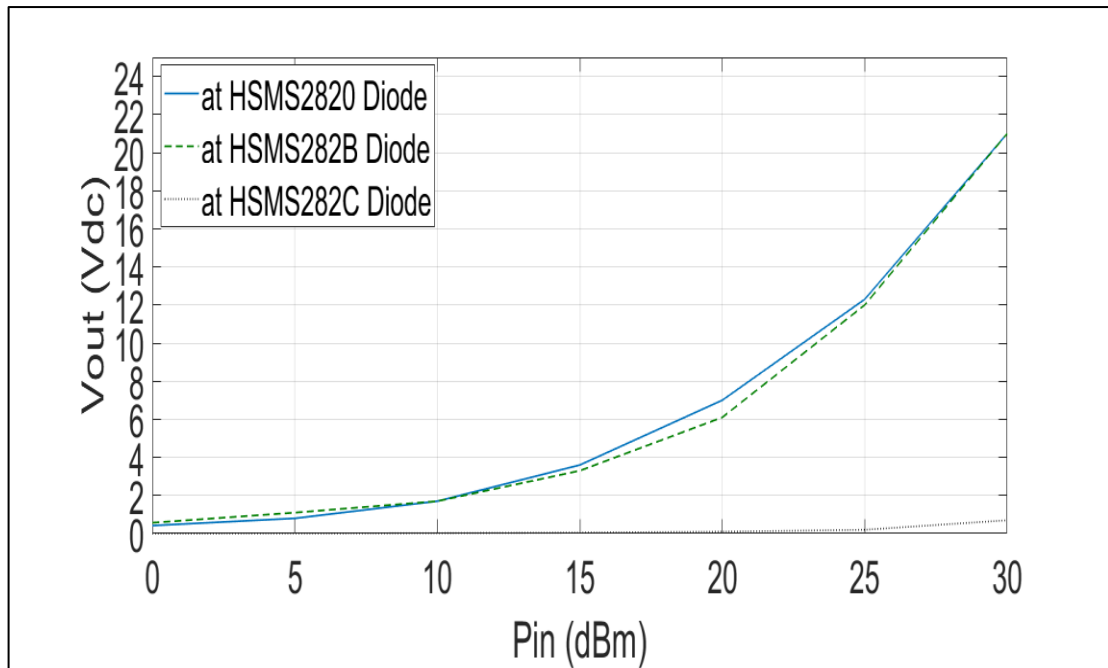


Fig. 3.51: Vout (V) versus Pin (dBm) of Dickson charge pump rectifier circuit for different Diodes at 2.4 GHz with LC-circuit.

Fig. 3.52 shows the comparison in Vout of the rectifier's performance when changing in ϵ_r , where 2.64, 3, 3.55, 4.3, 6, and 6.5 are used. It has been seen that the differences are almost negligible, except in the high of Pin where there is a trivial difference.

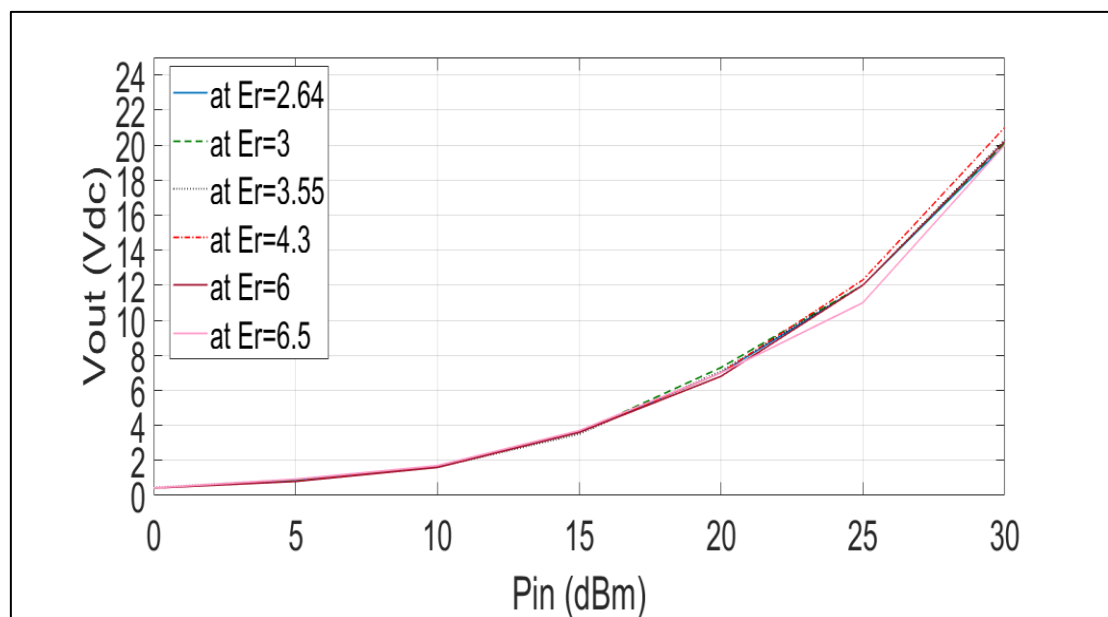


Fig. 3.52: Vout (V) versus Pin (dBm) of Dickson charge pump rectifier circuit for different ϵ_r at 2.4 GHz with LC-circuit.

Fig. 3.53 shows the comparison in efficiency (η) of the rectifier's performance when changes in resistance load (from 1 to 5 k Ω) are employed. It has been found that the efficiency (η) decreases at both sides (low and high) of P_{in} , except the highest (η) is achieved at (R_L) equals to 2 k Ω at 30 dBm of P_{in} , where the recorded value is $\eta = 16\%$.

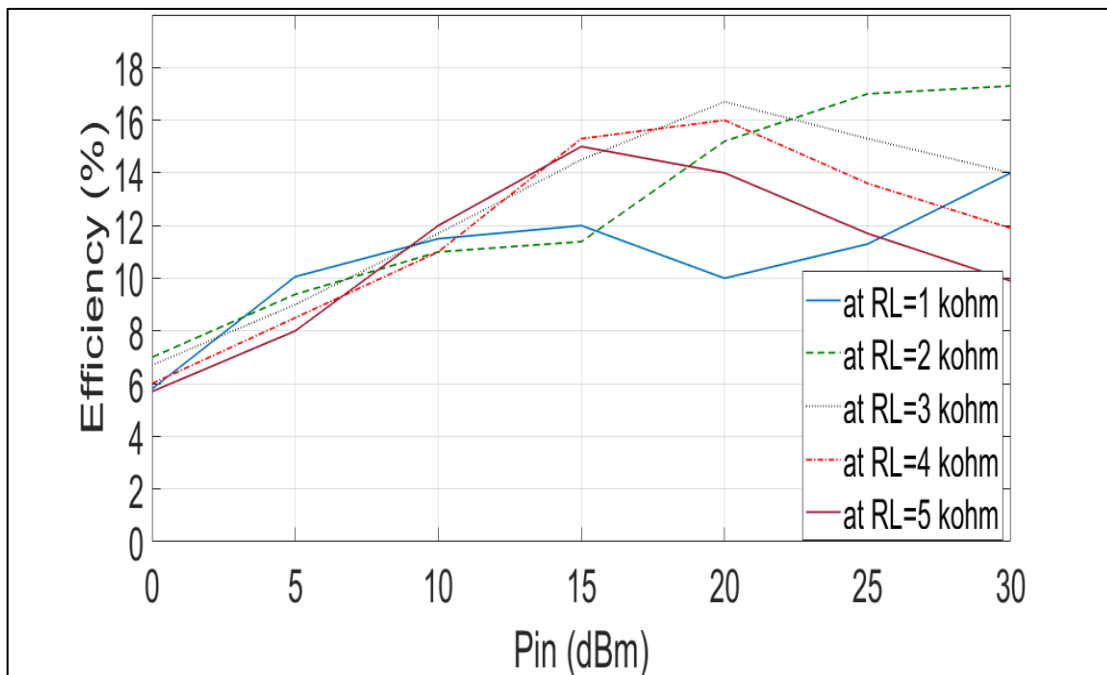


Fig. 3.53: Efficiency (η) versus P_{in} (dBm) of Dickson charge pump rectifier circuit for different values of resistance load (R_L) at 2.4 GHz with LC-circuit.

Fig. 3.54 shows the comparison in efficiency (η) of the rectifier's performance when changes in diode's type are made. It has been noted that the best efficiency (η) was with the use of the HSMS2820 diode and the worst with the HSMS282C diode.

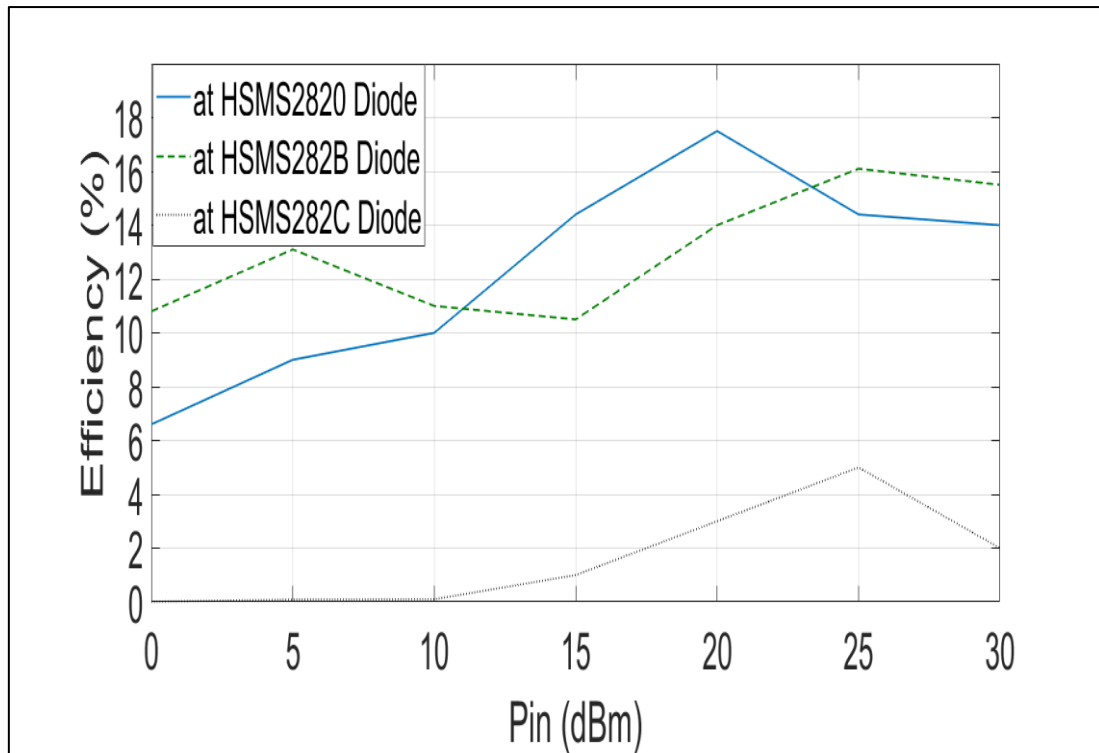


Fig. 3.54: Efficiency (η) versus Pin (dBm) of Dickson charge pump rectifier circuit for different Diodes at 2.4 GHz with LC-circuit.

Fig. 3.55 shows the comparison in efficiency (η) of the rectifier's performance when changes in ϵ_r are made. It has been investigated that the efficiency (η) almost differs by a different ϵ_r of substrate.

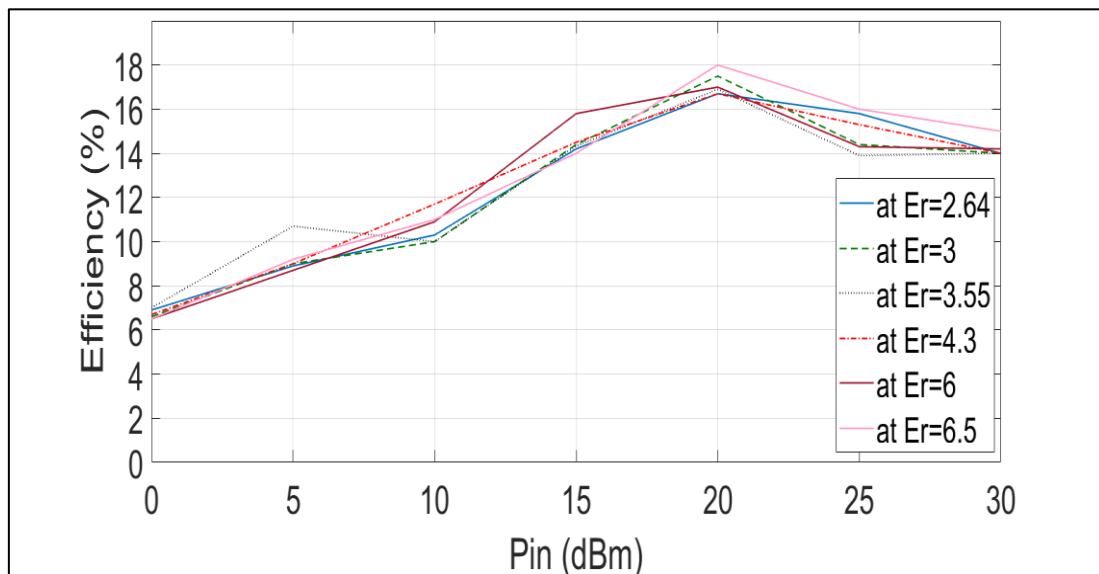


Fig. 3.55: Efficiency (η) versus Pin (dBm) of Dickson charge pump rectifier circuit for different ϵ_r at 2.4 GHz with LC-circuit.

Fig. 3.56 shows the comparison in V_{out} of the rectifier circuits performance at the resistance load ($3\text{ k}\Omega$), HSMS2820 diode, and ϵ_r equal to 4.3. It has been investigated that the highest V_{out} with the Graetz charge rectifier circuit is about 27 V.

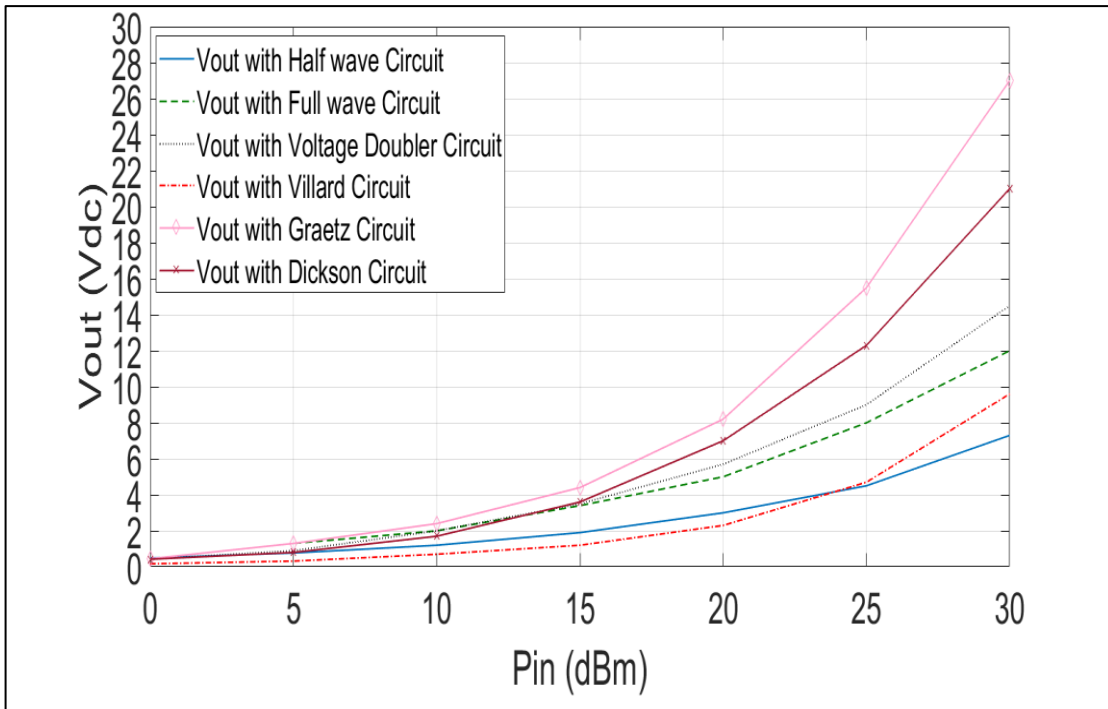


Fig. 3.56: V_{out} (V) versus P_{in} (dBm) of different rectifier circuits at 2.4 GHz with LC-circuit.

Fig. 3.57 shows the comparison in Efficiency (η) of the rectifier circuits performance at the resistance load ($3\text{ k}\Omega$), HSMS2820 diode, and ϵ_r equal to 4.3. It has been found that the highest η with the Graetz charge rectifier circuit is about 27%.

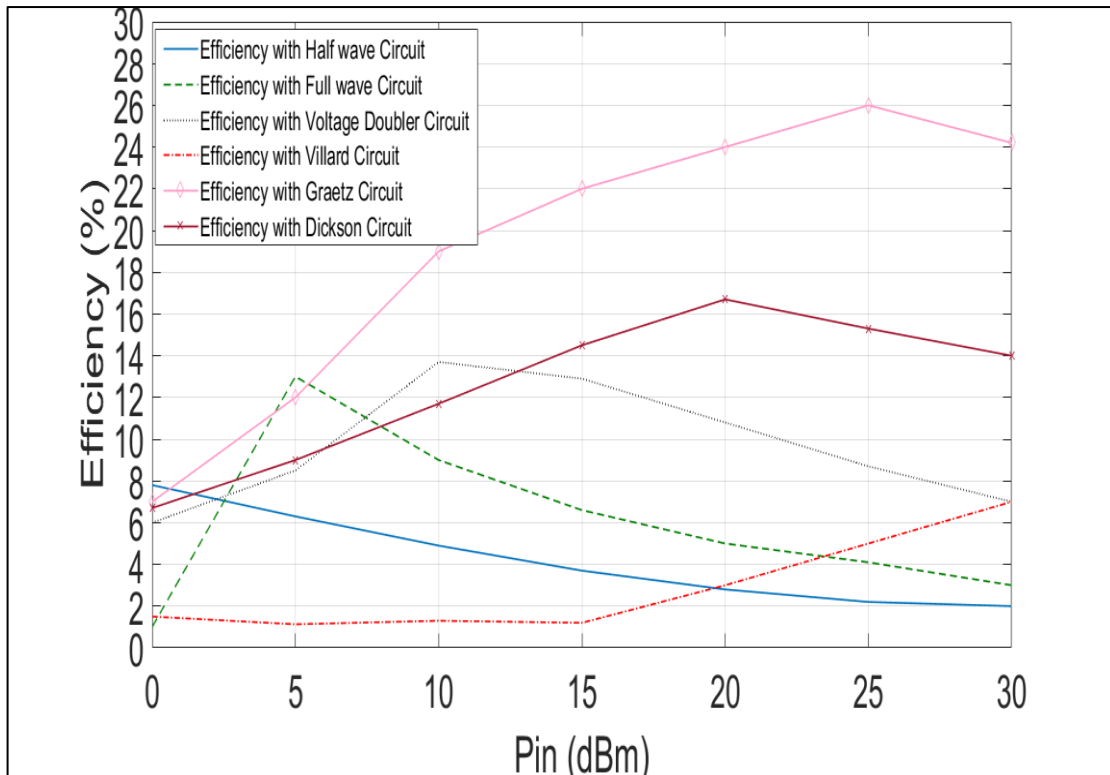


Fig. 3.57: Efficiency (η) versus P_{in} (dBm) of different rectifier circuits at 2.4 GHz with LC-circuit.

Table 3.1: The Efficiency (η) for different Rectifier circuits at 10 and 30 dBm of input power (P_{in}).

Rectifier circuits	Efficiencies (η) at $P_{in}= 10$ dBm	Efficiencies (η) at $P_{in}= 30$ dBm
Graetz charge pump	19%	24%
Voltage doubler	13%	7%
Dickson charge pump	12%	14%
Full-wave	9%	3%
Half-wave	5%	2%
Villard charge pump	1%	7%

CHAPTER FOUR

The Rectifier Circuits with TL-match method Compared with LC-match Method at 2.4 GHz

4.1 Impedance Matching Circuit using TL-match method

ADS is utilized to determine the matching at a certain frequency; however, this time, a Transmission Line (TL) matching for instance, the Graetz charge pump is utilized as a substitute for an LC matching since it produces a superior match and is simpler to manufacture. In order to modify the transmission lines at a certain frequency, such as 2.4 GHz, the steps listed below should be precisely followed:

Step 1: As shown in the circuit design in Fig. 4.1, start by using the Smith chart palette with two impedance terms.

Step 2: Utilizing two lines of length and two open stub blocks, choose the frequency at 2.4 GHz, source impedance (Z_{in}) at $50+j0$, and load impedance (Z_L) at $6.391-j77.056$ from the Smith chart circuit. The four TL blocks that first appeared at the location of (Z_L) in the Smith Chart Utility will be calibrated and then pull out the TL1 from the point of (Z_L) until it reaches the first arc that faces the Smith Chart. After that, pull out the TL2 from the TL1's end arc to the first arc that faces, the TL3 from the TL2's end arc to the first arc that faces, and lastly, pull out the TL4 from the TL3's end arc until it meets the Smith Chart's zero (reference) point. This will result in an excellent match of S_{11} at 2.4 GHz, as shown in Fig. 4.2.

Step 3: After modifying the S11 at 2.4 GHz, click the "Build ADS Circuit" button on the Smith chart to demonstrate the transmission line block diagram shown in Fig. 4.3.

Step 4: Using the Synthesize property in the LineCalc window of ADS, as illustrated in Fig. 4.4, determine the dimensions (W and L) for four blocks that are labeled with TL1, TL2, TL3, and TL4, respectively, based on the previous information in the block diagram of transmission lines.

Step 5: Lastly, open the LinCalc window to determine the dimensions (W and L) of each block of the matching network circuit at 2.4 GHz, which is composed of four TL blocks, as shown in Fig. 4.5.

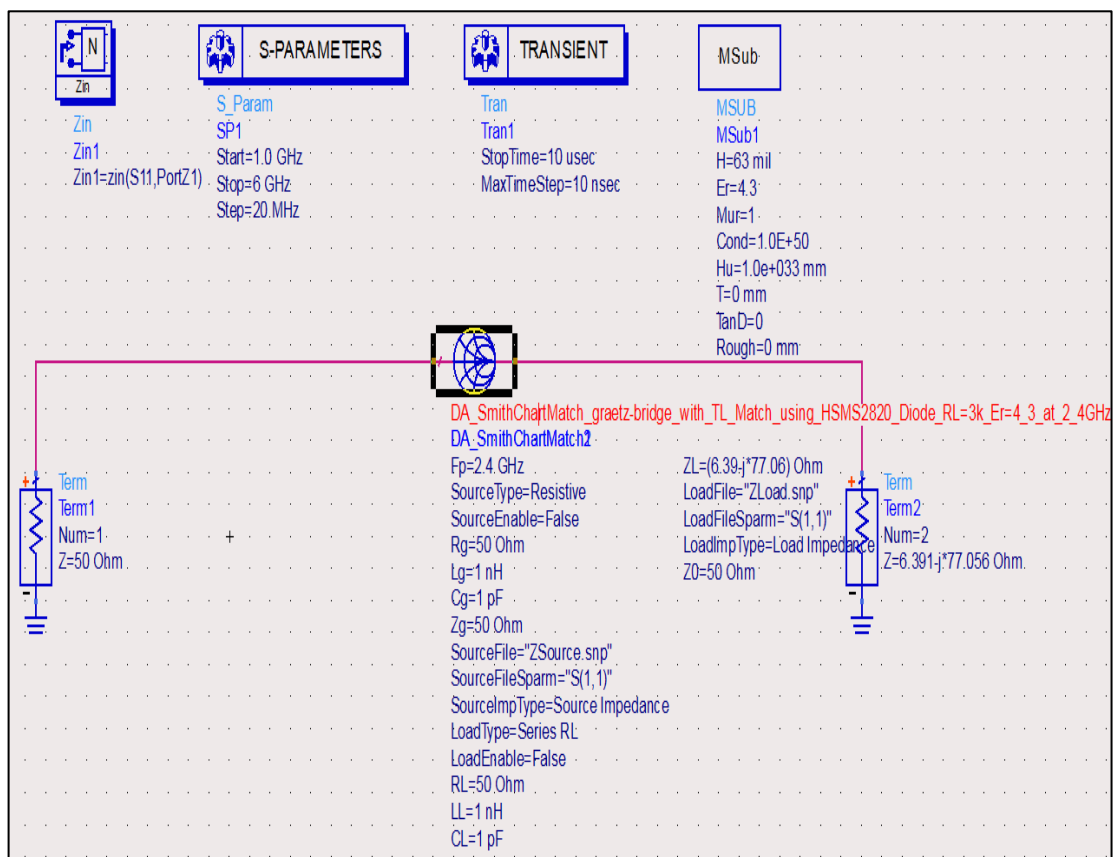


Fig. 4.1: Tools of Smith chart.

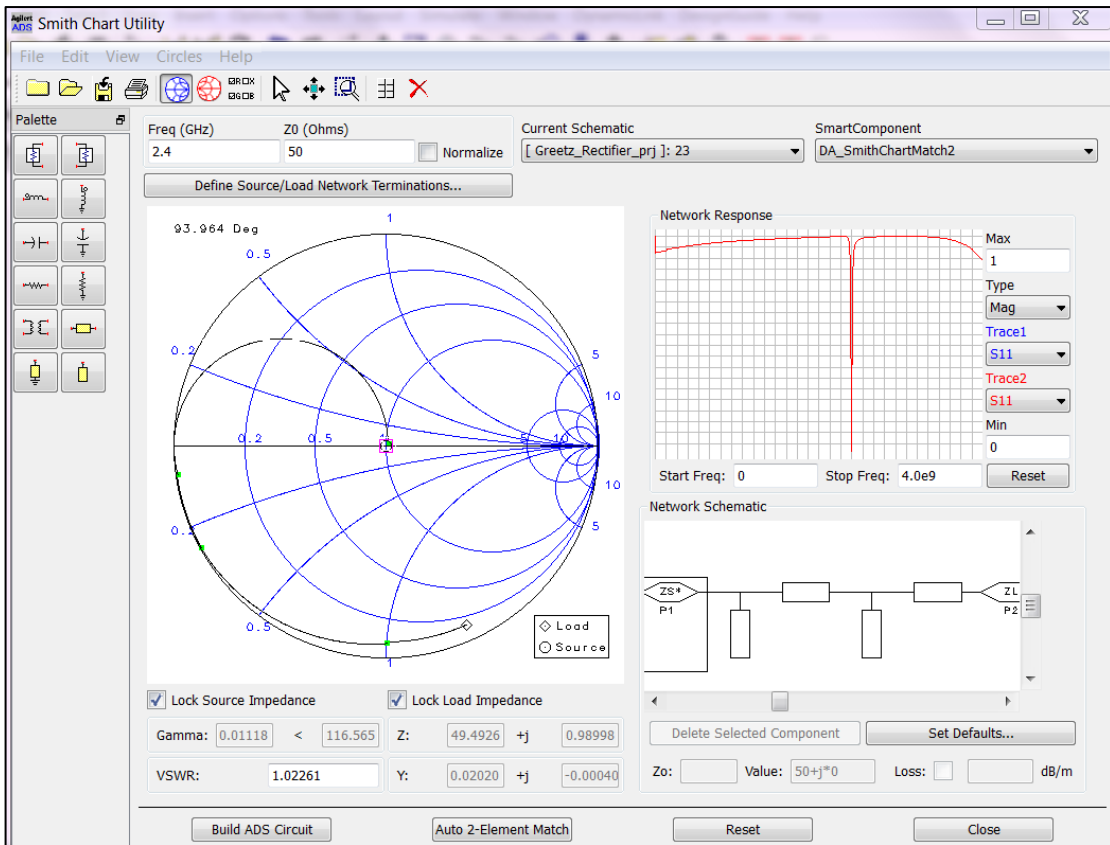


Fig. 4.2: Window of the Smith chart in ADS.

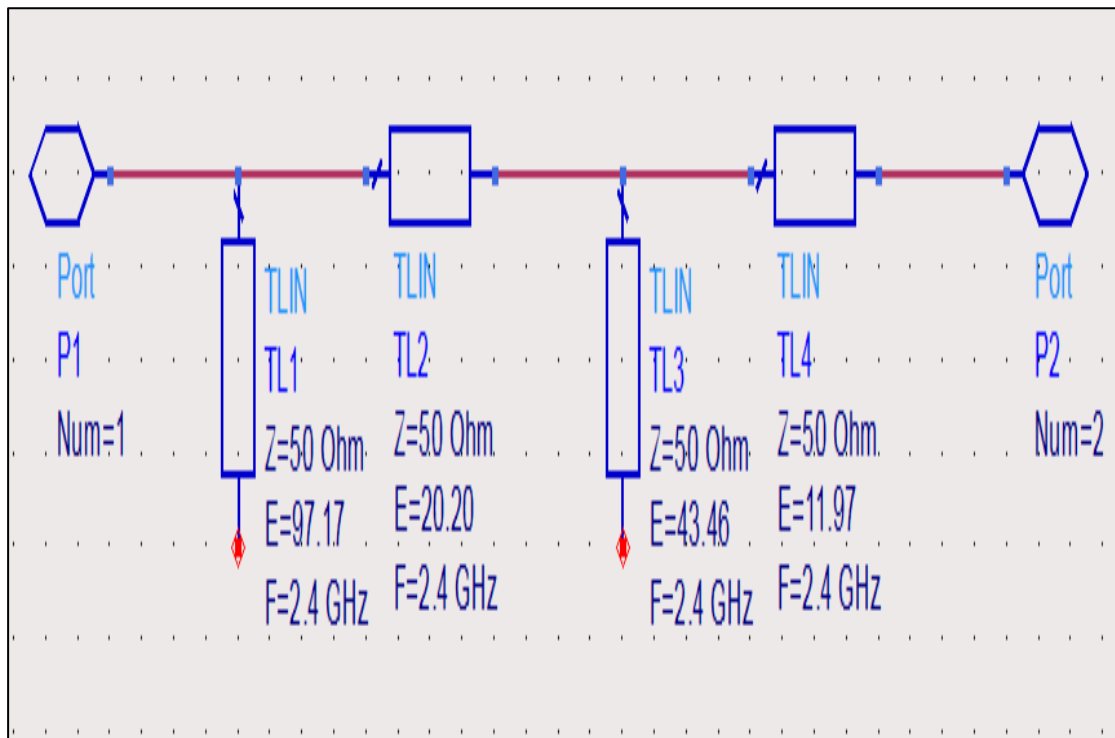


Fig. 4.3: Block diagram of Transmission Lines.

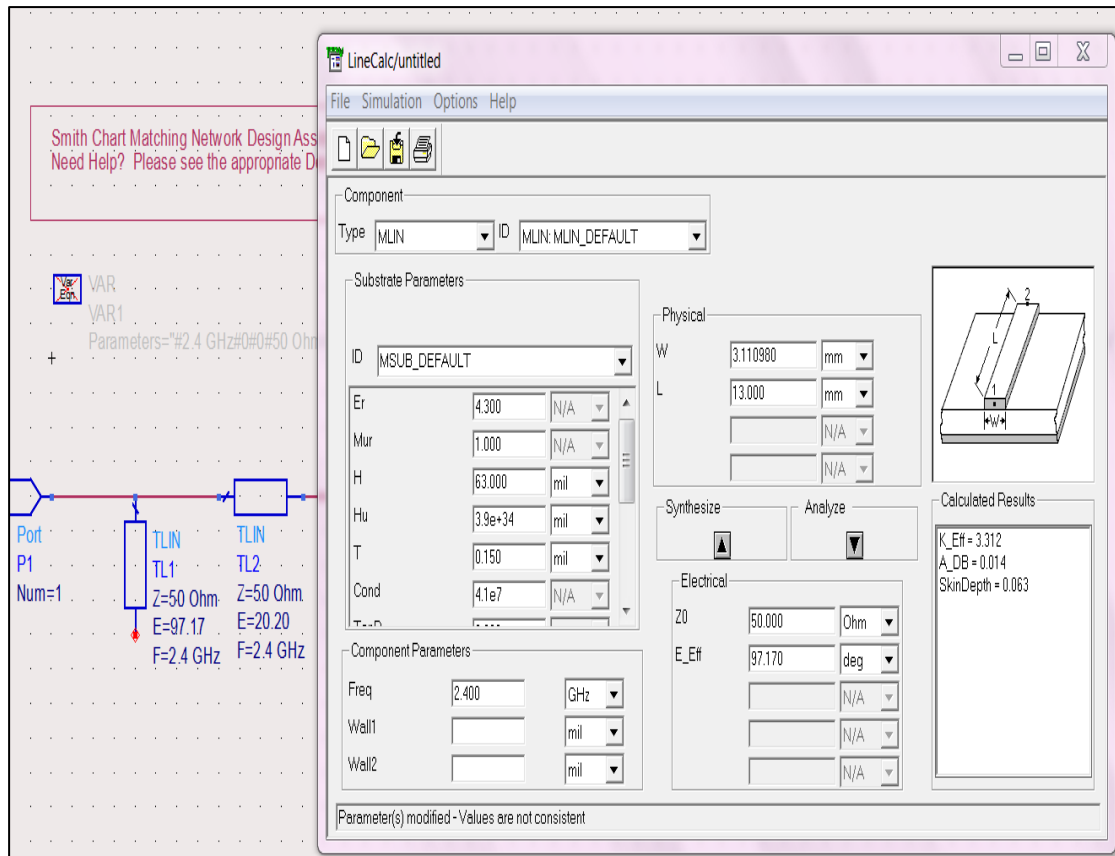


Fig. 4.4: Window of the LineCalc to compute Width and Length.

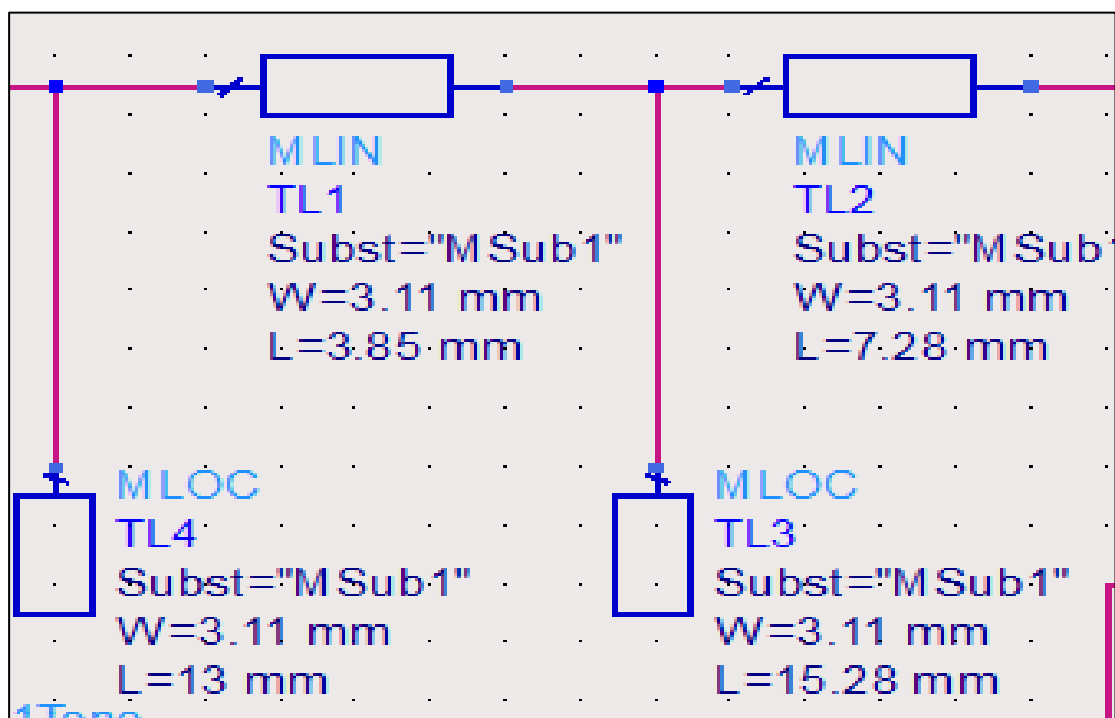


Fig. 4.5: Simulated Block diagram of Transmission Lines (TL) at 2.4 GHz.

4.2 Half-wave rectifier circuit using TL-match method

Impedance matching can also be implemented by applying the Smith Chart feature found in ADS software. As shown in Fig. 4.6, this technique matches the rectifier circuit to the source by using transmission line stubs at the circuit's input port. The transmission line stubs' length (L) and width (W) are critical factors in determining the quality of impedance matching. The rectifier circuit's simulated S11 at 2.4 GHz with TL-match method is shown in Fig. 4.7. At the given frequency, the return loss value dropped to below -29 dB.

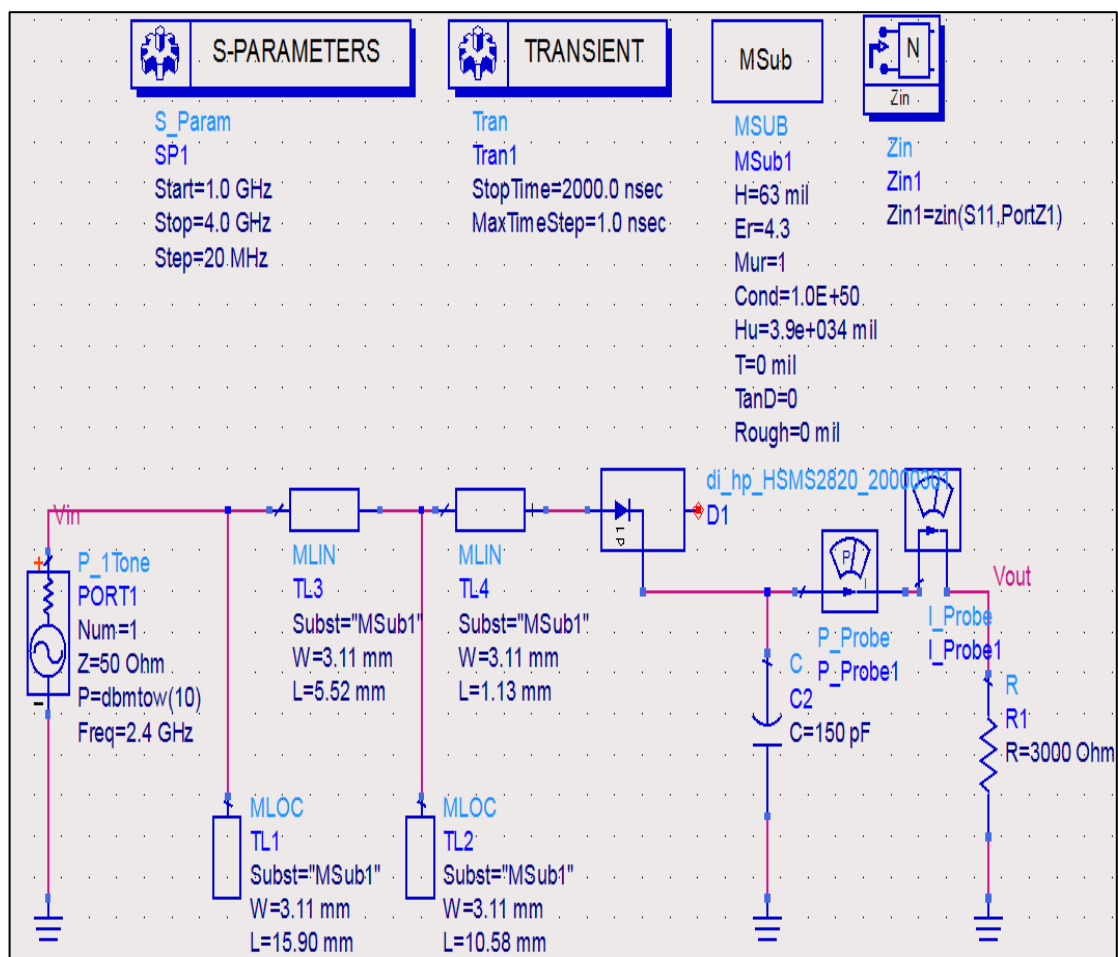


Fig. 4.6: Half-wave rectifier circuit operating at 2.4 GHz with TL-circuit.

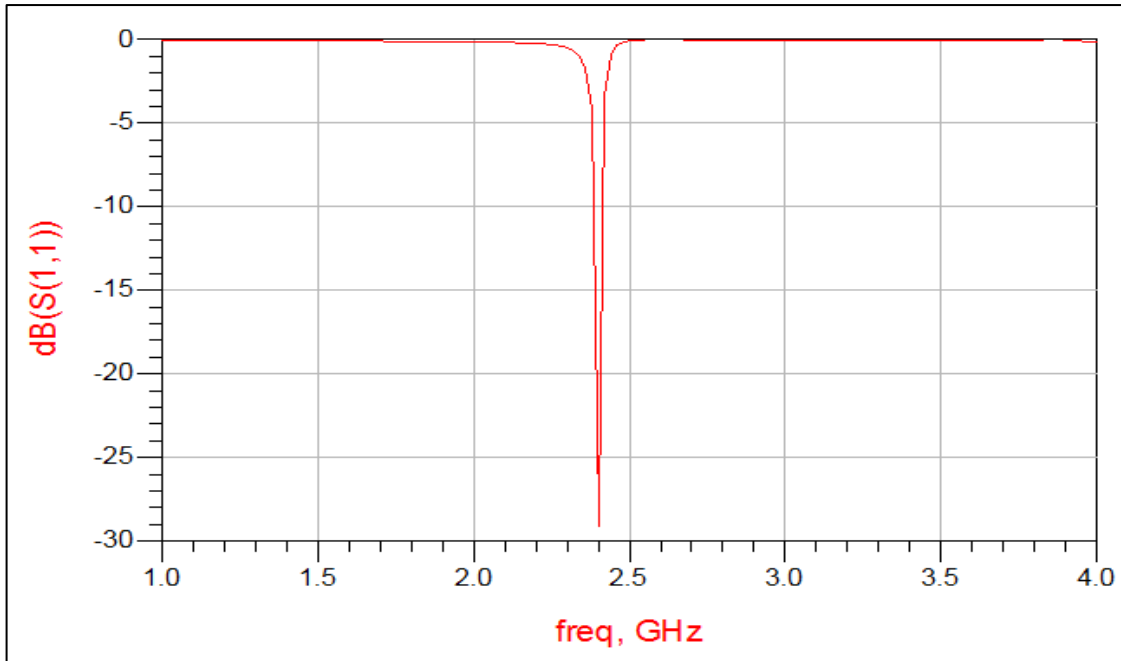


Fig. 4.7: Simulated S11 of half-wave rectifier circuit at 2.4 GHz with TL-circuit.

Fig. 4.8 displays the input voltage waveform that is fed to the half-wave rectifier circuit in the 2.4 GHz frequency band with a TL-circuit.

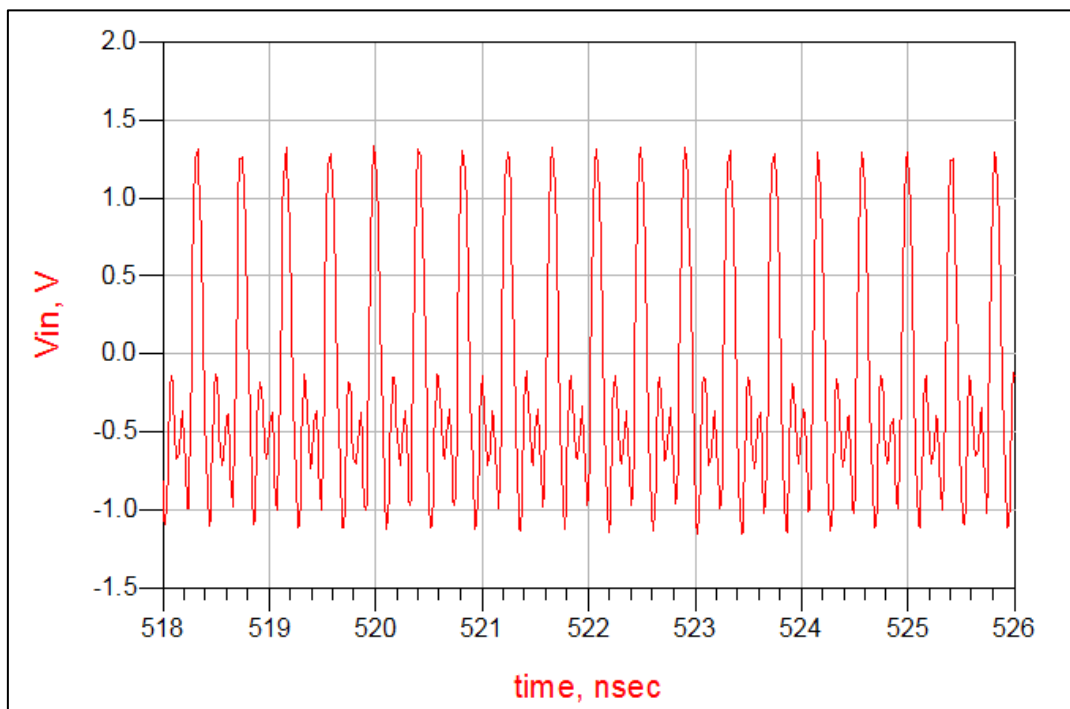


Fig. 4.8: Vin (Volt) vs. Time (nS) of half-wave rectifier circuit at 2.4 GHz with TL-circuit.

Fig. 4.9 illustrates the output voltage waveform for a half-wave rectifier circuit at 2.4 GHz. The achieved DC output voltage is around 10.8 V, as shown in Fig. 4.9.

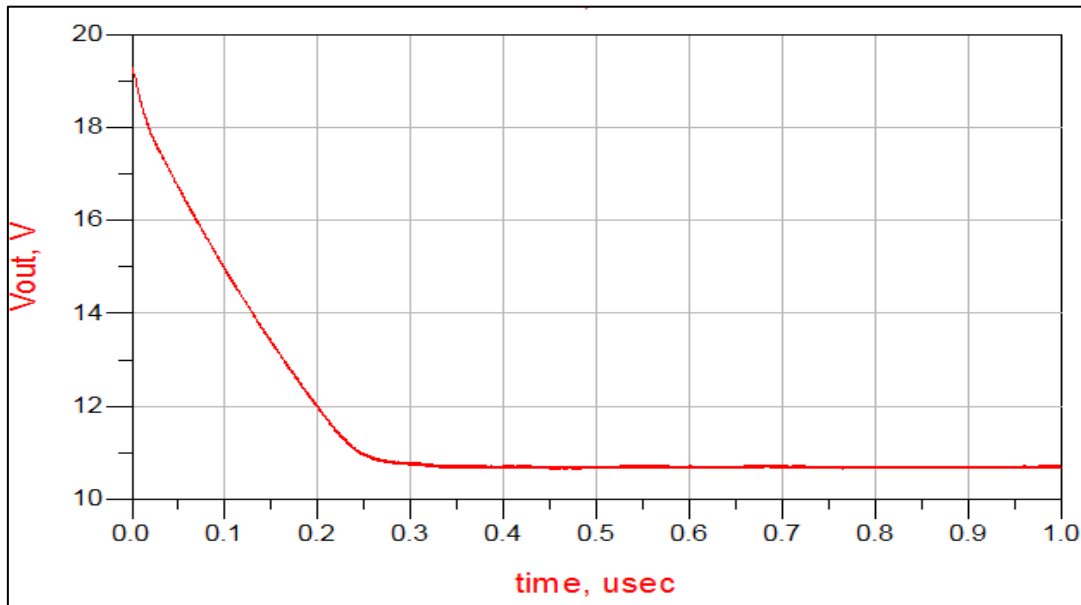


Fig. 4.9: V_{out} (V) of half-wave rectifier circuit at 2.4 GHz with TL-circuit.

Fig. 4.10 displays the waveform of output current for the half-wave rectifier circuit at 2.4 GHz. The output current is about 3.6 mA.

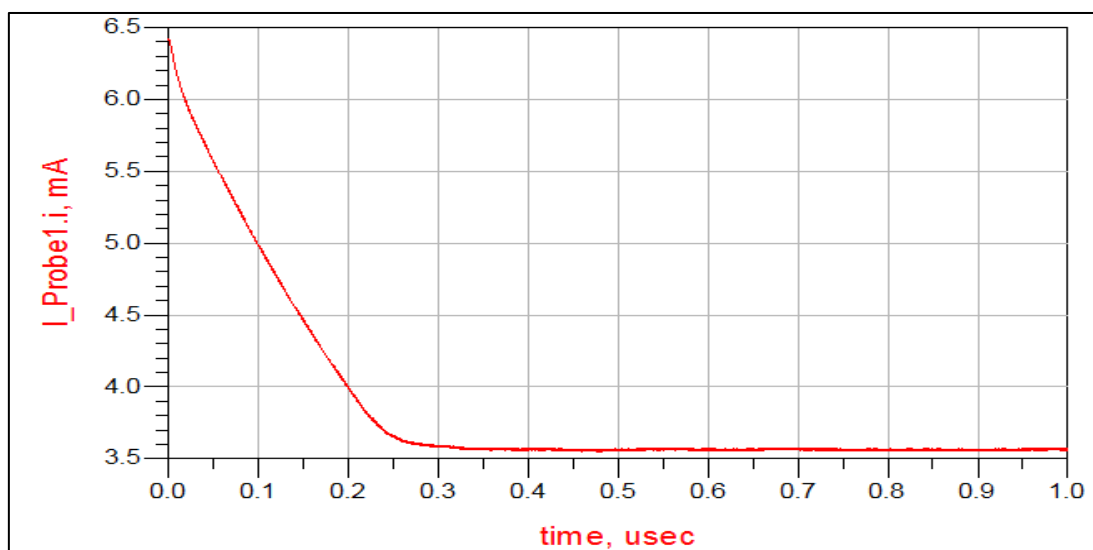


Fig. 4.10: Output current of half-wave rectifier circuit at 2.4 GHz with TL-circuit.

Fig. 4.11 shows the comparison in V_{out} of the rectifier's performance when using the LC-match method and the TL-match method. It has been investigated that there is little impact on the V_{out} at low input power (P_{in}) on the contrary at high input power (P_{in}), where using the TL-match method is higher in terms of V_{out} than using the LC-match method.

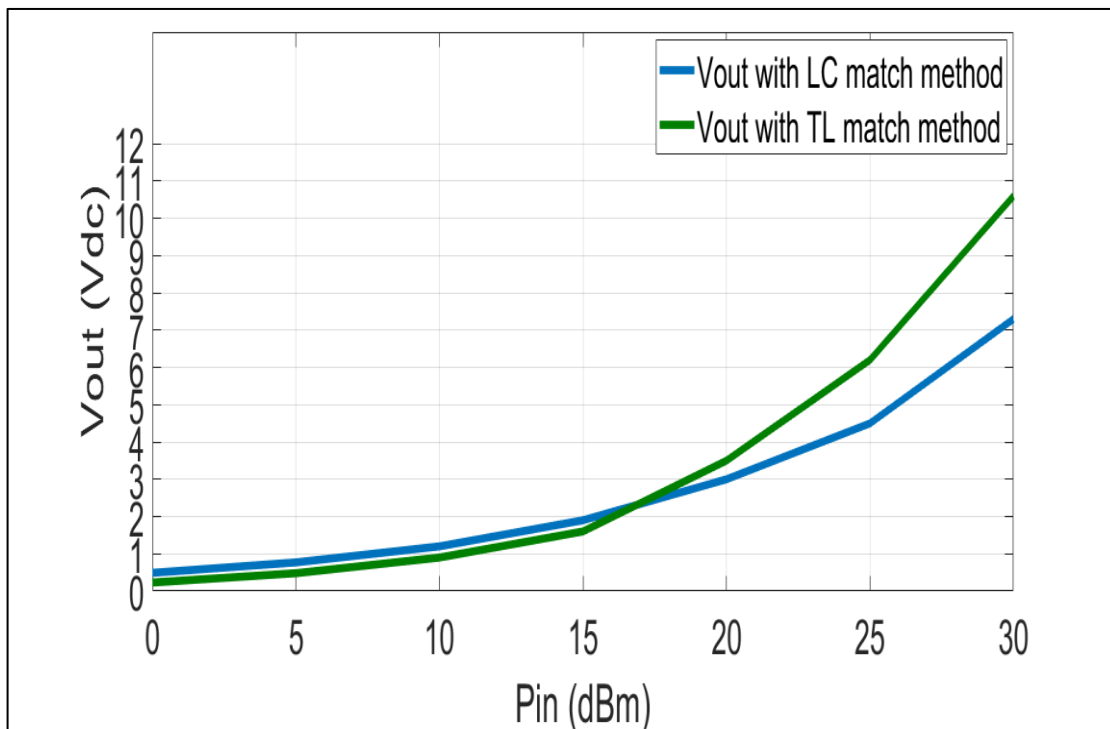


Fig. 4.11: V_{out} (V) versus P_{in} (dBm) of comparison between a half-wave rectifier circuit with an LC-circuit and a TL-circuit at 2.4 GHz.

Fig. 4.12 shows the comparison in efficiency (η) of the rectifier's performance when using the LC-match method and the TL-match method. It has been concluded that using the LC-match method provides higher efficiency (η) than using the TL-match method at low input power (P_{in}). On the other hand, at high input power (P_{in}), it is noticed that using the TL-match method provides higher efficiency (η) than using the LC-match method.

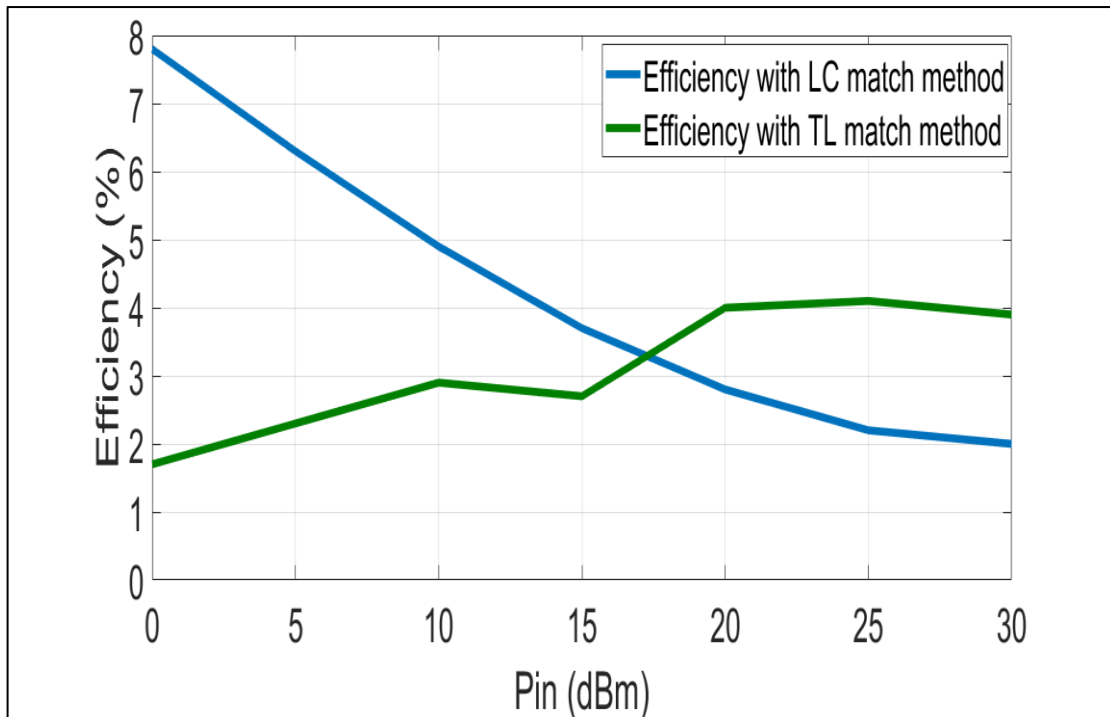


Fig. 4.12: Efficiency (η) versus Pin of comparison between a half-wave rectifier circuit with an LC-circuit and a TL-circuit at 2.4 GHz.

4.3 Full-wave rectifier circuit using TL-match method

The Smith Chart feature of ADS software may also be used to design the full-wave rectifier circuit with transmission line (TL) impedance matching. This method uses transmission line stubs at the circuit's input port to match the rectifier circuit to the source, as seen in Fig. 4.13. The width (W) and length (L) of the transmission line stubs are important parameters that affect how well the impedance matching works. Fig. 4.14 displays the rectifier circuit's simulated S11 at 2.4 GHz using the TL-match approach. The reflection coefficient value decreased to less than -15 dB at the specified frequency.

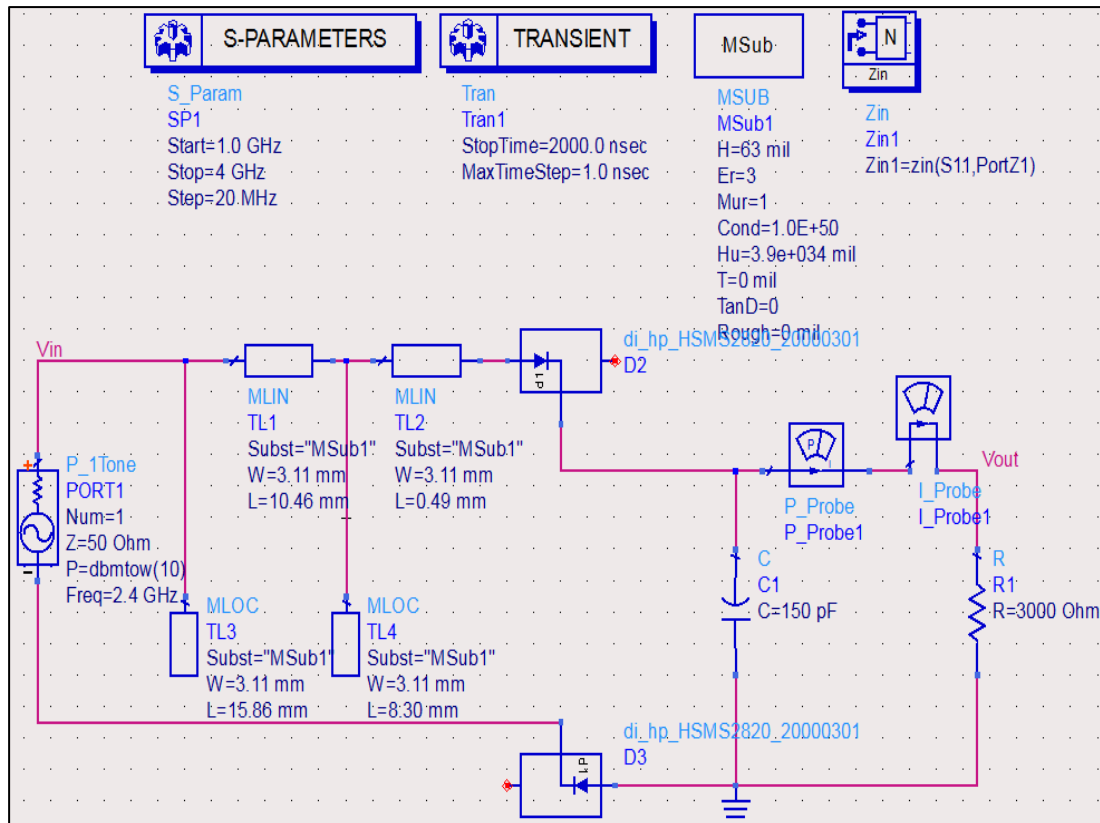


Fig. 4.13: Full-wave rectifier circuit operating at 2.4 GHz with TL-circuit.

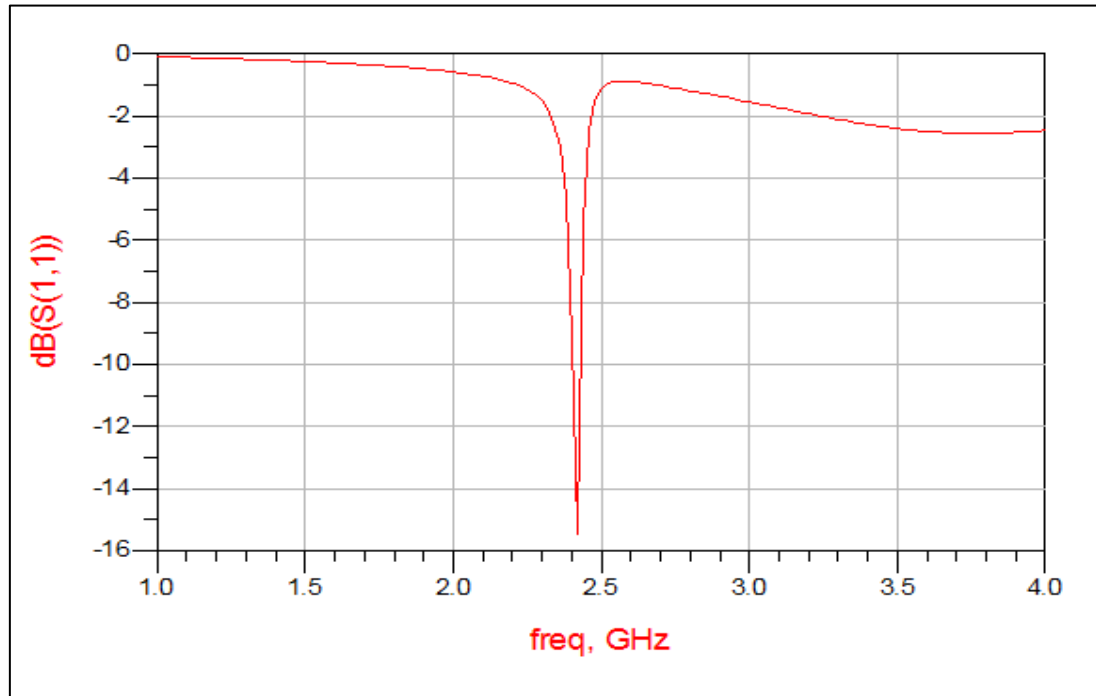


Fig. 4.14: Simulated S11 of full-wave rectifier circuit at 2.4 GHz with TL-circuit.

Fig. 4.15 shows the comparison in V_{out} of the rectifier's performance when using the LC-match method and the TL-match method. It has been investigated that using the TL-match method is higher in terms of V_{out} than using the LC-match method almost for all input power (P_{in}), except for high input power (P_{in}) between 25 and 30 dBm.

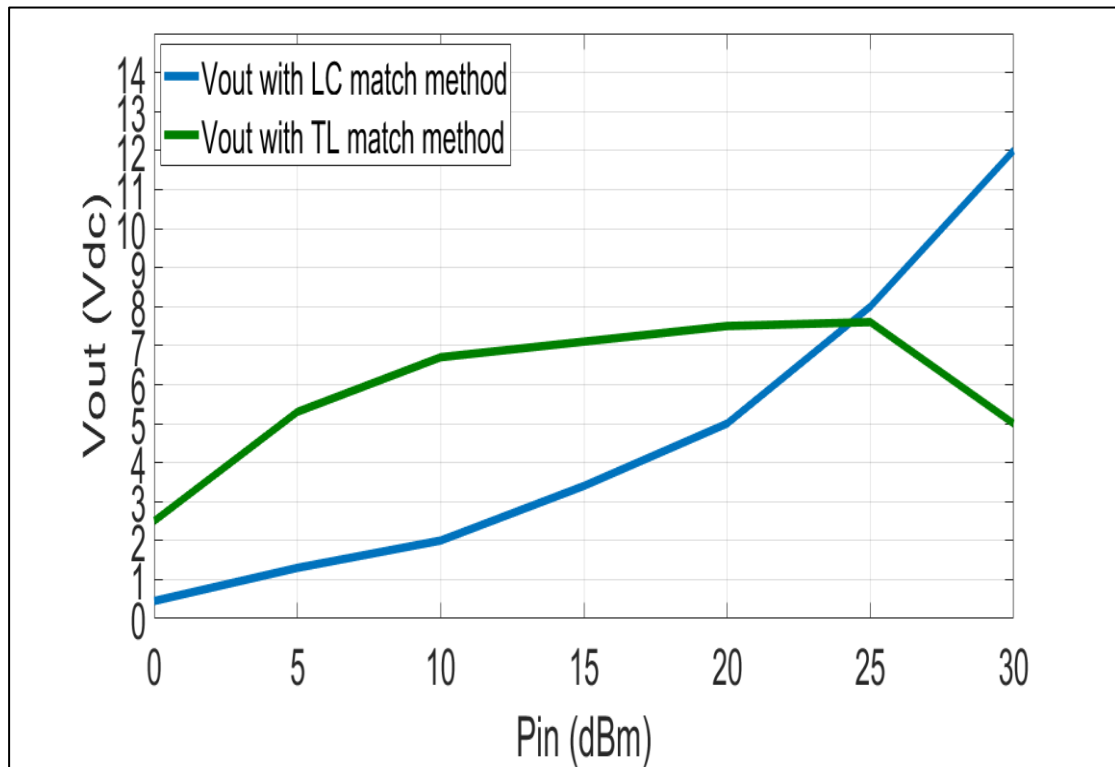


Fig. 4.15: V_{out} versus P_{in} of comparison between a full-wave rectifier circuit with an LC-circuit and a TL-circuit at 2.4 GHz.

Fig. 4.16 shows the comparison in efficiency (η) of the rectifier's performance when using the LC-match method and the TL-match method. It has been investigated that using the LC-match method is higher in terms of efficiency (η) than using the TL-match method at low input power (P_{in}); on the other hand, at high input power (P_{in}), using the TL-match method is bigger in terms of efficiency (η) than using the LC-match method. The higher recorded efficiency was 13% at 5 dBm of input power when using the LC-match method.

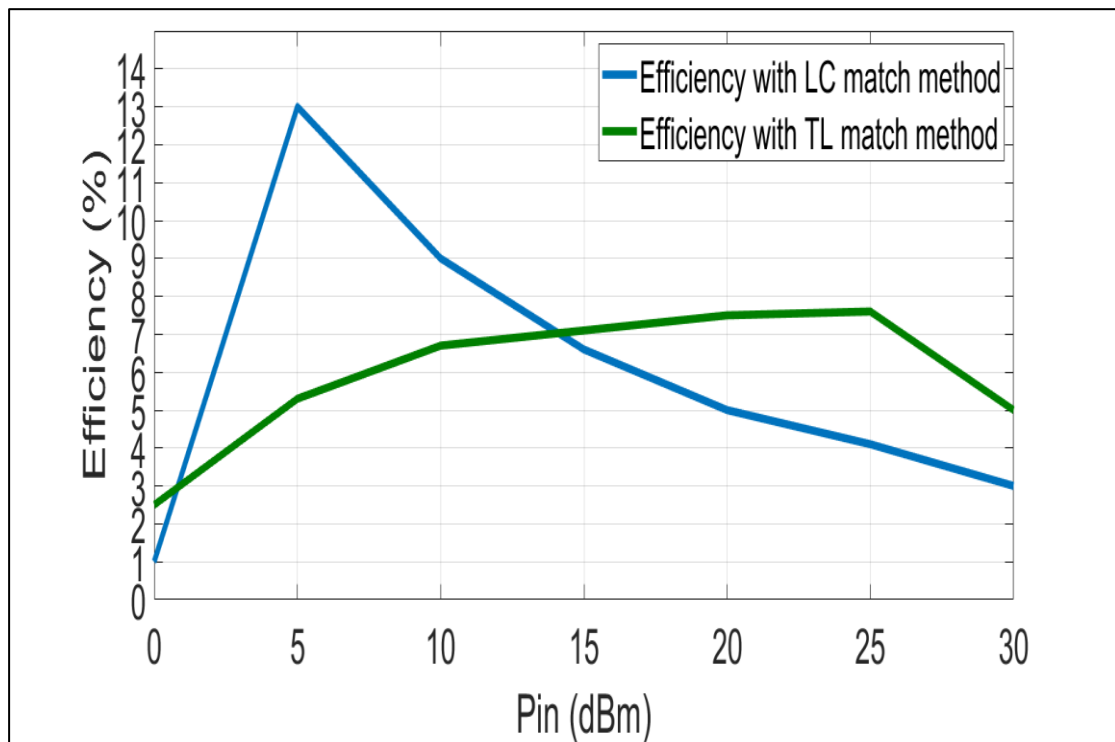


Fig. 4.16: Efficiency (η) versus Pin of comparison between a full-wave rectifier circuit with an LC-circuit and a TL-circuit at 2.4 GHz.

4.4 Voltage doubler rectifier circuit using TL-match method

The voltage doubler rectifier circuit with transmission line (TL) impedance matching is also constructed using the Smith Chart function of the ADS program as shown in Fig. 4.17. The simulated S11 of the rectifier circuit using the TL-match method is shown in Fig. 4.18 at 2.4 GHz. At the given frequency, the reflection coefficient value dropped to less than -38 dB, which means the validity of the execution procedure of the simulation in ADS software.

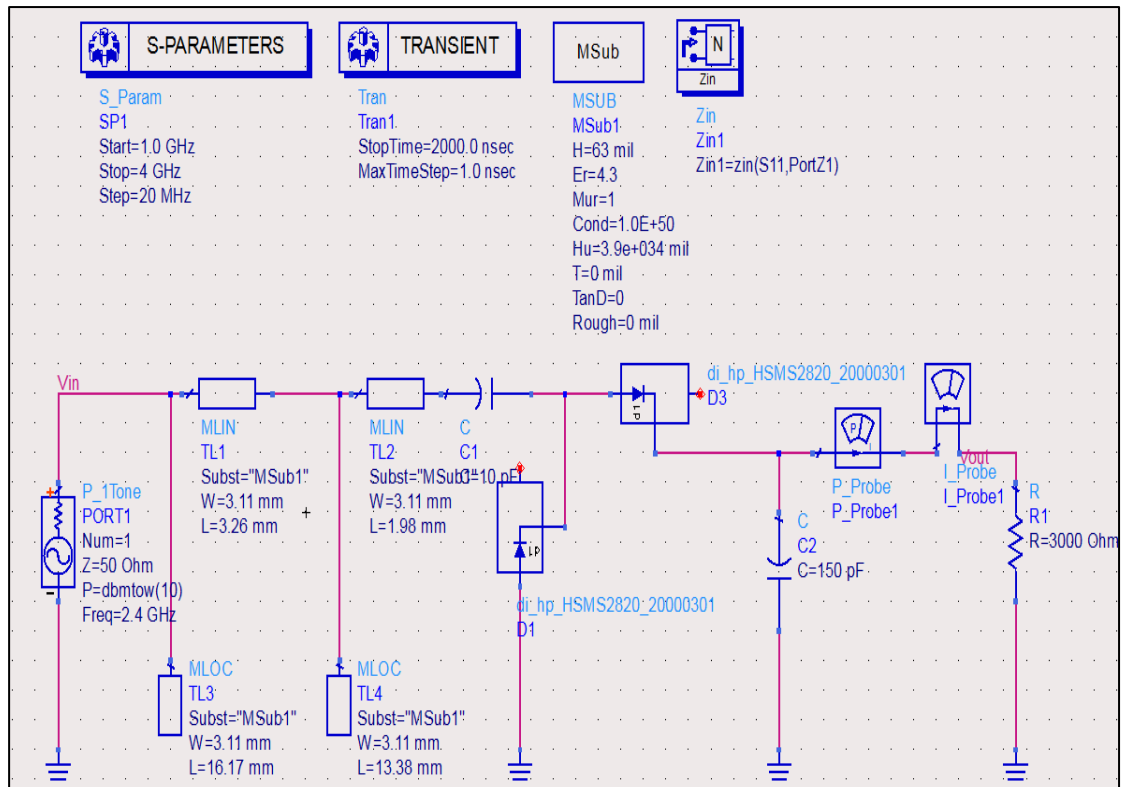


Fig. 4.17: Voltage doubler rectifier circuit operating at 2.4 GHz with TL-circuit.

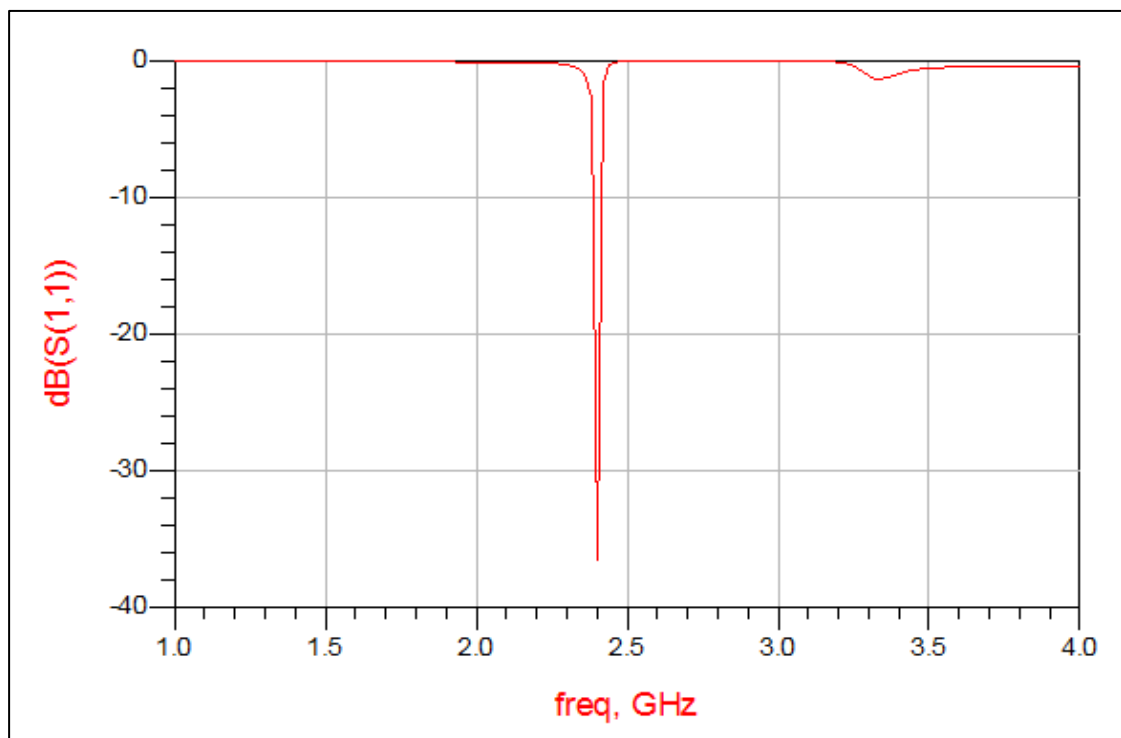


Fig. 4.18: Simulated S11 of voltage doubler rectifier circuit at 2.4 GHz with TL-circuit.

Fig. 4.19 shows the comparison in V_{out} of the rectifier's performance when using the LC-match method and the TL-match method. It has been found that there is little difference in terms of V_{out} at low input power (P_{in}); on the other hand, for high input power (P_{in}), the TL-match method has higher values than the LC-match method.

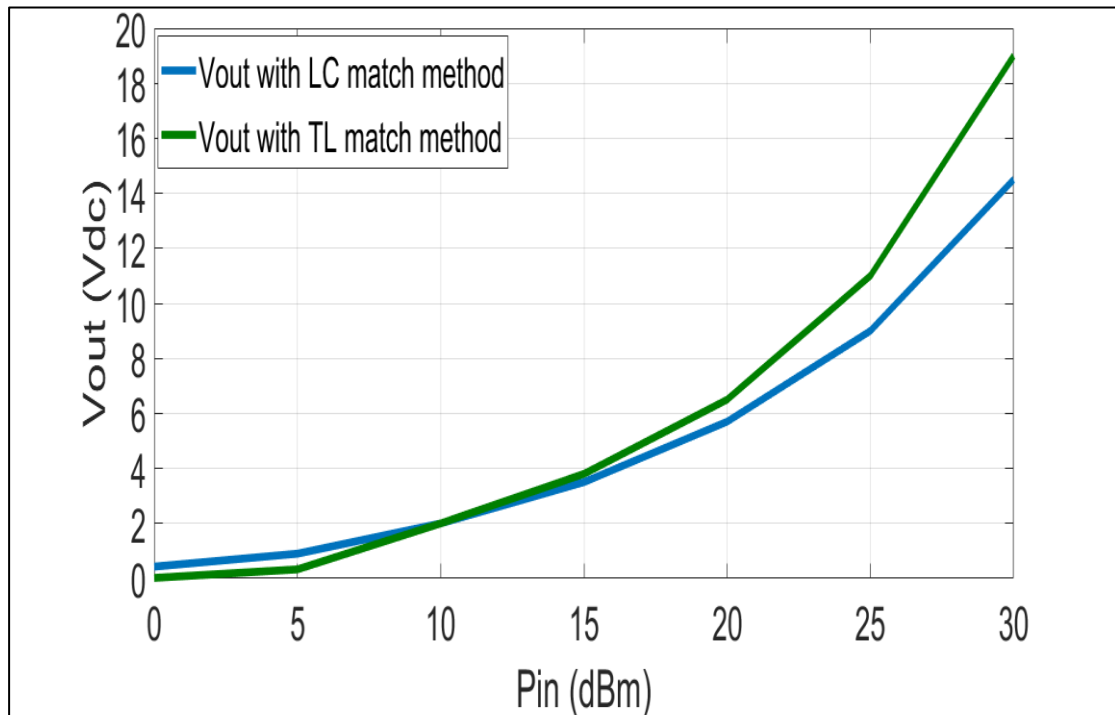


Fig. 4.19: V_{out} versus P_{in} of comparison between a voltage doubler rectifier circuit with an LC-circuit and a TL-circuit at 2.4 GHz.

Fig. 4.20 shows the comparison in efficiency (η) of the rectifier's performance when using the LC-match method and the TL-match method. It has been investigated that values vary between both the LC-match and TL-match in efficiency (η) at low input power (P_{in}). On the other hand, the efficiency (η) was higher at high input power (P_{in}) using the TL-match method than using the LC-match method. In addition, a better efficiency was 16% at 15 dBm of input power when using the LC-match method.

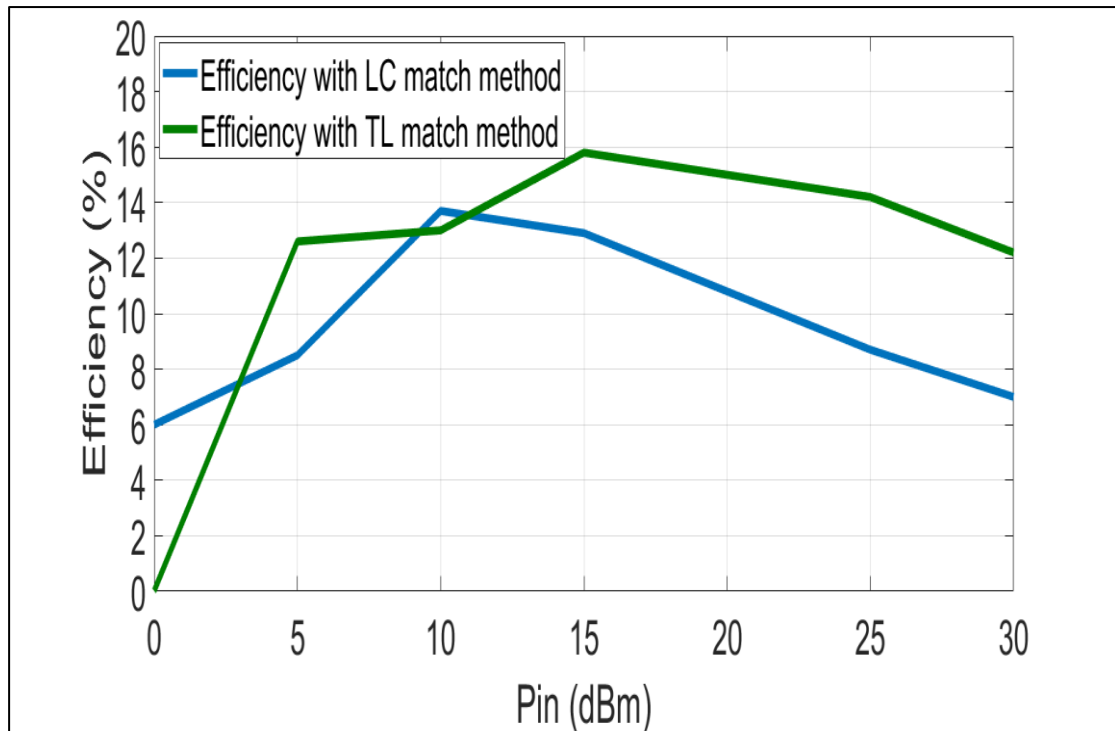


Fig. 4.20: Efficiency (η) versus Pin of comparison between a voltage doubler rectifier circuit with an LC-circuit and a TL-circuit at 2.4 GHz.

4.5 Villard charge pump rectifier circuit using TL-match method

Using the ADS program's Smith Chart tool, a Villard charge pump rectifier circuit with transmission line (TL) impedance matching was also built as seen in Fig. 4.21. Fig. 4.22 displays the rectifier circuit's simulated S11 using the TL-match approach at 2.4 GHz. The reflection coefficient value decreased to less than -31 dB at the specified frequency, indicating excellent impedance matching.

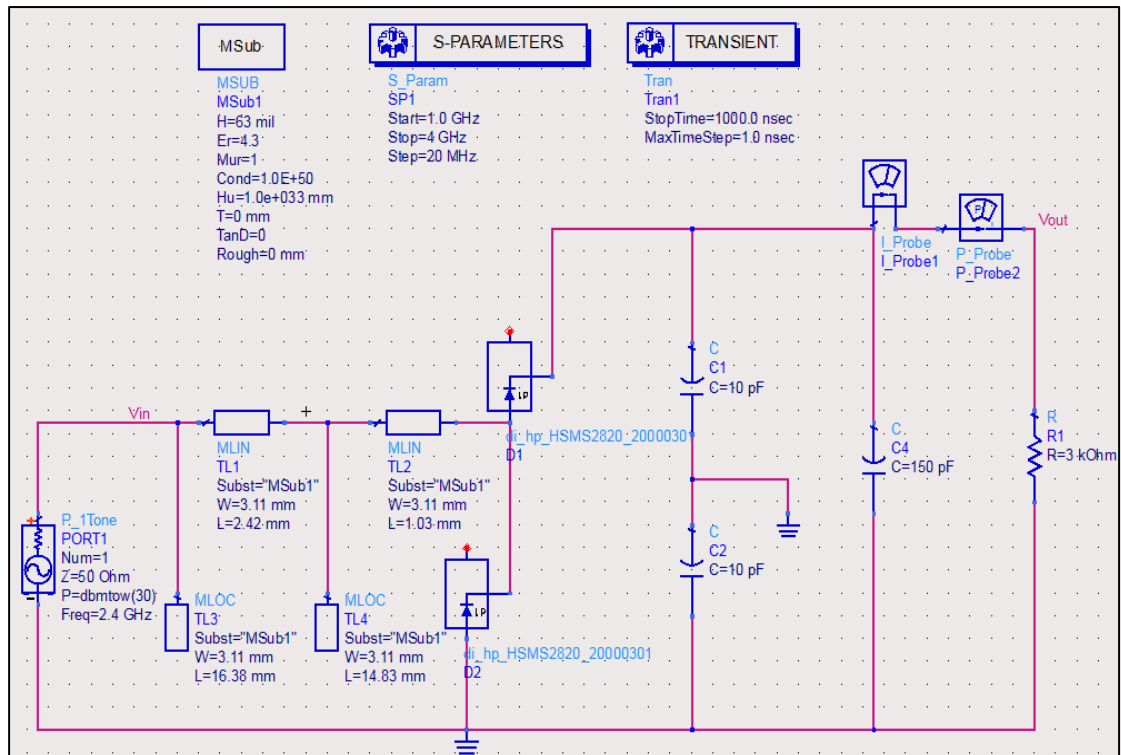


Fig. 4.21: Villard charge pump rectifier circuit operating at 2.4 GHz with TL-circuit.

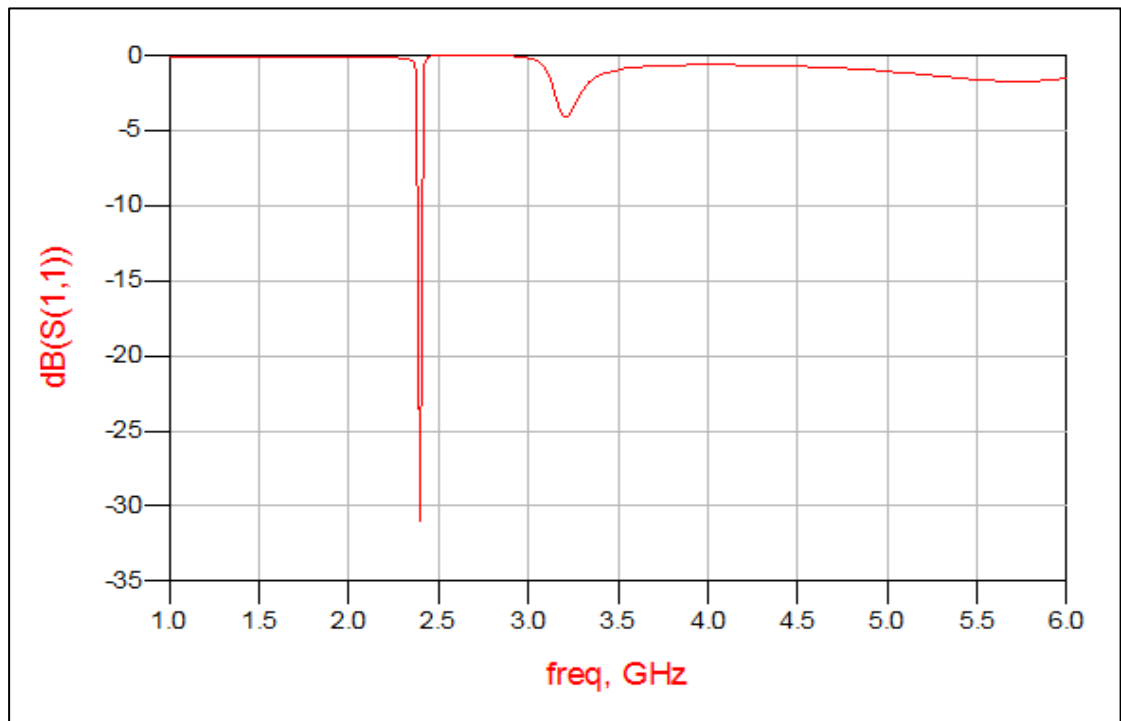


Fig. 4.22: Simulated S11 of Villard charge pump rectifier circuit at 2.4 GHz with TL-circuit.

Fig. 4.23 shows the comparison in V_{out} of the rectifier's performance when using the LC-match method and the TL-match method. It has been demonstrated that the LC-match method has higher values of DC voltage than the TL-match method at all input power.

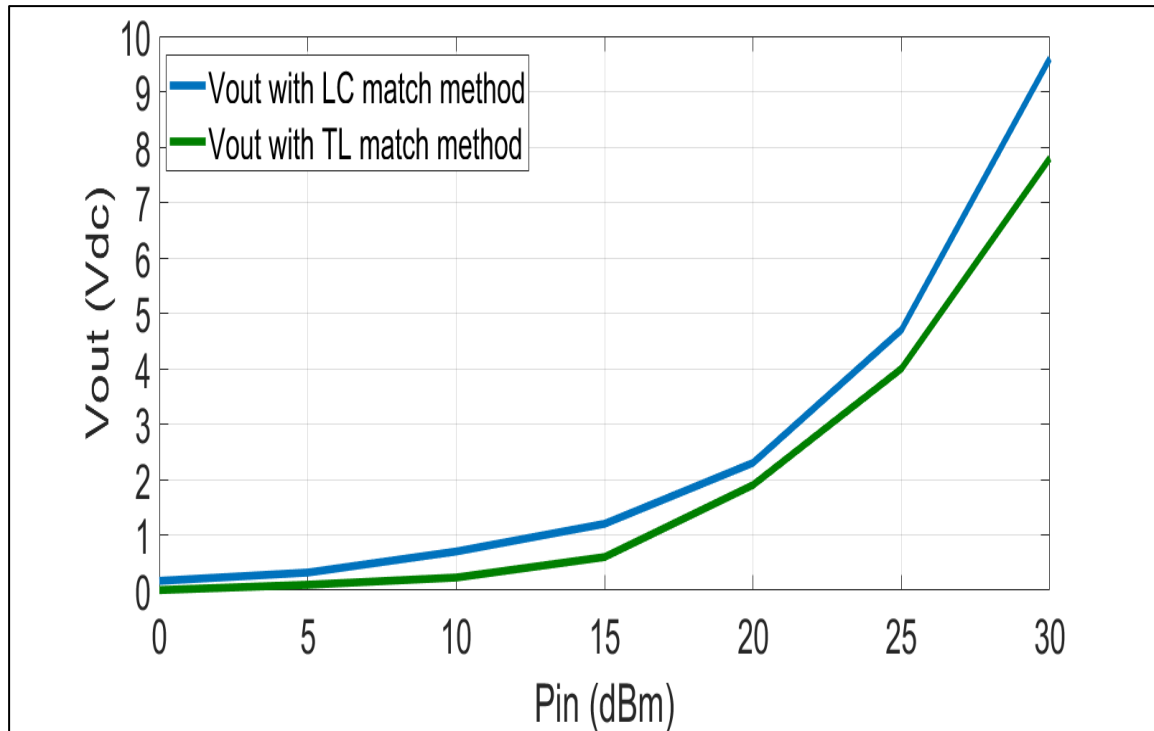


Fig. 4.23: V_{out} versus P_{in} of comparison between a Villard charge pump rectifier circuit with an LC-circuit and a TL-circuit at 2.4 GHz.

Fig. 4.24 shows the comparison in efficiency (η) of the rectifier's performance when using the LC-match method and the TL-match method. It has been investigated that the LC-match method has higher values of efficiency than the TL-match method at all input power. The higher efficiency was 7% at 30 dBm of input power when using the LC-match method. Overall, the efficiency was low in this kind among other rectifier circuits where the efficiency (η) is between 2 and 7%.

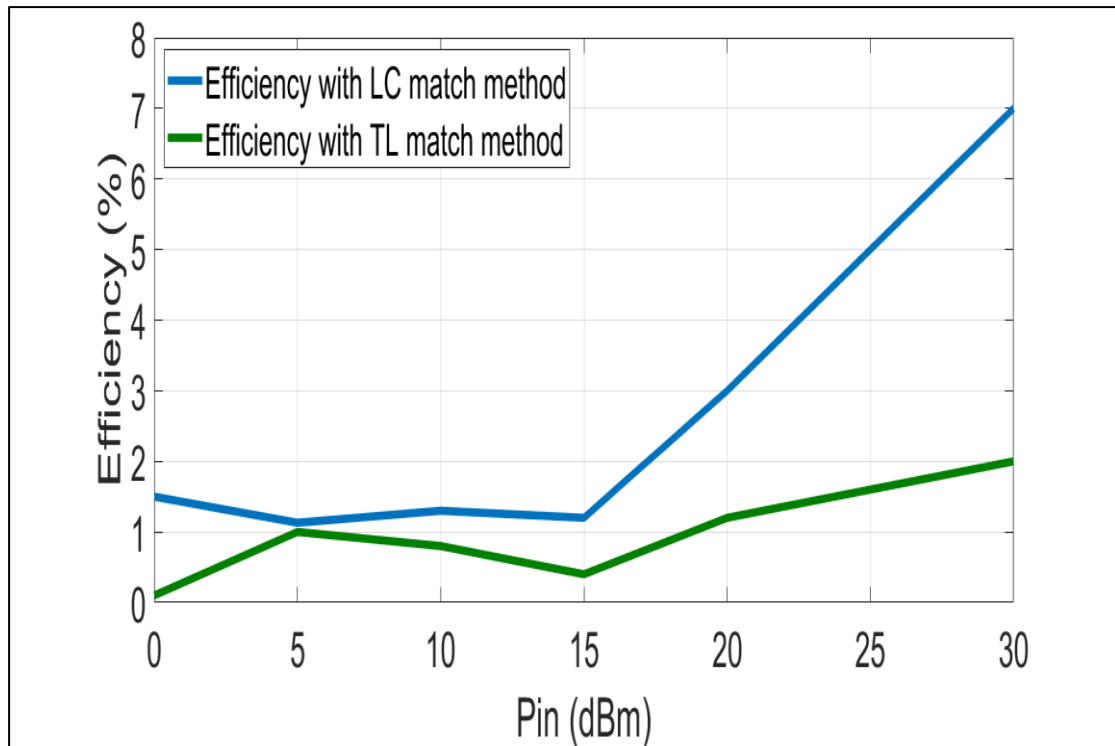


Fig. 4.24: Efficiency (η) versus Pin of comparison between a Villard charge pump rectifier circuit with an LC-circuit and a TL-circuit at 2.4 GHz.

4.6 Graetz charge pump rectifier circuit using TL-match method

A Graetz charge pump rectifier circuit with transmission line (TL) impedance matching is constructed using the Smith Chart tool included in the ADS software as shown in Fig. 4.25. The simulated S11 of the rectifier circuit using the TL-match technique is shown in Fig. 4.26 at 2.4 GHz. The simulation execution procedure of the ADS program was valid and acceptable when the reflection coefficient value dropped to less than -10 dB at the designated frequency.

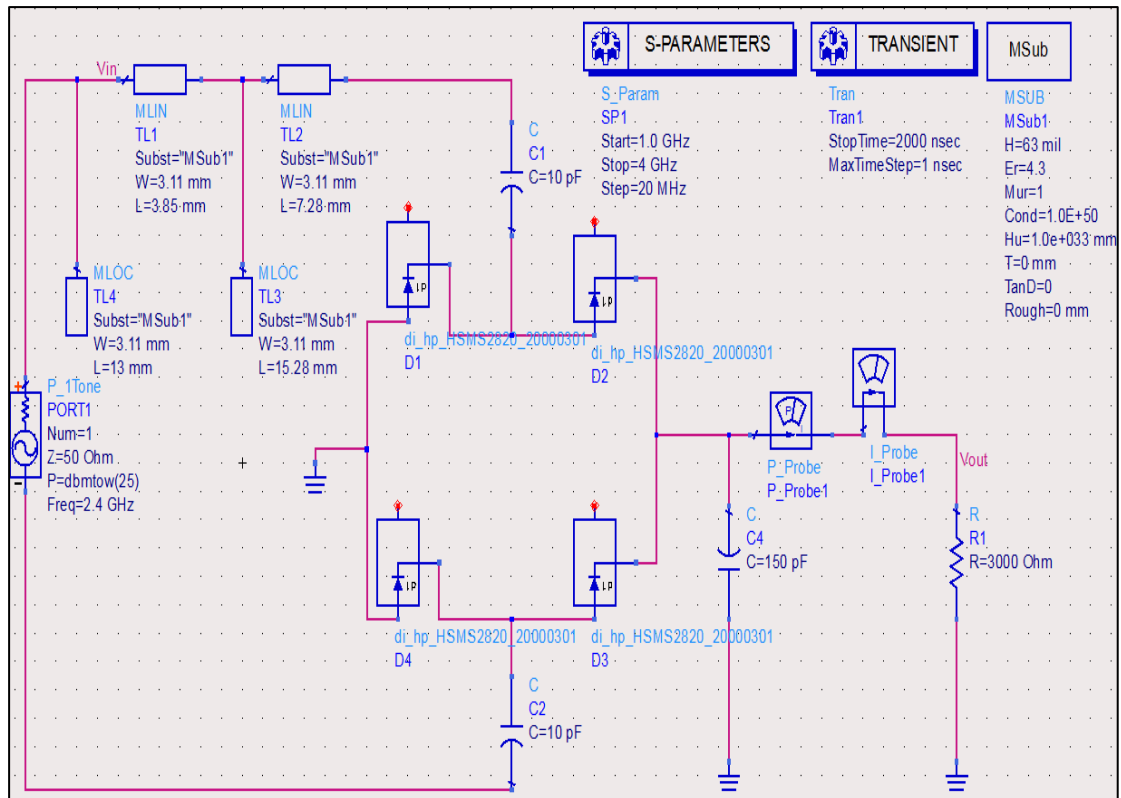


Fig. 4.25: Graetz charge pump rectifier circuit operating at 2.4 GHz with TL-circuit.

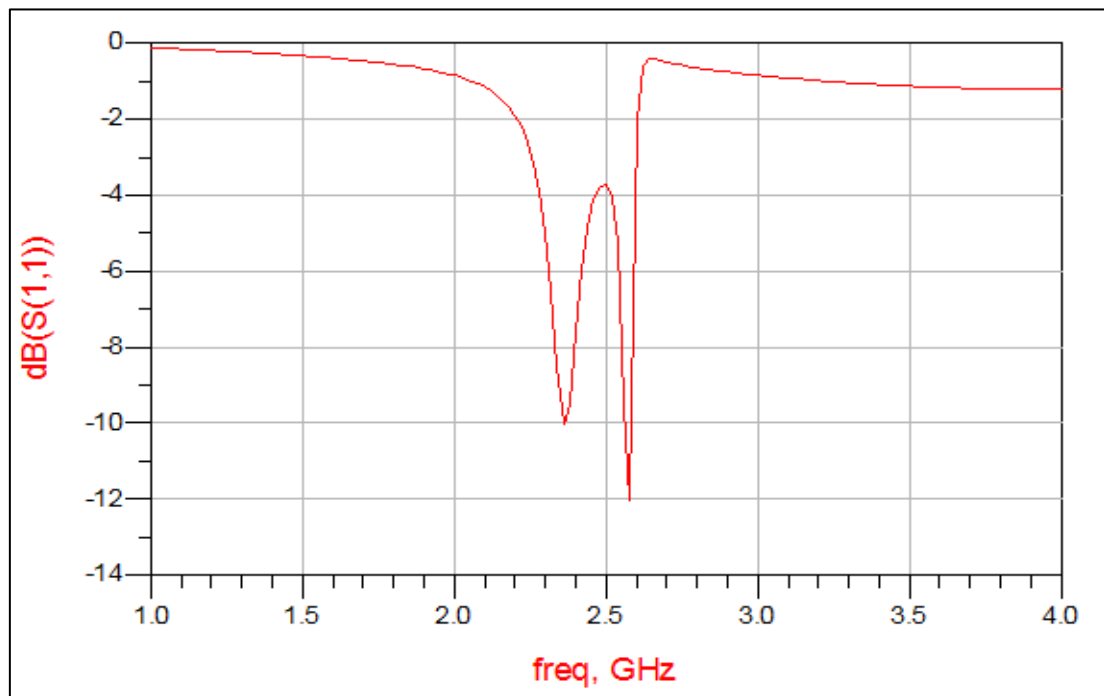


Fig. 4.26: Simulated S11 of Graetz charge pump rectifier circuit at 2.4 GHz with TL-circuit.

Fig. 4.27 shows the comparison in V_{out} of the rectifier's performance when using the LC-match method and the TL-match method. It has been demonstrated that the TL-match method has higher values than the LC-match method at all input power values, except at low input power beginning from 0 to 10 dBm, where there is little difference between them.

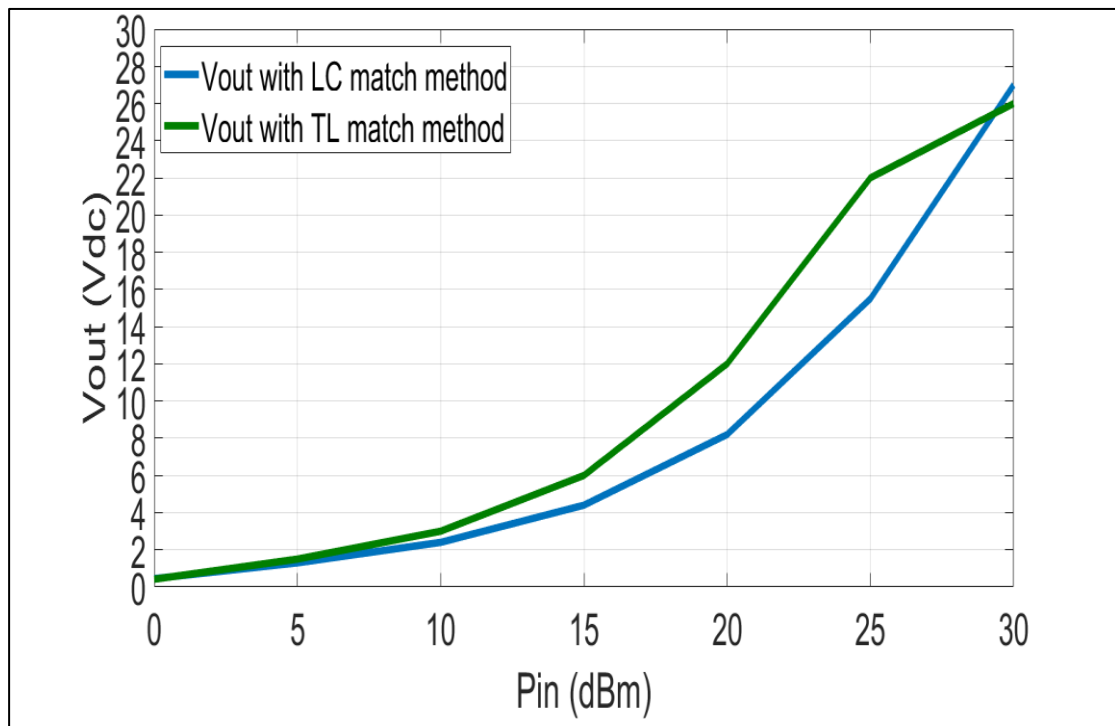


Fig. 4.27: V_{out} versus P_{in} of comparison between a Graetz charge pump rectifier circuit with an LC-circuit and a TL-circuit at 2.4 GHz.

Fig. 4.28 shows the comparison in efficiency (η) of the rectifier's performance when using the LC-match method and the TL-match method. It has been found that the TL-match method has higher values than the LC-match method at all input power. The best recorded efficiency was 50% at 20 dBm of input power when using the TL-match method. Overall, the efficiency of this type of rectifier circuit was higher than that of other rectifier circuit where the efficiency (η) lies between 7 and 50%.

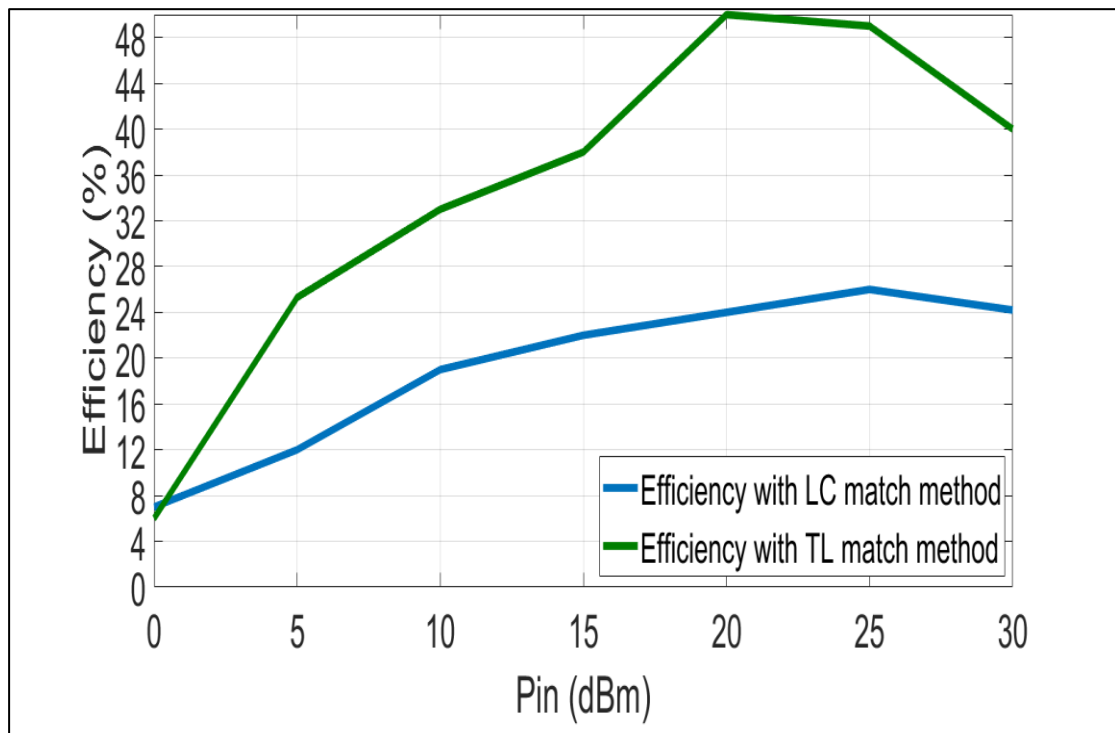


Fig. 4.28: Efficiency (η) versus Pin of comparison between a Graetz charge pump rectifier circuit with an LC-circuit and a TL-circuit at 2.4 GHz.

4.7 Dickson charge pump rectifier circuit using TL-match method

Lastly, The Smith Chart tool in the ADS program was used to build a Dickson charge pump rectifier circuit with transmission line (TL) impedance matching as illustrated in Fig. 4.29. Fig. 4.30 displays the rectifier circuit's simulated S11 at 2.4 GHz using the TL-match approach. The ADS program's simulation execution process was deemed valid when the reflection coefficient value at the assigned frequency fell to less than -35 dB indicating excellent impedance matching.

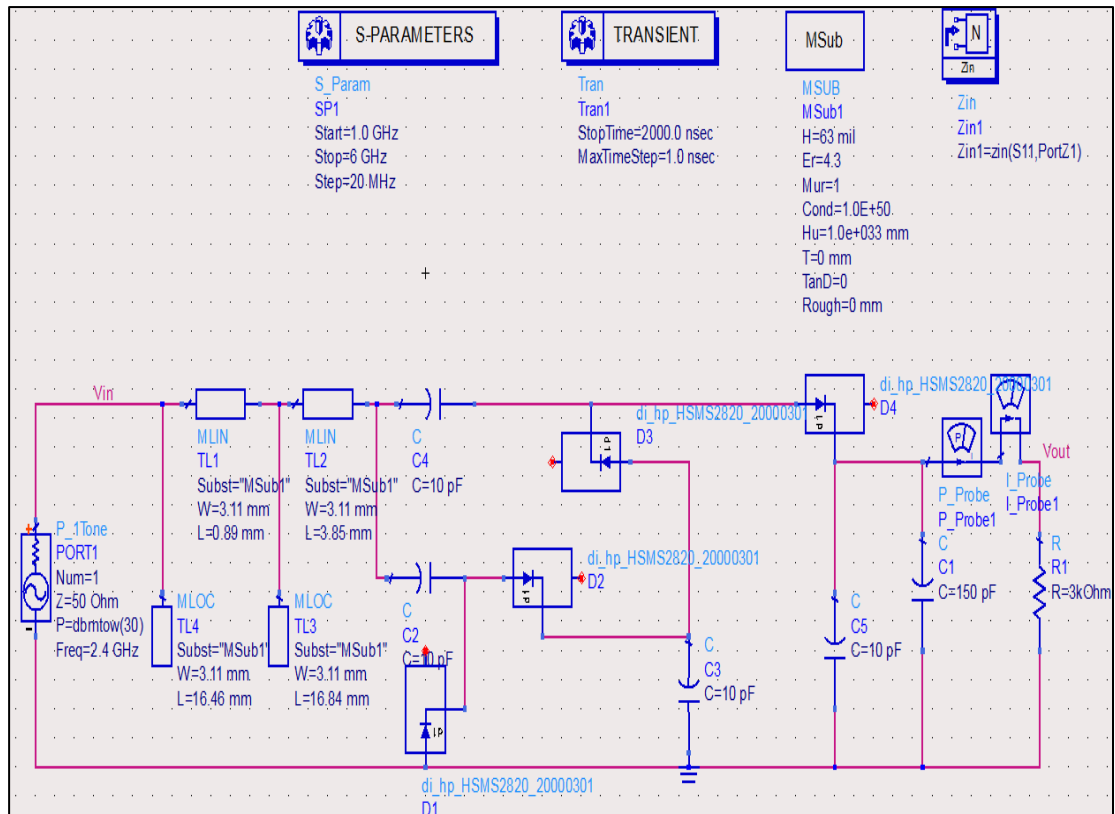


Fig. 4.29: Dickson charge pump rectifier circuit operating at 2.4 GHz with TL-circuit.

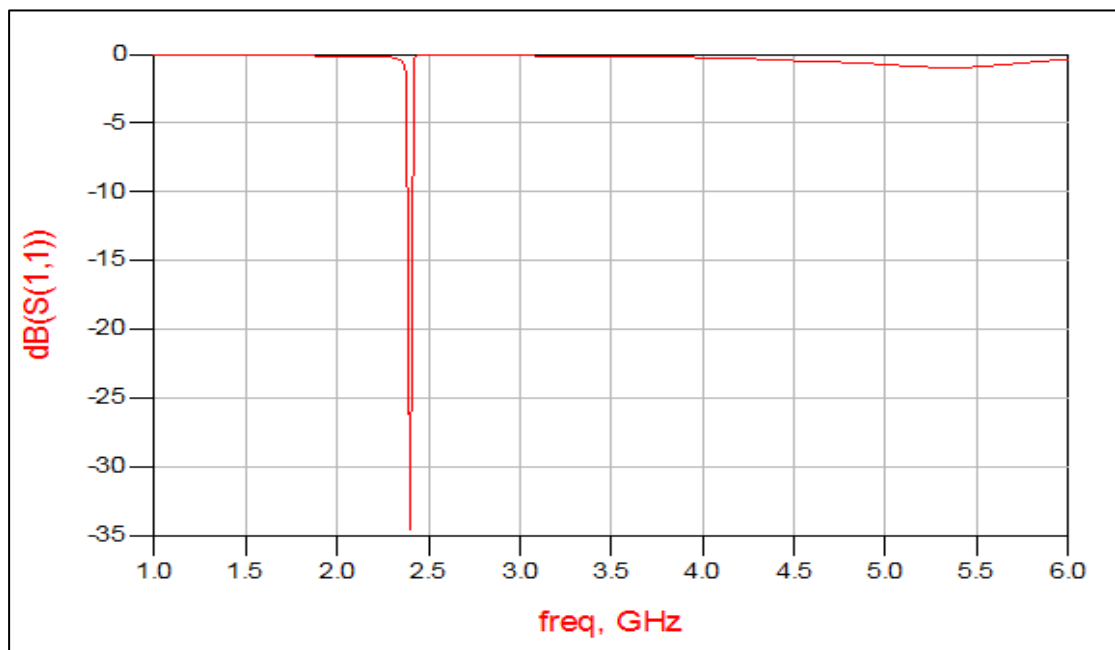


Fig. 4.30: Simulated S11 of Dickson charge pump rectifier circuit at 2.4 GHz with TL-circuit.

Fig. 4.31 shows the comparison in V_{out} of the rectifier's performance when using the LC-match method and the TL-match method. It has been investigated that the LC-match method has higher values of DC voltage than the TL-match method at all input power, where the high values with the LC-match method and the highest value is about 21 V at 30 dBm of P_{in} .

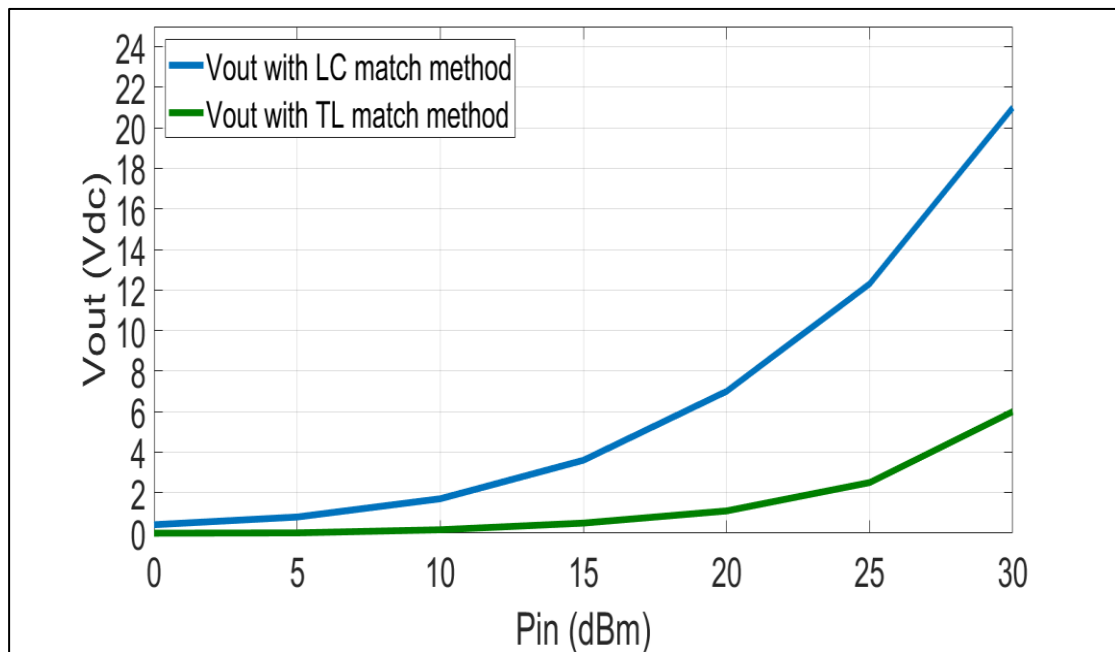


Fig. 4.31: V_{out} versus P_{in} of comparison between a Dickson charge pump rectifier circuit with an LC-circuit and a TL-circuit at 2.4 GHz.

Fig. 4.32 shows the comparison in efficiency (η) of the rectifier's performance when using the LC-match method and the TL-match method. It has been seen that the LC-match method has higher values of efficiency than the TL-match method at all input power. The higher efficiency was 17% at 20 dBm of P_{in} when using the LC-match method. Overall, the efficiency of this type of rectifier circuit was smaller than that of the Graetz charge pump rectifier circuit.

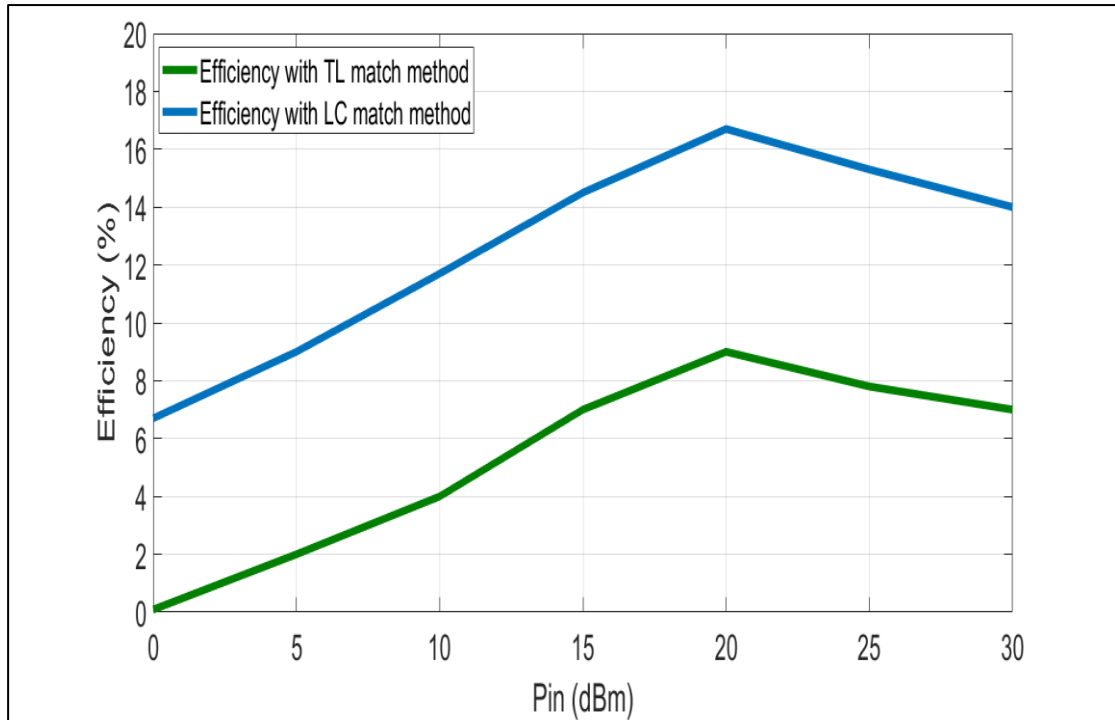


Fig. 4.32: Efficiency (η) versus Pin of comparison between a Dickson charge pump rectifier circuit with an LC-circuit and a TL-circuit at 2.4 GHz.

Fig. 4.33 shows the comparison in Vout performance of the rectifier circuits using the TL-match method at the resistance load (3 k Ω), HSMS2820 diode, and ϵ_r equal to 4.3. It has been investigated that the highest Vout with the Graetz charge rectifier circuit is about 27 V, followed by the voltage doubler rectifier circuit with a value around 19.7 V, followed by the full-wave rectifier circuit, then by the half-wave rectifier circuit. On the other hand, the smallest value between them was the Dickson charge pump rectifier circuit.

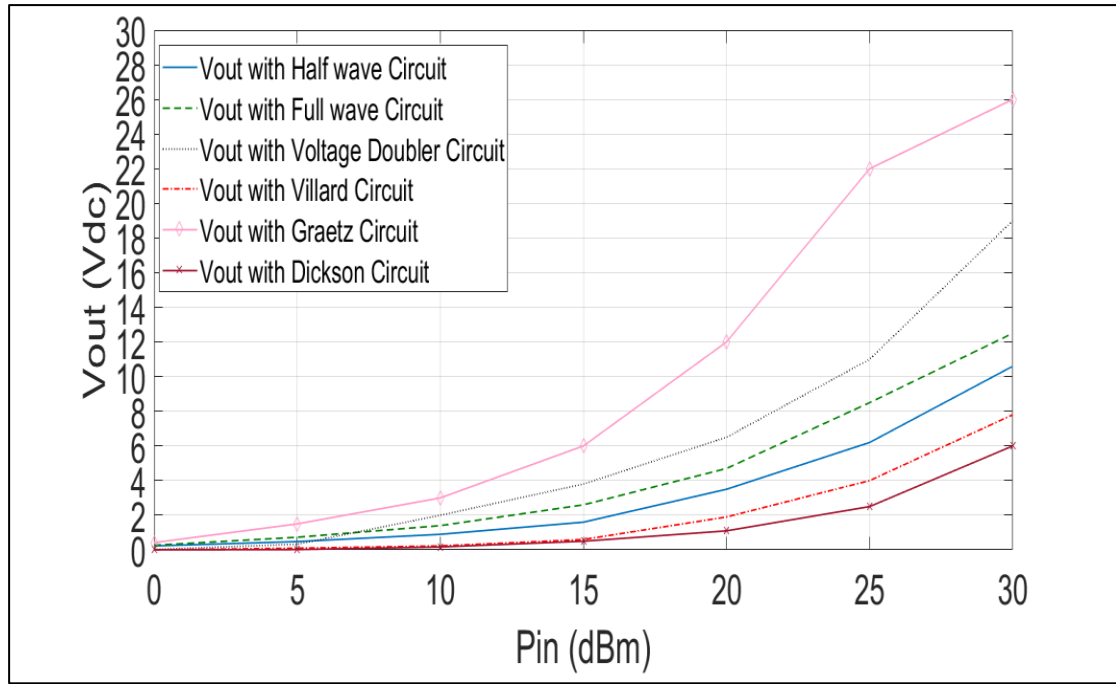


Fig. 4.33: Vout (V) versus Pin (dBm) of different rectifier circuits at 2.4 GHz with TL-circuit.

Fig. 4.34 shows the comparison in efficiency performance of the rectifier circuits using the TL-match method at the resistance load ($3 \text{ k}\Omega$), HSMS2820 diode, and ϵ_r equal to 4.3. It has been investigated that the highest efficiency with the Graetz charge rectifier circuit is about 50% at 20 dBm of input power, followed by the voltage doubler rectifier circuit with a value around 16.7 % at 15 dBm of input power Pin, followed by the full-wave rectifier circuit, then by the half-wave rectifier circuit. On the other hand, the smallest value between them was the Dickson charge pump rectifier circuit.

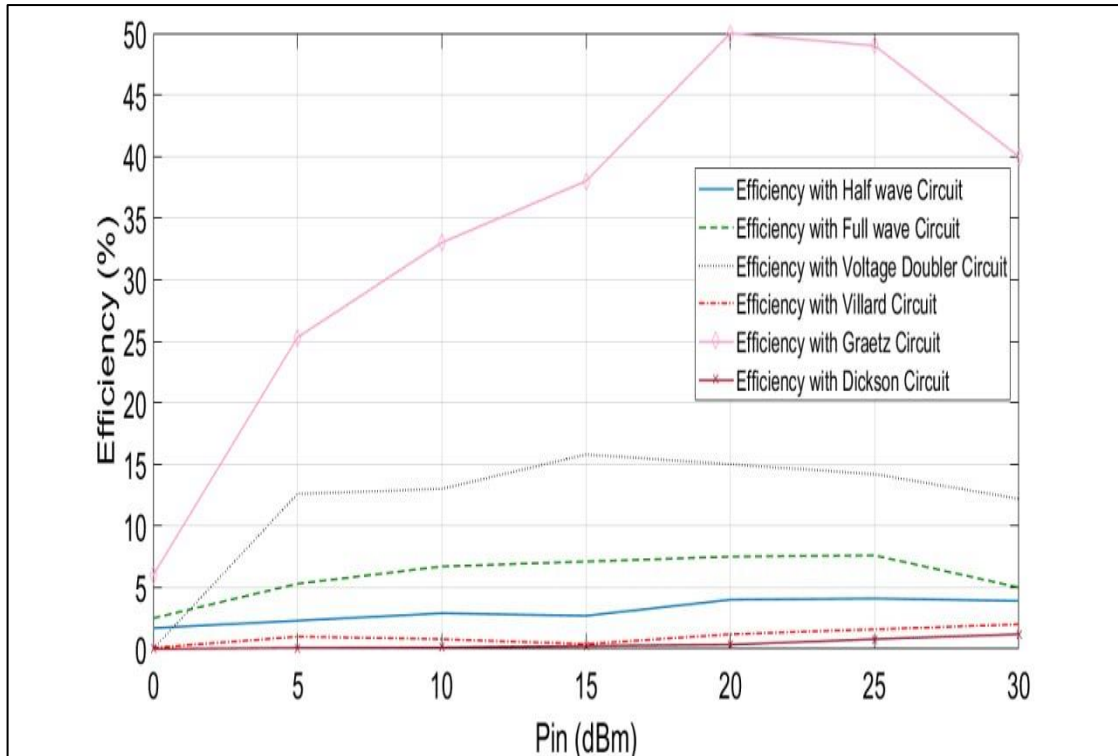


Fig. 4.34: Efficiency (η) versus Pin (dBm) of different rectifier circuits at 2.4 GHz with TL-circuit.

The comparison of the rectifier's performance efficiency (η) when the load resistance (from 1 to 5 k Ω) is changed is shown in Fig. 4.35. Research has shown that when load resistance increases, efficiency (η) declines. The maximum efficiency (η) of 73% is found at a load resistance equal to 1 k Ω at 25 dBm of P_{in} . Additionally, this efficiency rating is outstanding in comparison to other rectifier circuits that have relatively low efficiency.

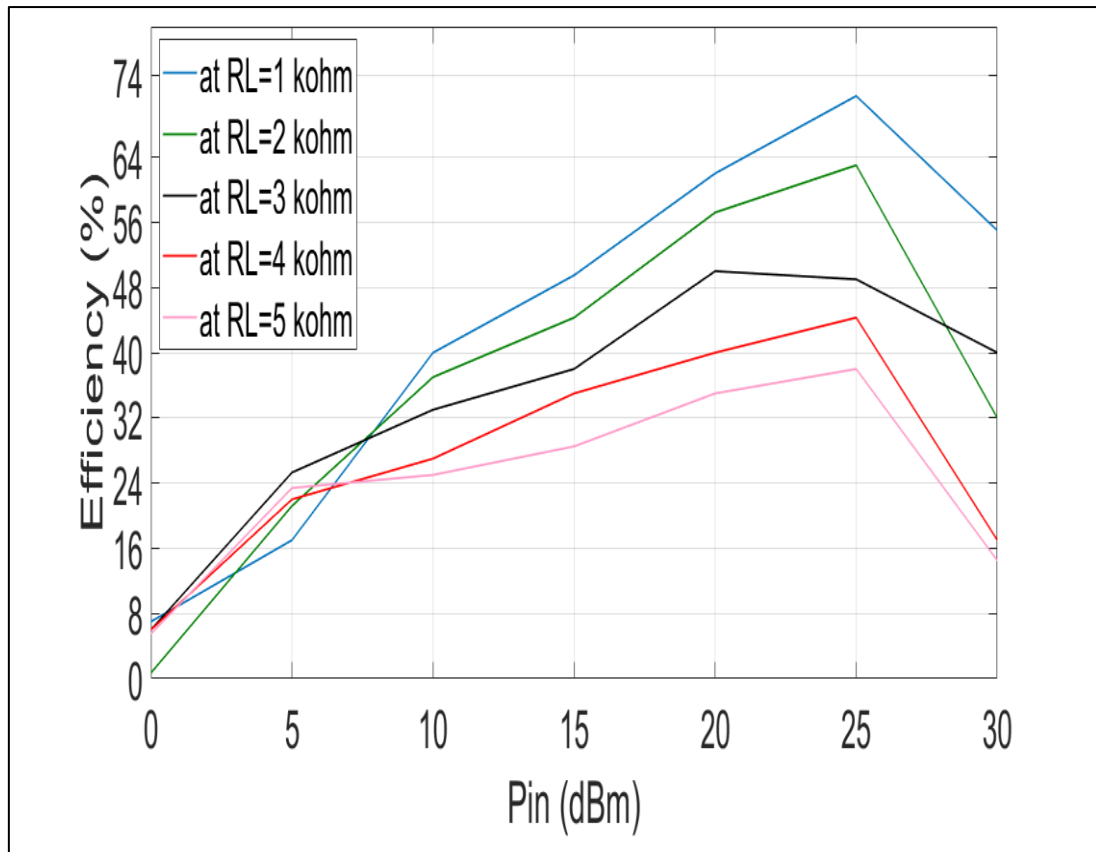


Fig. 4.35: Efficiency (η) versus Pin (dBm) of Graetz charge pump rectifier circuit for different values of resistance load (R_L) at 2.4 GHz with TL-circuit.

CHAPTER FIVE

CONCLUSIONS AND FUTURE WORKS

5.1 CONCLUSIONS

In this work, six types of rectifier circuits were designed and simulated, and they were compared in terms of Output Voltage and Efficiency. A comparison was made between all six types of rectifier circuits using the LC match method and the TL match method, in terms of Output Voltage and Efficiency. The aim is to present a full guidelines for rectifiers' designers to select the best rectifier circuit based on the application, power range, operating frequency, load condition, available diodes and substrate type. Thus, this study provides a detailed road map for RF-based energy harvesting systems.

Rectifier circuits using LC-match method

- This comparative study of rectifier types has demonstrated that the Graetz charge pump offers the highest output voltage and efficiency among the rectifier types considered.
- It concludes from this study that the half-wave and full-wave rectifier circuits are most affected by changing diodes in terms of the V_{out} .
- The full-wave rectifier circuit is mostly affected by changing the ϵ_r in terms of V_{out} . Furthermore, the voltage doubler was worrisome in terms of V_{out} at low resistance loads, while the half-wave and full-wave rectifier circuits are most stable.
- The Graetz charge pump, followed by the half-wave rectifier circuit, are the most affected by changing diodes in terms of efficiency.

- The Graetz charge pump is the best stable among rectifier circuits for changing ϵ_r in terms of efficiency.
- Finally, the Dickson charge pump is most stable in changing resistance load in terms of efficiency.

Rectifier circuits using TL-match method

- It has been obtained that the highest V_{out} with the Graetz charge rectifier circuit is about 27 V, followed by the voltage doubler rectifier circuit with a value around 19.7 V.
- The smallest value between them was the Dickson charge pump rectifier circuit in terms of V_{out} .
- It has also been obtained that the highest efficiency with the Graetz charge rectifier circuit is about 73% at 25 dBm of input power, followed by the voltage doubler rectifier circuit with a value around 16.7 % at 15 dBm of input power.
- In addition, the poorest performance among them was the Dickson charge pump rectifier circuit.
- The Graetz charge pump was the best among the other rectifier circuits, using both the LC-match method and the TL-match method.

5.2 FUTURE WORKS

There are several potential areas of work when comparing different rectifier circuits, including the half wave rectifier, full wave rectifier, voltage doubler, Villard charge pump, Graetz charge pump, and Dickson charge pump. Some potential future research directions and areas of interest in this field may include:

1. **Efficiency Optimization:** Developing methods to raise rectifier circuit efficiency might be the topic of research. Reduce power losses and raise total energy conversion efficiency, this may comprise investigating novel circuit topologies, choosing components, or using optimization methods.
2. **Power Density Enhancement:** Increasing rectifier circuit power density is a significant area of research. To allow increased power density and compact rectifier designs, researchers may look into new semiconductor materials, sophisticated packaging methods, or heat management techniques.
3. **Integration with Energy Storage:** Understanding the integration of rectifier circuits with energy storage devices, such as supercapacitors or batteries, can be a worthwhile endeavor. This could involve creating circuit designs that preserve minimal complexity and high conversion efficiency while effectively charging energy storage devices.
4. **System-Level Optimization:** Scholars may concentrate on rectifier circuit optimization in the context of bigger power electronic systems. Evaluating elements including fault tolerance, system-level control, electromagnetic interference (EMI) prevention, and overall system integration may be necessary.

References

- [1] Costanzo A, Masotti D. Energizing 5G: near- and far-field wireless energy and data transfer as an enabling technology for the 5G IoT. *IEEE Microw Mag*;18 (3):125–36, 2017.
- [2] Wagih M, Hilton GS, Weddell AS, Beeby S. Broadband millimeter-wave textile-based flexible rectenna for wearable energy harvesting. *IEEE Trans Microw Theory Tech* 2020;68(11):4960–72, 2020.
- [3] Yue X, et al. Development of an indoor photovoltaic energy-harvesting module for autonomous sensors in building air quality applications. *IEEE Internet Things J*;4:2092–103, 2017.
- [4] Halimi MA, Khan T, Surender D, Nasimuddin N, Rengarajan SR. Dielectric resonator antennas for RF energy-harvesting/wireless power transmission applications: a state-of-the-art review. *IEEE Antennas Propag. Mag.* 2023. <https://doi.org/10.1109/MAP.2023.3236270>. Early access.
- [5] Surender D, Khan T, Talukdar FA, Antar YMM. Rectenna design and development strategies for wireless applications: a review. *IEEE Antennas Propag Mag*;64 (5):16–29, 2022.
- [6] Halimi MA, Khan T, Nasimuddin AA, Kishk YMM, Antar. Rectifier circuits for RF energy harvesting and wireless power transfer applications: a comprehensive review based on operating conditions. *IEEE Microw Mag*; 24(1):46–61, 2023.
- [7] Hesham R, Soltan A, Madian A. Energy harvesting schemes for wearable devices. *AEU-Int J Electron Commun*;138:1–11, 2021.

- [8] Surender D, Halimi MA, Khan T, Talukdar FA, Nasimuddin, Rengarajan SR. 5G/ millimeter-wave rectenna systems for radio-frequency energy harvesting/wireless power transmission applications: an overview. *IEEE Antennas Propagat Mag* 2022. <https://doi.org/10.1109/MAP.2022.3208794>. Early access.
- [9] Shi Y, Jing J, Fan Y, Yang L, Li Y, Wang M. A novel compact broadband rectenna for ambient RF energy harvesting. *AEU-Int J Electron Commun*;95:264–70, 2018.
- [10] Halimi MA, Surender D, Khan T. Design of a 2.45 GHz operated rectifier with 81.5 % PCE at 13 dBm input power for RFEH/WPT applications. In: 2021 IEEE Indian conference on antennas and propagation (InCAP); p. 981–3, 2021.
- [11] Tran, L.-G.; Cha, H.-K.; Park, W.-T. RF power harvesting: A review on designing methodologies and applications. *Micro Nano Syst. Lett.* 2017, 5, 14
- [12] Shafiee N, Tewari S, Calhoun B, and Shrivastava A, “Infrastructure circuits for lifetime improvement of ultra-low power IoT devices,” *IEEE Trans. Circuits Syst. I, Reg. Papers*, vol. 64, no. 9, pp. 2598–2610, Sep. 2017.
- [13] Roy A, Klinefelter A, Yahya FB, Chen X, Gonzalez-Guerrero LP, Lukas CJ, Kamakshi DA, Boley J, Craig K, Faisal M, Oh S, Roberts NE, Shaksheer Y, Shrivastava A, Vasudevan DP, Wentzloff DD, Calhoun BH. A 6.45 μ W Self-Powered SoC With Integrated Energy-Harvesting Power Management and ULP Asymmetric Radios for Portable Biomedical Systems. *IEEE Trans Biomed Circuits Syst.* 2015 Dec;9(6):862-74. doi: 10.1109/TBCAS.2015.2498643. Epub 2015 Dec 28. PMID: 26731775.

- [14] Y. Zhang et al., "A Batteryless 19 μ W MICS/ISM-Band Energy Harvesting Body Sensor Node SoC for ExG Applications," in *IEEE Journal of Solid-State Circuits*, vol. 48, no. 1, pp. 199-213, Jan. 2013, doi: 10.1109/JSSC.2012.2221217.
- [15] Y. -P. Chen et al., "An Injectable 64 nW ECG Mixed-Signal SoC in 65 nm for Arrhythmia Monitoring," in *IEEE Journal of Solid-State Circuits*, vol. 50, no. 1, pp. 375-390, Jan. 2015, doi: 10.1109/JSSC.2014.2364036.
- [16] Saffari P, Basaligheh A, and Moez K, "An RF-to-DC rectifier with high efficiency over wide input power range for RF energy harvesting applications," *IEEE Trans. Circuits Syst. I, Reg. Papers*, vol. 66, no. 12, pp. 4862–4875, Dec. 2019.
- [17] Karami MA and Moez K, "Systematic co-design of matching networks and rectifiers for CMOS radio frequency energy harvesters," *IEEE Trans. Circuits Syst. I, Reg. Papers*, vol. 66, no. 8, pp. 3238–3251, Aug. 2019.
- [18] Xu P, Flandre D, and Bol D, "Analysis, modeling, and design of a 2.45-GHz RF energy harvester for SWIPT IoT smart sensors," *IEEE J. Solid-State Circuits*, vol. 54, no. 10, pp. 2717–2729, Oct. 2019.
- [19] A. Khalifa et al., "The Microbead: A 0.009 mm³ Implantable Wireless Neural Stimulator," in *IEEE Transactions on Biomedical Circuits and Systems*, vol. 13, no. 5, pp. 971-985, Oct. 2019, doi: 10.1109/TBCAS.2019.2939014.
- [20] F. Laiwalla et al., "A Distributed Wireless Network of Implantable Sub-mm Cortical Microstimulators for Brain-Computer Interfaces," 2019 41st Annual International Conference of the IEEE Engineering in

Medicine and Biology Society (EMBC), Berlin, Germany, 2019, pp. 6876-6879, doi: 10.1109/EMBC.2019.8857217.

[21] Zhao Y, Rennaker RL, Hutchens C, and Ibrahim T, "Implanted miniaturized antenna for brain computer Interface applications: Analysis and design," PLoS One, vol. 9, no. 7, 2014, Art. no. e103945.

[22] Yang K-W, Oh K, and Ha S, "Challenges in scaling down of free-floating implantable neural interfaces to millimeter scale," IEEE Access, vol. 8, pp. 133295–133320, 2020.

[23] Choi S, Salim A, Jeong H, Lim S. High efficiency and compact metamaterial-inspired 900 MHz rectifier. *J Microw Power Electromagn Energy*;50(3): 168–81, 2016.

[24] Hsu C, Lin S, Tsai Z. Quad-band rectifier using resonant matching networks for enhanced harvesting capability. *IEEE Microwave Wirel Compon Lett*;27(7): 669–71, 2017 .

[25] Gozel MA, Kahriman M, Kasar O. Design of an efficiency-enhanced Greinacher rectifier operating in the GSM 1800 band by using rat-race coupler for RF energy harvesting applications. *Int J RF Microw Comput Aided Eng*;29(1):1–8, 2018 .

[26] Chandravanshi S, Sarma SS, Akhtar MJ. Design of triple band differential rectenna for RF energy harvesting. *IEEE Trans Antennas Propag*;66(6):2716–26, 2018.

[27] P. Wu et al., "Compact High-Efficiency Broadband Rectifier With Multi-Stage-Transmission-Line Matching," in *IEEE Transactions on Circuits and Systems II: Express Briefs*, vol. 66, no. 8, pp. 1316-1320, Aug. 2019, doi: 10.1109/TCSII.2018.2886432.

- [28] Wu S, Wang J, Liu J, Cheng DY. A novel design of single branch wideband rectifier for low-power application. *Radioengineering*;29(1):125–31, 2020.
- [29] He Z, Liu C. A compact high-efficiency broadband rectifier with a wide dynamic range of input power for energy harvesting. *IEEE Microwave Wirel Compon Lett*;30(4):433–6, 2020.
- [30] Muhammad S, Jiat TJ, Kin WS, Iqbal A, Alibakhshikenari M, Limiti E. Compact rectifier circuit design for harvesting GSM/900 ambient energy. *Electronics*.; 9(10):1-11, 2020.
- [31] Mansour I, Mansour M, Aboualalaa M. Compact and efficient wideband rectifier based on π network with wide input power ranges for energy harvesting. *AEU-Int J Electron Commun* ;160:1–7, 2023.
- [32] Muhammad S, Tiang JJ, Wong SK, Smida A, Waly MI, Iqbal A. Efficient quad-band RF energy harvesting rectifier for wireless power communications. *AEU-Int J Electron Commun*; 139:1–9, 2021.
- [33] Ismail N, Abd KE. Reversed L-type matching impedance of RF-to-DC rectifier for energy harvesting system. *Journal of Electrical and Electronic Systems Research*.; 19:167-72, 2021.
- [34] Pinto D, Arun A, Lenka S, Colaco L, Khanolkar S, Betgeri S, et al. Design and performance evaluation of a Wi-Fi energy harvester for energizing low power devices. In *region 10 symposium* (pp. 1-8). IEEE, 2021.
- [35] Narayanan S and Thangavel S. A compact two sleeve microstrip patch rectenna system for ambient RF energy harvesting. *International Journal of Engineering Research & Technology*.; 10(6): 716-23, 2021.
- [46] Coskuner E, Garcia-Garcia JJ. Metamaterial impedance matching

network for ambient RF-energy harvesting operating at 2.4 GHz and 5 GHz. *Electronics.*; 10(10):1-14, 2021.

[36] Coskuner E, Garcia-Garcia JJ. Metamaterial impedance matching network for ambient RF-energy harvesting operating at 2.4 GHz and 5 GHz. *Electronics.*; 10(10):1-14, 2021.

[37] Yusoff SS, Malik SA, Ibrahim T. Simulation and performance analysis of a dual GSM band rectifier circuit for ambient RF energy harvesting. *Applications of Modelling and Simulation.*; 5:125-33, 2021.

[38] Li S, Cheng F, Gu C, Yu S, Huang K. Efficient dual-band rectifier using stepped impedance stub matching network for wireless energy harvesting. *IEEE Microwave and Wireless Components Letters.*;31(7):921-4, 2021.

[39] Halimi MA, Khan T, Kishk AA, Rengarajan SR. Design of a frequency selectable rectifier using tuned matching circuit for RFEH applications. *IETE J Res* 2022. <https://doi.org/10.1080/03772063.2022.2112986>.

[40] Surender D, Halimi MA, Khan T, Talukdar FA, Antar YMM. A 90° twisted quarter-sectored compact and circularly polarized DR-rectenna for RF energy harvesting applications. *IEEE Antennas Wirel Propag Lett*;21(6):1139–43, 2022.

[41] Surender D, Halimi MA, Khan T, Talukdar FA, Antar YMM. A triple band rectenna for RF energy harvesting in smart city applications. *Int J Electron*;110(5): 789–803, 2022. <https://doi.org/10.1080/00207217.2022.2062797>.

[42] Halimi MA, Surender D, Khan T, Kishk AA, Rengarajan SR. A multisteped transmission line matching strategy based triple-band

rectifier for RFEH/WPT applications. *IEEE Microwave Wirel Compon Lett*;32(8):1008–10, 2022.

[43] Surender D, Halimi MA, Khan T, Talukdar FA, Kishk AA, Antar YMM, Rengarajan SR. Semi-annular-ring slots loading for broadband circularly polarized DR-rectenna for RF energy harvesting in smart city environment. *AEU-Int J Electron Commun*; 147:154143, 2022.

[44] Muhammad S, Tiang JJ, Wong SK, Nebhen J, Smida A, Waly MI, Iqbal A. Broadband RCN-based RF-rectifier with a large range of power for harvesting ambient wireless energy. *AEU-Int J Electron Commun*; 152:1–10, 2022.

[45] Surender D, Halimi MA, Khan T, Talukdar FA, Antar YMM. A triple band rectenna for RF energy harvesting in smart city applications. *Int J Electron*;110(5): 789–803, 2022. <https://doi.org/10.1080/00207217.2022.2062797>.

[46] Wang C, Zhang J, Bai S, Chang D, Duan L. A multi-band compact flexible energy collector for wearable or portable IoT devices. *IEEE Antennas Wirel Propag Lett* 2023. <https://doi.org/10.1109/LAWP.2023.3235918>.

[47] D. Surender et al., "Analysis of Facet-Loaded Rectangular DR-Rectenna Designs for Multisource RF Energy-Harvesting Applications," in *IEEE Transactions on Antennas and Propagation*, vol. 71, no. 2, pp. 1273-1284, Feb. 2023, doi: 10.1109/TAP.2022.3231014.

[48] Halimi MA, Khan T, Koul SK, Rengarajan SR. A dual-band rectifier using half-wave transmission line matching for 5G and Wi-Fi bands RFEH/MPT applications. *IEEE Microwave Wirel Compon Lett* 2023;33(1):74–7.

- [49] S. Kim, "RF Energy Harvesting techniques for wirelessly Powered devices," School of Integrated Technology and Yonsei Institute of Convergence Technology, Yonsei University, Songdo, Incheon, 406-840, Korea.
- [50] Sallan, J.; Villa, J.; Llombart, A.; Sanz, J. Optimal Design of ICPT Systems Applied to Electric Vehicle Battery Charge. *IEEE Trans. Ind. Electron.*, 56, 2140–2149, 2009.
- [51] Villa, J.L.; Sallán, J.; Llombart, A.; Sanz-Osorio, J. Design of a high frequency Inductively Coupled Power Transfer system for electric vehicle battery charge. *Appl. Energy*, 86, 355–363, 2009.
- [52] Wang, C.-S.; Covic, G.; Stielau, O. Power Transfer Capability and Bifurcation Phenomena of Loosely Coupled Inductive Power Transfer Systems. *IEEE Trans. Ind. Electron.*, 51, 148–157, 2004.
- [53] Wang, C.-S.; Stielau, O.; Covic, G. Design Considerations for a Contactless Electric Vehicle Battery Charger. *IEEE Trans. Ind. Electron.*, 52, 1308–1314, 2005.
- [54] Batarseh, Issa, Ahmad Harb, Issa Batarseh, and Ahmad Harb. "Uncontrolled Diode Rectifier Circuits." *Power Electronics: Circuit Analysis and Design*, pp: 461-524, 2018.
- [55] H. W. Cheng, T. C. Yu, and C. H. Luo, "Direct current driving impedance matching method for rectenna using medical implant communication service band for wireless battery charging," *IET Microwaves Antennas & Propagation*, vol. 7, pp. 277-282, Mar , 19, 2013.

[56] Avago Technologies, "Schottky Diode Voltage Doubler," Application Note 956-4, 2010.

[57] X. Chen, L. Huang, J. Xing, Z. Shi, and Z. Xie, "Energy harvesting System and circuits for ambient wifi energy harvesting," in 2017 12th International Conference on Computer Science and Education (ICCSE). IEEE, pp. 769–772, 2017.

[58] R. Yuan and D. P. Arnold, "An input-powered active AC/DC converter with zero standby power for energy harvesting applications," in Energy Conversion Congress and Exposition (ECCE), IEEE, pp. 4441-4446, 2010.

[59] M. Awad, P. Benech, J. -M. Duchamp and N. Corrao, "Performance Comparison of Two Stage of Dickson Voltage Rectifier Realized in FD-SOI 28 nm and BiCMOS 55 nm for RF Energy Harvesting," 2018 IEEE/MTT-S International Microwave Symposium - IMS, Philadelphia, PA, USA, 2018, pp. 980-983, doi: 10.1109/MWSYM.2018.8439412.

[60] Sobot, R. (2020). "Wireless Communication Electronics". Springer International Publishing.

[61] Nasimuddin, & Halimi, Md & Khan, Taimoor & Kishk, Ahmed & Antar, Yahia. (2023). Rectifier Circuits for RF Energy Harvesting and Wireless Power Transfer Applications: A Comprehensive Review Based on Operating Conditions. 24. 46-61. 10.1109/MMM.2022.3211594.

الملخص

حصاد الطاقة هو أسلوب أخذ الطاقة من البيئة الخارجية للنظام وتحويلها إلى طاقة كهربائية قابلة للاستخدام. قد تعمل الإلكترونيات بدون مصدر طاقة تقليدي بفضل تجميع الطاقة، مما يلغي الحاجة إلى توصيلات الكابلات المتكررة وتغيير البطارية. عادةً ما يتم تضمين دوائر التحكم في الكهرباء وحماية خلية تخزين الطاقة في نظام حصاد الطاقة. في هذا العمل، تم إجراء مقارنة بين أنواع مختلفة من دوائر المقومات لحصاد طاقة الترددات اللاسلكية. تم تصميم ومحاكاة ستة أنواع من دوائر المقومات التي تتكون من نصف الموجة، والموجة الكاملة، ومضاعف الجهد، ومضخة شحن فيلارد، ومضخة شحن غرايتز، ومضخة شحن ديكسون. تم تصميم هذه الأنواع المختلفة من الدوائر المقومات مع مقاومات أحمال مختلفة، دايودات نوع (HSMS-282X) ومواد قياسية للركيزة التي تمثل (ϵ_r). عندما يتم تصميم مقومات على FR-4 مع سمك الركيزة من 1.6 ملم باستخدام مرحلة واحدة مع طريقة LC-match عند 2.4 جيجاهرتز. كان النطاق المدروس لجهد الدخل من 0 ديسيبل إلى 30 ديسيبل. ثابت العزل الكهربائي هو 4.3، مقاومة الحمل هي 3 كيلو أوم، دايود من نوع (HSMS-2820) كان قد استخدم. كان أعلى جهد خرج مسجل لمضخة شحن غرايتز حوالي 27 فولت، بينما كانت أعلى كفاءة مسجلة لمضخة شحن غرايتز 27%. أيضا. مرة أخرى، يتم إعداد دراسة مقارنة بين دوائر المقومات باستخدام طريقة LC-match ودوائر المقومات باستخدام طريقة TL-match. وعلاوة على ذلك، فإن مضخة الشحن غرايتز هي الأفضل بين دوائر المقومات الأخرى، بعد أن سجلت كفاءة 73% و 26.8 فولت من حيث الفولتية عند استخدام طريقة مطابقة TL-match. من ناحية أخرى، فإن مضخة شحن ديكسون هي الأسوأ من حيث الأداء مقارنة بدوائر المقومات الأخرى. تم تصميم المقومات في هذا العمل وتمت محاكاتها بواسطة برنامج نظام التصميم المتقدم (ADS).

تحليل مقارن لدوائر المعدل عند 2.4 جيجا هرتز لتطبيقات حصاد الطاقة

رسالة تقدم بها

عثمان أنور محمد

إلى

مجلس كلية هندسة الإلكترونيات- جامعة نينوى
وهي جزء من متطلبات نيل شهادة الماجستير
علوم في هندسة الإلكترونيك

بإشراف

الأستاذ المساعد الدكتور

احمد محمد احمد سلامة السبعاعي



جامعة نينوى
كلية هندسة الالكترونيات
قسم الالكترونك

تحليل مقارن لدوائر المعدل عند 2.4 جيجا هرتز لتطبيقات حصاد الطاقة

عثمان أنور محمد

رسالة في هندسة الالكترونك

بإشراف

الاستاذ المساعد الدكتور

احمد محمد احمد سلامة السبعاعي